

# STUDY OF THE OPTICAL AND DC ELECTRICAL PROPERTIES OF PLASMA POLYMERIZED THIN FILMS OF DIETHYLANILINE

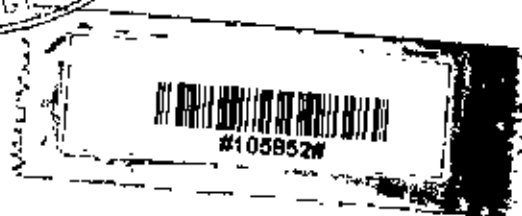
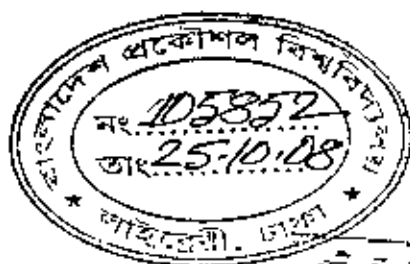
A thesis submitted to the Department of Physics, Bangladesh University of Engineering  
and Technology (BUET) in partial fulfillment of the requirement for the degree of  
**MASTER OF PHILOSOPHY (M. Phil.) IN PHYSICS**

By

**Rummana Matin**

**Roll No: 100514010 F**

**Session: October, 2005**



**DEPARTMENT OF PHYSICS**  
**BANGLADESH UNIVERSITY OF ENGINEERING AND TECHNOLOGY (BUET)**  
**DHAKA- 1000, BANGLADESH**  
**MARCH, 2008**

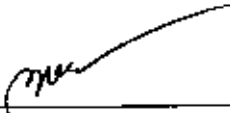

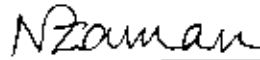

BANGLADESH UNIVERSITY OF ENGINEERING & TECHNOLOGY (BUET)  
DHAKA  
DEPARTMENT OF PHYSICS



**Certification of thesis work**

The thesis titled "*STUDY OF THE OPTICAL AND DC ELECTRICAL PROPERTIES OF PLASMA POLYMERIZED THIN FILMS OF DIETHYLANILINE*", submitted by **RUMMANA MATIN**, Roll No: 100514010F, Registration No: 1005370, Session: October-2005, has been accepted as satisfactory in partial fulfillment of the requirement for the degree of **Master of Philosophy ( M.Phil.) in Physics** on **30 March, 2008**.

**BOARD OF EXAMINERS**

1.   
\_\_\_\_\_  
**Dr. Md. Abu Hashan Bhuiyan** (Supervisor) Chairman  
Professor  
Department of Physics, BUET, Dhaka
2.   
\_\_\_\_\_  
**Dr. Md. Feroz Alam Khan** (Ex-Officio) Member  
Head, Department of Physics  
BUET, Dhaka
3.   
\_\_\_\_\_  
**Dr. Nazma Zaman** Member  
Professor  
Department of Physics, BUET, Dhaka
4.   
\_\_\_\_\_  
**Prof. Dr. R. I. M. A. Rashid** Member (External)  
Department of Physics  
University of Dhaka, Dhaka

## **Candidate's Declaration**

**It is hereby declared that this thesis or any part of it has not been submitted elsewhere for the award of any degree or diploma.**

Signature of the candidate

*Rummana Matin*

(Rummana Matin)

Roll no: 100514010 F

Session : October, 2005.

## Contents

Declaration	i
Dedication	ii
List of Figures	v
List of Tables	viii
Glossary	viii
Acknowledgements	x
Abstract	xii
<b>CHAPTER 1</b>	<b>INTRODUCTION</b>
<b>1.1. Introduction</b>	1
<b>1.2. Review of Earlier Research Work</b>	3
<b>1.3. Objectives of the Present Study</b>	10
<b>1.4. Thesis Layout</b>	11
References	11
<b>CHAPTER 2</b>	<b>FUNDAMENTAL ASPECTS OF PLASMA, POLYMER, AND PLASMA POLYMERIZATION</b>
<b>2.1. Introduction</b>	16
<b>2.2. Plasma</b>	16
<b>2.3. Polymer</b>	17
2.3.1. Classification based upon different factors related to polymers	17
2.3.2. Crystalline and amorphous states of polymer	18
2.3.3. Classification based upon polymerization mechanism	20
2.3.4. Cross-link in polymers	23
<b>2.4. Plasma Polymerization</b>	23
2.4.1. Control parameters of plasma polymer thin film properties	25
2.5.2. Overall reactions and growth mechanism in plasma polymerization	26
<b>2.6. Glow Discharge</b>	29
2.6.1. DC Glow Discharges	30
2.6.2. AC and RF glow discharges	32
2.6.3. Different variants to glow discharge plasmas	33

<b>2.7. Some characteristic differences of plasma polymers from the conventional polymers</b>	33
References	34
<b>CHAPTER 3            EXPERIMENTAL DETAILS</b>	
<b>3.1. Introduction</b>	36
<b>3.2. The Monomer</b>	36
<b>3.3. Substrate Material and its Cleaning Process</b>	37
<b>3.4. Capacitively Coupled Plasma Polymerization Set-up</b>	37
<b>3.5. Generation of Glow Discharge Plasma in the Laboratory</b>	40
<b>3.6. Deposition of Plasma Polymerized Thin Film</b>	41
<b>3.7. Contact Electrodes for Electrical Measurements</b>	42
<b>3.8. Measurement of Thickness of the Thin Films</b>	43
<b>3.9. Multiple-Beam Interferometry</b>	44
References	46
<b>CHAPTER 4            STRUCTURAL ANALYSES OF PPDEA</b>	
<b>4.1. Introduction</b>	47
<b>4.2. Scanning Electron Microscopy (SEM)</b>	47
4.2.1. Theoretical background	48
4.2.2. Energy Dispersive X-ray (EDX) analysis	49
4.2.3. Experimental procedure	50
4.2.4. Results and discussion	50
<b>4.3. Infrared Spectroscopy</b>	55
4.3.10. Results and discussion	61
References	64
<b>CHAPTER 5            UV-VIS SPECTROSCOPY OF PPDEA</b>	
<b>5.1 Introduction</b>	66
<b>5.2. Ultraviolet Visible Optical Absorption Spectroscopic Analysis</b>	66
5.2.1. UV-vis spectrophotometer	67
5.2.2. The Beer-Lambert law	69
5.2.3. Electronic transitions	69

5.2.4. Absorbing species containing $\pi$ , $\sigma$ , and $n$ electrons	71
5.2.5. Direct and indirect optical transitions	73
<b>5.3. Experimental Procedure</b>	74
<b>5.4. Results and Discussion</b>	74
References	78

## **CHAPTER 6 DC ELECTRICAL PROPERTIES OF PPDEA**

<b>6.1 Introduction</b>	79
<b>6.2. DC Electrical Conduction Mechanism</b>	79
6.2.1. Schottky Mechanism	80
6.2.2. Poole-Frenkel mechanism	82
6.2.3. Space charge limited conduction (SCLC) mechanism	84
<b>6.3. Thermally activated conduction processes</b>	86
<b>6.4. Experimental Procedure</b>	88
<b>6.5. Results and Discussion</b>	90
6.5.1. Current density-voltage (J-V) characteristics	90
6.5.2. Temperature dependence of current	96
References	99

## **CHAPTER 7 CONCLUSIONS**

<b>7.1 Conclusions</b>	101
<b>7.2 Suggestions for Further Research</b>	102

### **List of Figures**

2.1 Crystalline and amorphous states of polymer.....	18
2.2 Disordered region in amorphous polymer .....	19
2.3 Network structure of (a) thermoplastic, (b) thermoset, (c) elastomer .....	20
2.4 Block Copolymer, Graft Copolymer, Random Copolymer.....	23
2.5 Competitive ablation and polymerization	
scheme of glow discharge polymerization.....	24
2.6 Plasma polymerization reactor.....	25
2.7 General hierarchy for the production of active species in molecular gas plasma ...	27

2.8 Schematic representation of bicyclic step-growth mechanism in plasma polymerization.....	29
2.9 Schematic representation of the basic processes in a glow discharge.....	30
2.10 Normal glow discharge; (a) the shaded areas are luminous, (b) distribution of potential among luminous zones.....	31
3.1 The structure of 2,6 diethylaniline .....	36
3.2 Schematic diagram of the plasma polymerization set-up.....	37
3.3 Plasma polymerization set-up in laboratory .....	38
3.4. Glow discharge in laboratory.....	40
3.5. Glow discharge plasma during deposition.....	41
3.6 Electrode assembly.....	43
3.7. Samples for electrical measurement (2 samples from left) and for thickness measurement (sample on right).....	43
3.8. Multiple Beam Interferometric set-up in laboratory.....	44
3.9. Interferometer arrangement for producing reflection Fizeau fringes of equal thickness .....	45
4.1 Schematic diagram of a scanning electron microscope .....	47
4.2 Phenomena occurring in scanning electron microscope .....	48
4.3 Micrographs of PPDEA thin films onto glass substrate (magnification 500x) (a) $d = 250$ nm (b) $d = 350$ nm.....	51
4.4 Micrographs of PPDEA thin films onto glass substrate (magnification 6.00kx) (a) $d = 250$ nm (b) $d = 350$ nm .....	52
4.5 Micrographs of PPDEA thin film ( $d=350$ nm) onto glass substrate (a)magnification 12.0 k (b) magnification 35.0 kx.....	53
4.6 EDX spectrum and weight percentages of PPDEA thin films.....	54
4.7. Different vibrational modes .....	56
4.8 Infrared spectroscopy correlation Table.....	57
4.9 Molecular responses to radiation .....	58
4.10 Schematic diagram of a double beam infrared spectrometer .....	61
4.11 The IR spectra of DEA monomer, spectrum M and PPDEA, spectrum P.....	62
5.1 Schematic of an uv-vis spectrophotometer.....	67
5.2 Vibrational and rotational energy levels of absorbing materials.....	71
5.3 Electronic transitions in different energy level.....	71

5.4 Examples of $\pi \rightarrow \pi^*$ Excitation.....	72
5.5 Variation of absorbance (ABS) with wavelength, $\lambda$ for PPDEA thin films of different thicknesses. (inset: DEA monomer).....	76
5.6 Plot of absorption co-efficient, $\alpha$ , as a function of photon energy, $h\nu$ , for PPDEA thin films of different thicknesses .....	76
5.7 $(\alpha h\nu)^{1/2}$ vs. $h\nu$ curves for PPDEA thin films of different thicknesses .....	77
5.8 $(\alpha h\nu)^2$ vs. $h\nu$ curves for PPDEA thin films of different thicknesses .....	77
6.1 Schottky effect at a neutral contact.....	81
6.2 Poole-Frenkel effect at a donor center.....	83
6.3. Energy diagram for different regions under space charge limited conduction mechanism.....	84
6.4. Space charge limited conduction characteristic for an insulator containing shallow traps.....	86
6.5 Diagram of electron-transfer mechanisms between adjacent sites separated by a potential-energy barrier.....	88
6.6 A schematic circuit diagram of DC measurements.....	89
6.7 Arrangement for DC measurement.....	89
6.8 log J-log V plot for PPDEA thin film at different temperatures ( $d = 400$ nm).....	92
6.9 log J-log V plot for PPDEA thin film at different temperatures ( $d = 300$ nm).....	92
6.10 log J-log V plot for PPDEA thin film at different temperatures ( $d = 250$ nm).....	93
6.11 log J-log V plot for PPDEA thin film at different temperatures ( $d = 150$ nm).....	93
6.12 Plots of log J-log d for PPDEA thin films in the non-Ohmic region.....	94
6.13 ln J vs. $V^{1/2}$ at room temperature for PPDEA thin films of different thicknesses.....	94
6.14 ln J vs. $V^{1/2}$ at different temperatures for a PPDEA thin film ( $d = 150$ nm) .....	95
6.15 Plots of ln J vs $d^{1/2}$ for PPDEA thin films at higher voltage region.....	95
6.16 Plots of Current density vs. inverse of absolute temperature for PPDEA thin film in Ohmic and non-Ohmic regions ( $d = 400$ nm).....	97
6.17 Plots of Current density vs. inverse of absolute temperature for PPDEA thin film in Ohmic and non-Ohmic regions ( $d = 300$ nm).....	97
6.18 Plots of Current density vs. inverse of absolute temperature for PPDEA thin film in Ohmic and non-Ohmic regions ( $d = 250$ nm).....	98
6.19 Plots of Current density vs. inverse of absolute temperature for PPDEA thin film in Ohmic and non-Ohmic regions ( $d = 150$ nm).....	98



## List of Tables

2.3.1 Classification based upon different factors related to polymer.....	18
3.1 General properties of 2,6 diethylaniline.....	36
4.1 EDX spectrum and weight percentages of as deposited PPDEA thin film.....	54
4.2 Assignments of IR absorption peaks for DEA and PPDEA.....	63
5.1 The optical parameter of thin films of PPDEA.....	75
6.1 The slopes in the two voltage regions at different temperatures for samples of different thicknesses.....	90
6.2 Comparison of experimental and theoretical $\beta$ co-efficient.....	91
6.3 Values of activation energy $\Delta E$ (eV) for PPDEA thin films of different thicknesses.....	96

## Glossary

ABS	Absorbance
AC	Alternating Current
Al	Aluminum
Cr-Al	Chromel-Alumel
CBD	Chemical Bath Deposition
cc	Capacitively Coupled
CRT	Cathode-ray tube
d	Sample Thickness
DC	Direct Current
DEA	2,6 Diethylaniline
DSC	Differential Scanning Calorimetry
DTA	Differential Thermal Analysis
$E_g(d)$	Direct transition energy gap,
$E_g(i)$	Indirect transition energy gap,
FL	Fermi Level
FTIR	Fourier Transform Infrared
I	Current
J	Intensity of Radiation
IR	Infrared



k	Boltzmann Constant
k	Extinction Co-efficient
MHz	Mega Hertz
PECVD	Plasma Enhanced Chemical Vapor Deposition
PPDEA	Plasma Polymerized 2, 6 Diethylaniline
PPDP	Plasma-polymerized Diphenyl
PPm-X	Plasma-Polymerized m-Xylene
PPPA	Plasma-Polymerized Polyaniline
PVD	Physical Vapour Deposition
rf	Radio Frequency
SCLC	Space Charge Limited Conduction
SEM	Scanning Electron Microscopy
$T_g$	Glass Transition Temperature
$T_m$	Melting Point
TGA	Thermo Gravimetric Analysis
TSDC	Thermally Stimulated Depolarization Current
UV-vis	Ultraviolet-Visible
V	Voltage
XPS	X-ray Photoelectron Spectroscopy
$\alpha$	Absorption Coefficient
$\beta_{exp}$	Experimental $\beta$ Co-efficient
$\beta_S$	Schottky Co-efficient
$\beta_{PF}$	Poole-Frenkel Co-efficient
$\phi$	Columbic barrier height of the electrode polymer interface
$\phi_c$	Ionization potential of the PF centers
$\lambda$	Wavelength
$\Delta E$	Activation Energy
$\sigma$	Electrical Conductivity
$\epsilon$	Dielectric Constant
$\epsilon_0$	Permittivity of Free Space
$\mu$	Mobility of Charge Carrier
$\theta$	Trapping Factor

## Acknowledgements

I would like to express my sincere thanks and gratitude to my respected supervisor Dr. Md. Abu Hashan Bhuiyan, Professor, Department of Physics, Bangladesh University of Engineering and Technology (BUET) for his kind cooperation, encouragement, and proper guidance to carry out the thesis work. I am immensely grateful to my supervisor for making me familiar with the interesting field of plasma deposition and processing of the present-time research activities.

I am grateful to Prof. Dr. Md. F. A. Khan, Head, Department of Physics, Bangladesh University of Engineering and Technology (BUET), for providing the research facilities available in the department.

I would like to extend my thankfulness to Prof. Dr. M. Huq, Prof. Dr. J. Podder, Prof. Dr. N. Zaman, Dr. A. K. M. A. Hossain, Dr. Md. M. Hossain, Dr. Md. Nazrul Islam, Mrs. F. Khanam, Mrs. Afia Begum, and Dr. Md. F. Mina for their inspiration throughout the research work.

I am grateful to Head, Department of Materials and Metallurgical Engineering for allowing me to take the Scanning Electron Microscopy of my samples. I am also thankful to Mr. Md. Yousuf Khan of the same department for giving me assistance to carry out the SEM and EDX.

My sincere thanks to Dr. M. A. Gafur, Research Engineer, PP & PDC and the authority of the Bangladesh Council of Scientific and Industrial Research (BCSIR), Dhaka, for giving me the opportunity to take the Ultraviolet-visible (UV-vis) spectra.

Mr. Sudhandshu Kumar Roy, Principle Scientific Officer, chemical research division, BCSIR, Dhaka, and Mr. S. M. Mahmudul Hassan, Scientific Officer of the same division, deserve my thankfulness for giving me opportunity to accomplish the Infrared spectroscopy.

I am also grateful to Dr. Tofazzal Hossain, Principle Scientific Officer, Industrial Physics Division, BCSIR, Dhaka, for permitting me to verify the SEM and EDX results.

I would like to give special thanks to Mr. Rama Bijoy Sarker, Ms. H. Akther, Ms. Tamanna Afroze, Ms. Sharmin Seema Ms. Nasima Banu, Ms. Hosne Ara, Mr. Ali Ashraf, Mr. Md. Maidul Islam, Mr. M. Jellur Rahman, Lecturer, Department of Physics (BUET), Md. Raquibul Islam Lecturer, Department of Physics (BUET), all the newly appointed Lecturers and other post graduate students in our laboratory for their help and support.

I am thankful to all staff members of the department of physics, BUET for their co-operation.

I am thankful to the authority of Bangladesh University of Engineering and Technology (BUET), for providing me the financial grant.

I am ever grateful to my father, mother, brother and all of my friends for their continued encouragement and moral support during research work.

Finally, I do express my heartiest gratitude to almighty Allah for giving me patience and courage to complete the work.

## Abstract

Plasma polymerized organic thin films have recently attained considerable attention due to their extensive application in the fields of electronics, optics. Our present investigation aims at to study the dc electrical conduction mechanism from the voltage, thickness and temperature dependent current density measurements and structure-property relation of plasma polymerized 2, 6, diethylaniline (PPDEA) thin film. The uniform, pinhole-free PPDEA thin films were deposited at room temperature onto glass substrates by a parallel plate capacitively coupled glow discharge reactor. The thicknesses of the films were measured by Multiple Beam Interferometric method. The structure, surface morphology, and compositions of PPDEA thin films were characterized by scanning electron microscopy (SEM), energy dispersive X-ray (EDX) analysis, and Infrared (IR) spectroscopy. The optical properties of the thin films were investigated by Ultraviolet visible (UV-vis) absorption spectroscopic analysis.

In SEM analysis, a smooth, flawless and pinhole free surface was observed for PPDEA thin films. No significant change was observed in PPDEA thin films of different thicknesses. The EDX analysis indicated the presence of C, N and O in the samples. The presence of O in PPDEA which is not present in DEA implies incorporation of carbonyl and hydroxyl groups through the reaction of the free radicals. IR analysis reveals that the PPDEA thin film deposited by plasma polymerization technique does not exactly resemble to that of the DEA monomer and the presence of carbonyl group is detected. The absorption coefficient  $\alpha$ , at various wavelengths was calculated using the UV-vis data. The direct transition energy  $E_{g(d)}$  and indirect transition energy  $E_{g(i)}$  were obtained by extrapolating the linear portion of the plots of  $(\alpha hv)^2$  vs  $hv$  and  $(\alpha hv)^{1/2}$  vs  $hv$  respectively to intercept the photon energy axis. The current density-voltage (J-V) characteristics of PPDEA thin films of different thickness have been studied at different temperatures. In the low voltage region, the conduction current obeys Ohm's law while the charge transport phenomenon appears to be electrode limited Schottky type conduction in the higher voltage region. The temperature dependence of the current density for different bias voltages was also investigated. From the arrhenius plots of  $J$  vs.  $1/T$ , it is found that the activation energies ( $\Delta E$ ) decrease as the bias voltage increases. The activation energies are about  $0.10 \pm 0.03$  eV and  $0.20 \pm 0.05$  eV at the lower temperature region and about  $0.69 \pm 0.06$  eV and  $0.63 \pm 0.03$  eV at the higher temperature region for 8 and 14 V respectively. The low activation energy in the low temperature region and the higher activation energy in the higher temperature region may be attributed to a transition from a hopping regime to a regime dominated by distinct energy levels.

# **CHAPTER 1**

## **INTRODUCTION**

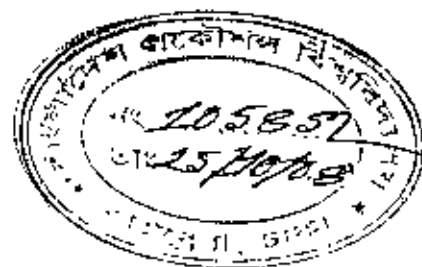
**1.1. Introduction**

**1.2. Review of Earlier Research Work**

**1.3. Objectives of the Present Study**

**1.4. Thesis Layout**

References



## 1.1. Introduction

Plasma polymerization is one of the modern techniques to deposit uniform, pinhole-free and flawless thin polymer film on any surface that is in contact with the plasma of the organic monomer. It is a unique and rather unconventional thin film technology which yields polymers having properties completely different from those of conventional polymers. The plasma polymer films have cross-linked structure and have good chemical and physical stability. So these are used in the areas where mechanical, thermal, and electrical strengths are necessary [1-3].

A variety of techniques for producing polymer thin films have been studied. Thin polymer thin films can be prepared in two ways: one includes wet processes like Langmuir-Blodgett, spreading, dipping, or solvent casting methods. The other is dry processing, such as physical vapor deposition (PVD) and chemical vapor deposition (CVD). Of these methods, plasma polymerization is frequently used to make polymer thin films [32-34]. The technique of most interest to plasma polymerization is the glow discharge, in which free electrons gain energy from an imposed electrical field, and subsequently loses it through collisions with neutral molecules in the gas. The transfer of energy to gas molecules leads to the formation of a host of chemically reactive species, some of which become precursors to the plasma polymerization reaction. Although the recognition of thin film formation by glow discharge polymerization can be traced back to 1874, and of chemical reactions in electrical discharges to 1868, systematic investigation of plasma polymerization began only in the 1960s.

Plasma polymers are deposited on surfaces contacting a glow discharge of organic or organometallic feed gases in the form of a thin film and /or as a powder. Plasma polymerization is a specific type of plasma chemistry, which involves reactions between plasma species, between plasma and surface species and between surface species. In the cases of a free radical mechanism, two types of reaction may be postulated: i) plasma induced polymerization and ii) plasma state polymerization. Plasma induced polymerization is the conventional free-radical induced polymerization of molecules containing unsaturated carbon-carbon bonds, while plasma state polymerization depends on the presence, in a plasma, of electrons and other species energetic enough to break any bond. A cursory survey of the literature concerning plasma polymerization reveals that due to the complexity of plasma the bulk of the research has been concentrated on establishing

the dependence of the macroscopic and spectroscopic properties of the product on the major process variables e.g. power, monomer type, gas flow rate, pressure etc.

Yasuda [2] proposed the CAP (Competition - Ablation - Polymerization) mechanism for glow discharge polymerization. Bell et al [7] by combining a certain number of kinetic modeling studies reported a model for the plasma polymerization of hydrocarbons. A more general description was given by Yasuda who identified two regimes of plasma polymerization in which the mechanisms differ dramatically i.e. the monomer - deficient and the energy deficient plasma.

Yasuda surveyed 28 monomers and found that monomers containing aromatic groups, nitrogen (e.g., -NH, -NH<sub>2</sub>, -CN), silicon and olefinic double bonds are more polymerizable while those containing oxygen (e.g. -C=O, -O-, -OH), chlorine, aliphatic hydrocarbon and cyclic hydrocarbon tend to decompose.

An increasing number of applications have been found for plasma polymerized thin films in a wide variety of fields. Several excellent papers of the optical, electrical and electrically conductive mechanism have been published. Most investigators studied the electrode and bulk limited conduction processes which are operative in these films. Simultaneously the optical properties such as direct or indirect transitions and refractive index have also been frequently reported.[5-35]

Plasma polymer films have been employed to increase the adhesion and compatibility in immiscible systems. Their good adhesion to metals, ceramics, and other polymers has potential applications to adhesion promoters, surface protective coatings, etc. For this reason many investigations were made on their morphological, structural and chemical properties.[36-47]

Electronic and photonic properties of polyaniline have attracted considerable research interest due to its potential applications in a wide range of fields. In our laboratory, investigations have been done on several plasma polymerized organic thin films including N, N, 3, 5 tetramethyl aniline thin film. Reviewing the early research work it was found that DC electrical and structural investigations on 2,6 diethylaniline thin films have not yet been done. In the present research work, 2,6 diethylaniline thin film is prepared by using the plasma polymerization technique and their electrical and structural properties have been investigated.



## 1.2. Review of earlier research work

Plasma polymerization is a unique technique where uniform pinhole-free and flawless thin layer of polymer film is deposited on any surface that is in contact with the plasma of the organic monomer. Plasma polymerized films have molecular structures different from the conventional polymers. The most significant is that the plasma polymer films have cross linked structure so that these films are chemically and physically stable and used for the area in which mechanical, thermal, and electrical strengths are necessary [1,2,3].

Plasma polymers have many applications such as resist in Micro fabrication process, Electronic elements (thin film transistor, diode switching elements, dielectric sensors, and capacitors), opto-electronic devices (light guide material, optical fibers, photovoltaic energy converters, photodiodes, optical coatings to inhibit corrosion) etc. [1].

Electrical conduction in polymers has been studied extensively during the last couple of decades to understand the nature of charge transport in these materials. Various mechanisms, such as Schottky emission, Poole-Frenkel emission, and Space-charge limited conduction have been suggested for the charge transport [4, 6]. The first of various electrically conductive polymers was polyacetylene. Other specialty polymers in this class that have been extensively studied includes polyaniline, polythiophene, poly(p-phenylene) and polypyrrole [5].

Plasma polymerized thin organic film gains increasing scientific interest for their remarkable optical and electrical properties. H. Akther and A. H. Bhuiyan [5,6] deposited plasma polymerized N, N, 3, 5 tetramethylaniline (PPTMA) thin film onto glass substrates at room temperature by a capacitively coupled plasma polymerization system. They reported from the IR spectroscopy, Elemental analysis (EA), and UV-vis spectroscopy that this film contains more conjugation as compared to the monomer. The  $\pi$ - $\pi^*$  transition in PPTMA thin film demonstrated the presence of an increased degree of conjugation in the resulting films for different thickness and its current density-voltage (J-V) characteristics indicated the space charge limited conduction. Electrical and optical measurements suggested that the top of valance band and the bottom of the conduction band may have gap states and the middle of the energy gap may be equal to the high-temperature activation energy. F-U-Z Chowdhury and A. H. Bhuiyan [7] investigated the optical properties and chemical structure of plasma polymerized diphenyl (PPDP) thin films. The IR spectroscopic analysis revealed that the structure of PPDP thin films are not structurally the same as that of the monomer and cyclization / aggregation by conjugation occurs in the PPDP structure on heat treatment which is partially relieved on aging. The band gap was

not affected appreciably by heat treatment whereas it is modified on aging. Mustari Zaman and A. H. Bhuiyan [8] deposited plasma polymerized tetraethylorthosilicate (PPTEOS) thin films by a capacitively coupled parallel plate glow discharge reactor. From EA and IR spectroscopic analysis they showed that the PPTEOS film deposited by the plasma polymerization technique does not exactly resemble to that of monomer tetraethylorthosilicate (TEOS) structure. From UV-vis spectroscopy it was found that the extinction co-efficient,  $K$ , on photon energy indicates the probability of electron transfer across the mobility gap, rises with the photon energy. Al-mamun, Islam and A. H. Bhuiyan [9] used a chemical bath deposition (CBD) technique for the preparation of thin films onto glass substrates and investigated structural, electrical and optical properties of these films and their studies revealed that the films with cubic structure show very low resistivity and optical absorption of the films result from free carrier absorption in the near infrared region. F-U-Z Chowdhury and A. H. Bhuiyan [10] investigated on plasma polymerized diphenyl (PPDP) films which were deposited using a capacitively coupled glow discharge reactor and showed that Poole-Frenkel mechanism was operative in the heat-treated PPDP films. A. H. Bhuiyan and A-B-M Shah Jalal [11] deposited plasma polymerized *m*-Xylene thin films using a capacitively coupled glow discharge reactor. From the I-V characteristics they found that Pool-Frenkel conduction mechanism was most probable in these films. N. Nagaraj et.al. [12] studied the I-V characteristics of doped polyvinyl films as a function of film temperature and dopant concentration and found that the dominant charge transport mechanism in this film is Schottky type. C. J. Mathai et.al. [13, 14] found the Schottky type conduction mechanism in Polyaniline thin films with asymmetric electrode configuration. They also prepared the radio frequency (rf) and ac plasma polymerized aniline thin films and found that the optical band gap of these films differ considerably and the band gap was further reduced by in situ doping of iodine. It has been shown that electrical conductivity of this film in the case of rf plasma polymerized thin films has a higher value compared to that of ac. Iodine doping enhanced conductivity of the polymer thin films considerably. Tamirisa et.al. [15] synthesized polyaniline thin films on several substrates positioned at various distance from the center of the coil of an inductively coupled pulsed-plasma reactor. FTIR spectroscopy results revealed that the chemical composition and structure of the films were very dependent on the substrate's position with respect to the rf coil. SEM studies indicated that as the films became thicker they developed nodules atop a somewhat smoother underlayer. The impedance measurements were consistent with relatively rough films possibly containing pinholes.

M. M. Nahass et.al. [16] reported the dependence of electrical conductivity (dc.ac) and dielectric properties on temperature and on frequency of thermally deposited thin films of N-(p-dimethylaminobenzylidene)-p-nitroaniline (DBN). The dc conductivity indicated a thermally activated carrier hopping rate which increased with increasing temperature. The obtained experimental results of ac conductivity showed that the correlated barrier hopping model is the appropriate mechanism for the electron transport in the DBN film. Both the dielectric constant and dielectric loss showed a decrease with increasing frequency. Several investigations were carried out on polypyrrole thin films. K. Rajan et.al. [17] found that iodine doping increased the conductivity of the film and decreased the optical band-gap energy. A comparative study of the IR spectra of the monomer and the polymer pyrrole gave information that the ring structure was retained during plasma polymerization. R. Valasky et.al. [18] demonstrated that the thickness strongly influences the electrical behavior in the electrodeposited polypyrrole (PPY) films. Thinner PPY films presented better morphological characteristics, which permitted higher charge carrier mobility. M. S. Silverstein et.al. [19] investigated structural, electrical, optical properties of plasma polymerized thiophene (PPT<sub>h</sub>) and found that the PPT<sub>h</sub> films differed from the monomer structure, the band gap for the PPT<sub>h</sub> films is similar to that for conventional PTh. Undoped films exhibited nonlinear I-V behavior typical of Schottky metal-semiconductor barrier with breakdown at reverse bias. Iodine doping yielded Ohmic I-V behavior. X. Zhao et.al. [20] investigated on the plasma polymerized 4-phenylbenzonitrile and FTIR, X-ray photoelectron spectroscopy (XPS) and Atomic force microscopy (AFM) characterizations on this film showed that the homogeneous film with a large  $\pi$ -conjugated system and high retention of aromatic ring structure was obtained when a low discharge power was used. A blue emission with relatively high photoluminescence intensity for thin films was observed. Xiao Hu et.al. [21] prepared plasma polymerized 4-cyanopyridine (PPCPD) thin films of desired thickness through plasma polymerization under different glow discharge conditions. The effect of the discharge power on this film was investigated by FTIR, UV-vis and XPS measurements. A high retention of aromatic ring structure of the starting monomer in the deposited plasma films was obtained when a low discharge power was used. A red shift in the maximum absorption wavelength for the films was observed as compared with the monomer absorption spectrum. The AFM showed that the PPCPD film with quite smooth surface could be grown under a relatively low discharge power. M.M. El-Nahas et.al. [22] investigated on physical characteristics of 4-tricyanovinyl-N, N-diethylaniline. The differential scanning calorimetry (DSC) showed

the stability of this compound up to 423 K. The temperature dependence of the electrical conductivity was found typical for semiconducting compounds. The J-V characteristics revealed that, the conduction current obeys Ohm's law while the charge transport phenomenon appears to be space-charge limited in the higher voltage region. S. Saravanan et.al. [23] prepared polyaniline thin films by employing an rf plasma polymerization technique. Measurements on capacitance, dielectric constant, dielectric loss and ac conductivity which were evaluated in the frequency range 100 Hz - 1 MHz showed that the capacitance and dielectric loss decreased with increase of frequency and increased with increase of temperature. The ac conductivity was calculated from the observed dielectric constant and was explained based on the Austin - Mott model for hopping. The FTIR studies revealed that the aromatic ring is retained in the polyaniline, thereby increasing the thermal stability. T. Liang et.al. [24] demonstrated the effect of film thickness on the electrical properties of polyimide thin films. With decreasing film thickness, the dielectric constant decreased but the conduction current increased. Using IR spectroscopy, polyimide chains were found to be oriented parallel to the electrodes. The dependence of the dielectric constants on film thickness was explained by the orientation of polymer chains. X. Y. Zhao et.al. [25] characterized the plasma polymerized 1-Cyanoisoquinoline thin films. From IR, XRD and SEM studies it was found that a high retention of aromatic ring structure of the starting monomer was found in the films. As the films were homogeneous it was used for dielectric measurements and it showed a low dielectric constant which was obtained for this film for the first time. M. Campos et.al. [26] saw the influence of methane in the electrical properties of polypyrrole films doped with dodecylbenzene sulfonic acid. Measurements on dc electrical current and capacitance as a function of voltage revealed that a metal with low work function could be used to form a non-ohmic contact with doped polypyrrole (PPy). The junction parameter, the saturation current density and the ideality current factor were influenced by the methane gas. The response to methane was in agreement with those for Schottky diodes using a thermionic emission theory. The interaction of the PPy with methane was explained by changes in the Schottky barrier height and in the carrier concentration of the diodes which were confirmed by capacitance-voltage measurements. F. Brovelli et.al. [27] synthesized 1-furfuryl pyrrole thin films and characterized them. The surface morphology showed a high coverage efficiency of the deposition process. I-V characteristics on Indium tin oxide/polymer/Al structures exhibited a turn-on voltage of 0.70 V. The charge injection mechanism in this structure was related to a Fowler-Nordheim tunneling effect.

F. Yukuphanoglu [28, 29] determined the optical band gap, refractive index, optical absorption properties, type of optical transitions, extinction co-efficient, and dielectric constant of some organic thin films. For some organic thin films it was found that the absorption spectra mechanism is due to both direct and indirect transition. The Urbach energies were calculated and it was found that the refractive index values were decreased with wavelength. Jinmo Kim et.al. [30] did a quantitative analysis of the surface density of amine groups on a plasma polymerized ethylenediamine thin film deposited on a platinum surface using inductively coupled plasma chemical vapor deposition method. They showed that the chemical derivatization in FT-IR spectroscopy is a useful way of quantifying the surface density of amine groups on PPEDA films. After a comparative analysis they indicated that chemical derivatization in all three independent surface sensitive analysis tools (FT-IR, UV-vis, XPS) can be used to quantify surface amine density. Tsuyoshi Michinobu et.al. [31] investigated the optical and electrochemical properties of carbazole containing donor-acceptor (D-A) type conjugated polymers by acceptor moieties and  $\pi$  spacer groups. They found that copolymerization with a stronger electron acceptor leads to more efficient intermolecular D-A coupling, which was evaluated by the optical absorption spectra of the charge transfer band as well as the electrochemical oxidation potential. S.H. Cho L. S. Bae, M. L. Kim et.al. [32-34] deposited polymer like organic thin films at room temperature and different radio-frequency powers by PECVD method using ethylcyclohexene as precursor. In this study, they especially compared the difference of corrosion resistant and optical properties of plasma polymerized organic thin films grown at various rf powers. The protective efficiency, crosslinking density, optical refractive index and contact angle increased with increasing rf power. AFM and SEM data showed quite smooth and dense surface morphology with increasing rf power. Another preparation with methylcyclohexane and ethylcyclohexane as organic precursors and hydrogen and Ar as a bubbler and carrier gas indicated that as the plasma power was increased, the contact angle, refractive index, and main absorption peak of thin films were increased while the optical transmittance was decreased, signifying that the plasma polymerized organic films have more low surface energy with increasing rf power. The Uv-vis spectra showed an energy band gap shift from 3.78 to 4.02 eV with increasing rf power. X. Y. Zhao et.al. [35] studied the effect of discharge power on the chemical structure and surface compositions of plasma-prepared poly (4-biphenylcarbonitrile) (PBPCN) thin films using FTIR, UV-vis and XPS. The results showed that a large  $\pi$  conjugated system can be formed in the PBPCN thin films at

low plasma discharge power of 30 W, and the plasma polymerization of 4-biphenylcarbonitrile monomer took place mainly through the opening of the  $\pi$  bonds of the  $C\equiv N$  functional group. A high discharge power of 50 W brought about more severe molecular (aromatic ring) fragmentation and thus the conjugation length of PBPCN films decreases due to the formation of non-conjugated polymer. Wu Li-guang et.al. [36] deposited 1,1,1-trifluoroethane thin film using a parallel plate plasma reactor. The chemical structure of this film was analyzed by FTIR and XPS which showed that the polymerization was divided into two regions: energy deficient and monomer deficient. The deposition rate of the film increased with an increase of W/Fm, reached a maximum value and then decreased. Tamirisa et.al. [37] deposited hydrogel films of N-isopropylacrylamide in a parallel plate capacitively coupled rf plasma reactor. Chemical bonding structures in these films were studied using FTIR and the thermo responsive nature of the film was confirmed through contact angle geometry. A reversible temperature dependent contact angle change was observed. A. K. M Farid ul Islam et.al. [38] studied the effects of temperature on electrical transport properties on spray deposited  $MnO_2$  thin films which revealed that the samples were non-degenerate n-type semiconductors and the transport properties were interpreted in terms of Seto's model which was proposed for polycrystalline semiconducting films. Hidenobu Aizawa [39] prepared plasma polymerized tert-butylacrylate (pp-t-BA) film using tert-butylacrylate monomer under 100pa of vapor pressure with varying rf power of 10-250W and continuous wave rf power of 13.56 MHz. Deposition amounts of this film were measured using QCM (quartz crystal microbalance) technique during polymerization. They showed that the deposition rates of pp-t-BA film were proportional to the polymerization time at 100pa of monomer pressure under the same rf power and increasing the rf power on plasma polymerization, decreased the amount of ester groups in pp-t-BA films. The FT-IR, XPS characterizations on these film suggested that some ester groups in pp-t-BA might decomposed during plasma polymerization. J. Stejskal et.al. [40] exposed polyaniline to iodine in an ethanol-water suspension. Polyaniline (PANI) base reacted with iodine and its conductivity increased by five orders of magnitude. The FTIR results showed that the increase in conductivity was due to protonation of PANI with the hydriodic acid that was produced in the oxidation of the emeraldine base to the pernigraniline form.

B. Despax et.al. [41] deposited polysiloxane thin films containing silver particles by an rf asymmetrical discharge. The presence of silver in the gas phase was detected by optical

emission spectroscopy. The FTIR spectra revealed the presence of Si-O-Si, Si-C-Si, SiCH<sub>3</sub> and C=C groups whose amount varied with the silver content. Transmission electron micrograph (TEM) analysis showed Ag nanoparticles with sizes varying from 4 to 70 nm depending on the silver volume fraction. E. Vassallo et.al. [42,43] deposited thiophene-like films by Plasma enhanced chemical vapor deposition (PECVD) in pulse mode using 3-methyl-thiophene as monomer and investigated by varying the rf peak powers in the range of 30-120 W. XPS and FT-IR showed thiophene-like structural properties. The energy gap decreased from 2.69 to 1.86 eV with increase in rf plasma power and showed semiconductive polymer properties. They also used XPS, IR and electrochemical methods to characterize the plasma deposited SiO<sub>x</sub> thin films for iron coatings with corrosive resistance capabilities. The IR spectroscopic analysis revealed that the increase of power in the glow discharge resulted in the formation of CO<sub>x</sub> gaseous species and of higher oxidized silicon species in the film. A major oxygen content in plasma phase produced more inorganic compact and cross-linked films, with anticorrosive properties. R. Clergereaux et.al. [44] studied the effects of oxygen plasma post-treatment by dc and microwave (mw) processes on plasma polymerized hexamethyldisiloxane (PPHMDSO) layers was compared in terms of post-treated layer thickness, composition, structure and properties. It was found that mw processes were more effective than dc due to the differences in the density of the obtained coatings (the oxygen diffusion coefficient decreases when the film density increases and the reaction rate is linked to the film structure). Furthermore the PPHMDSO film properties, such as band gap energies, refractive index, wettability and hardness, change with the oxygen post-treatment. V. Cech et.al. [45] deposited plasma polymer thin films on silicon wafer using an rf glow discharge operated in pulsed mode. Microscopic and spectroscopic technique revealed that physico-chemical properties of plasma polymer depend on the effective power used if the flow rate was constant. The deposition rate and surface roughness of films varied with the rf power. The refractive index and extinction coefficient increased with rf power. H. L. Luo et.al. [46] did the plasma polymerization of styrene with carbon dioxide under glow discharge conditions. The XPS and FTIR studies revealed that chemical composition of the plasma polymerized films was different from that of the thermal polymerized film and the oxygen content on the plasma polymerized films increased with the flow rate of CO<sub>2</sub>. Furthermore the presence of oxygen containing groups on the surface of films was confirmed. It was also found that the composition and morphology of the plasma polymerized films were controlled by the flow rate of CO<sub>2</sub>. R. Jafari et.al. [47] deposited plasma polymerized

acrylic acid (PPAA) coating on polyethylene films, in a 70 kHz low pressure plasma reactor at various plasma powers. The COOH retention of PPAA coatings and its stability to washing in water were investigated by XPS, water contact angle (WCA), FTIR, ellipsometry and SEM analysis. The results showed that the use of higher powers leads to an increase of stability of the coating due to a high degree of cross-linking. Optical emission spectroscopy (OES) measurements showed good correlation between the CO density in the gas phase and the carboxylic content of PPAA coating.

### 1.3. Objectives of the Present Study

The objectives of this work are to prepare thin film of 2, 6 diethylaniline (DEA) by well established glow discharge polymerization technique and characterizing those using different physical techniques. To get the desired sample deposition the plasma process parameters would be controlled properly. The structure, absorption coefficient, optical energy gaps, direct, and indirect transitions, dc electrical conduction mechanism of the plasma polymerized 2, 6 diethylaniline (PPDEA) would be investigated. Finally, the structure - property relation of the thin films would be analyzed with a view to find its suitability in electrical and optical devices.

Scanning electron microscopic (SEM) and an Energy Dispersive X-ray (EDX) analysis would be done to investigate the surface morphology and compositional analysis of PPDEA thin films.

The chemical structure of the DEA monomer and PPDEA thin film would be investigated by Infrared (IR) spectroscopy. A comparative study between the two spectra would be done to ascertain the chemical changes occurred in PPDEA thin film in contrast to the monomer DEA.

The Ultra-violet-Visible (UV-vis) optical absorption spectroscopic analysis would be done to determine the absorption coefficient, direct and indirect transition energy gaps in PPDEA thin films.

In current-voltage measurements, the variation of current with temperature at different applied voltages of samples of different thicknesses will be measured to specify the charge transport mechanism in the plasma polymerized 2, 6 diethylaniline thin film.



## 1.4. Thesis Layout

The thesis is comprised of seven chapters which includes following contents.

Chapter 1 presents the introduction, review of some earlier and recent work of interest, objectives of the present study.

Chapter 2 gives a brief discussion on plasma, classification of polymers, plasma polymerization, reaction and growth mechanism in plasma polymerization, different types of glow discharge, some characteristic differences of plasma polymers from the conventional polymers etc.

Chapter 3 describes about the monomer and the experimental details of plasma polymerization which have been done in the laboratory.

Chapter 4 contains the experimental procedure, results and discussion of scanning electron microscopy, energy dispersive X-ray analysis and infrared spectroscopic analysis which are done on PPDEA thin films.

Chapter 5 includes the experimental procedure, results and discussions of Ultra violet visible absorption spectroscopic analysis on PPDEA thin films.

Chapter 6 involves the brief description of dc conduction mechanisms, which are generally operative in plasma polymerized thin films. The nature of J-V characteristics and temperature dependence of current of PPDEA thin films are included in this chapter.

Chapter 7 finally gives the conclusions and suggestions of future research work.

## References

- [1] Riccardo d'Agostino (Ed.), 'Plasma Deposition, Treatment and Etching of Polymers' Academic Press, Boston (1990).
- [2] Yasuda H., 'Plasma Polymerization', Academic Press, Inc, New York (1985).
- [3] Joel R. Fried, 'Polymer Science and Technology' Printic, Hall of India PV. LTD. New Delhi, (2002).
- [4] Morita S. and Hattori S., in 'Application of plasma polymers in Plasma Deposition Treatment and Etching of polymers' Ed. Riccardo d'Agostino, Academic Press. San Diego. CA, USA, (1990).
- [5] Akther H. and Bhuiyan A. H., 'Infrared and ultra violet- visible spectroscopic investigation of plasma polymerized N, N, 3, 5,-tetramethylaniline thin films', Thin Solid Films, 474, 14-18,(2005).
- [6] Akther H. and Bhuiyan A. H., 'Electrical and optical properties of plasma polymerized N, N, 3, 5,-tetramethylaniline thin films', New J. Phys. 7. 173, (2005).

- [7] Shen M., Bell A T., 'Plasma polymerization', American Chemical Society, (1979).
- [8] Zaman M., Bhuiyan A.H., 'Optical properties of plasma polymerized Tetraethylorthosilicate thin films. Bangladesh J. Phys. **2(1)**, 107-113, 2006.
- [9] Al-Mamun, Islam A.B.M.O, Bhuiyan A.H. 'Structural Electrical and Optical properties of copper selenide thin films deposited by chemical bath deposition technique'. J. of Materials for Electronics. **16**,263-268, (2005).
- [10] Chowdhury F-U-Z, Bhuiyan A. H., 'The DC electrical conduction mechanism of heat-treated plasma polymerized diphenyl thin films', Indi. J.Phy. **76**, 239-244,(2002).
- [11] Bhuiyan A. H. Shah Jalal A.B.M, Ahmed S., Ibrahim M. , 'On the conduction mechanism in plasma polymerized m-xylene thin films' Thin solid films, **295**, 125-130, (1997).
- [12] Nagaraj N., Subba Reddy Ch. V., Sharma A. K., Narasimha Rao V. V. R. 'DC conduction mechanism in polyvinyl alcohol films doped with potassium thiocyanate' J. Power Sources, **112**, 326-330, (2002).
- [13] Mathai C. J., Saravanan S., Jayalekshmi S., Venkatachalam S., Anantharaman M. R., 'Conduction mechanism in plasma polymerized aniline thin films', Mater. Lett, **57**, 2253-2257, (2003).
- [14] Sajeev U. S., Mathai, C. J., Saravanan S, Ashokan R, Venkatachalam S., Anantharaman M. R., 'On the optical and electrical properties of rf and a.c. plasma polymerized aniline thin films', Bull. Mater. Sci., **29**, No.2 (2006).
- [15] Tamirisa Prabhakar A., Liddell KNona C., Pedrow Patric D., Osman. Mohammed A. 'Pulsed-plasma-polymerized aniline thin films'. J. Appl. Polym. Sci., **93**, 1317-1325 (2004).
- [16] El-Nahass M. M., Zeyada H. M., El-Samanoudy M. M., El-Menyawy E. M., 'Electrical conduction mechanisms and dielectric properties of thermally evaporated N-(p-dimethylaminobenzylidene)-p-nitroaniline thin films'. J. Phys. Condens Mat., **18**, 5163-5173, (2006).
- [17] Johan R. K. Sakthi Kumar D. 'Structural, Electrical, and Optical studies of plasma polymerized and iodine-doped polypyrrole'. J. Appl. Polym. Sci. **83**, 1856-59, (2002).
- [18] Valasky R., Ayoub S., Micaroni L., Hummelgen I. A. , 'Influence of film thickness on charge transport of electrodeposited polypyrrole thin films' Thin Solid Films. **415**, 206-210, (2002).
- [19] Silverstein M. S., Visoly-Fisher I., 'Plasma polymerized thiophene: molecular structure and electrical properties'. Polymer **43**, 11-20, (2002).

- [20] Zhao X. Wang, M. Xiao, J. 'Deposition of plasma conjugated polynitrile thin films and their optical properties'. *Euro. Poly. J.*, **42**, 2161-2167, (2006).
- [21] Hu Xiao, Zhao Xiongyan, Uddin A., Lee C. B. 'Preparation characterization and electronic and optical properties of plasma polymerized nitriles', *Thin Solid Films*, **477**, 81-87, (2005).
- [22] El-Nahass M. M., Abd-El-Rahman K. F., Darwish A. A. A., 'Electrical conductivity of 4-tricyanovinyl-N,N-diethylaniline' *Physica*, **B 403**, 219-223, (2008).
- [23] Saravanan S., Mathai C J., Venkatachalm S., 'Low k thin films based on r plasma-polymerized aniline', *New J. of Phy.*, **6**, 64, (2004).
- [24] Liang T., Makita Y., Kimura S., 'Effect of film thickness on the electrical properties of polyimide thin films', *Polymer*, **42**, 4867-4872, (2001).
- [25] Zhao X. Y., Wang M. Z., Wang Z., 'Deposition of plasma polymerized 1-Cyanoisoquinoline thin films and their dielectric properties', *Plasma Process Polym.*, **4**, 840-846, (2007).
- [26] Campos M., Simos F. R., Pereira E. C., 'Influence of methane in the electrical properties of polypyrrole films doped with dodecylbenzene sulfonic acid', *Sensors and Actuators*, **B 125**, 158-166, (2007).
- [27] Brovelli F., Rivas B. L., Bernede J. C., 'Synthesis of polymeric thin films by electrochemical polymerization of 1-furfuryl pyrrole. Characterization and charge - injection mechanism', *J. Chil. Chem. Soc.*, **52 No. 1**, (2007).
- [28] Yakuphanoglu F., Cukurovali A., Yilmaz I., 'Determination and analysis of the dispersive optical constants of some organic films', *Physia B* **351**, 53-58. (2004).
- [29] Yakuphanoglu F., Arslan M., 'The fundamental absorption edge and optical constants of some charge transfer compounds', *Optical Materials*, **27**, 29-37, (2004).
- [30] Kim Jinmo, Jung Donggeun, Park Yongsup, Kim Yongki, Won Moon Dae, Geol Lee Tae, 'Quantitative analysis of surface amine groups on plasma-polymerized ethylenediamine films using UV-visible spectroscopy compared to chemical derivatization with FT-IR spectroscopy, XPS and TOF-SIMS', *Appl. Surf. Sci.*, **253**. 4112-4118, (2007).
- [31] Michinobu T., Okoshi K., Osaka H., Kumazawa H., Shigehara K., 'Band gap tuning of carbazole- containing donor-acceptor type conjugated polymers by acceptor moieties and  $\pi$  spacer groups', *Polymer*, **49**, 192-199, (2008).

- [32] Cho S. H., Park Z. T., Kim J. G., Boo J. H., 'Physical and optical properties of plasma polymerized thin films deposited by PECVD method', *Surface and Coating Technology*, **174-175**, 1111-1115, (2003).
- [33] Bae L. S., Cho S. H., Kim Y., Boo J. H., 'Growth of plasma polymerized thin films by PECVD method and study of their surface and optical characteristics', *Surface and Coating Technology*, **193**, 142-146, (2005).
- [34] Kim M. C., Cho S. H., Hong B. Y., Kim Y. J., Yang S. H., Boo J. H., 'High rate deposition of plasma polymerized thin films using PECVD method and characterization of their optical properties', *Surface and Coating Technol.*, **169-170**, 595-599, (2003).
- [35] Zhao Xion-Yan, Wang Ming-Zhu, Zhang Bing-Zhu, Mao Lei, 'Synthesis, Characterization and nonlinear optical properties of plasma-prepared poly (4-biphenylcarbonitrile) thin films', *Polym. Int.*, **56**, 630-634, (2007).
- [36] Wu L., Zhu C., Liu M., 'Study on plasma polymerization of 1.1.1-trifluoroethene: deposition and structure of plasma polymer films'. *Desalination*, **192**, 234-240, (2006).
- [37] A. Tamirisa Prabhakar, Koskinen Jere, W. Hess Dennis. 'Plasma polymerized hydrogel thin films', *Thin Solid Films*, **515**, 2618-2624, (2006).
- [38] Farid ul Islam A. K. M., Islam R., Khan K. A., Yamamoto Yoshiyuki, 'Temperature effect on the electrical properties of pyrolytic  $MnO_2$  thin films prepared from  $H_3Mn(C_2O_4)_2 \cdot 4H_2O$ ', *Renewable Energy*, **32**, 235-247, (2007).
- [39] Aizawa Hidenobu, Kawashima Shoji, Kurosawa Shigeru, Noda Kazutoshi, Fujii Takayoshi, Hirata Mitsuo, 'Synthesis and characterization of plasma-polymerized tert-butylacrylate films', *Thin Solid Films*, **515**, 4141-4147, (2007).
- [40] Stejskal J., Trchova M., Blinova N. V., Konyshenko E. N., Reynaud S., Prokes J., 'The reaction of polyaniline with iodine', *Polymer*, **49**, 180-185, (2008).
- [41] Despax B., Reynaud P., 'Deposition of polysiloxane thin films containing silver particles by an rf asymmetrical discharge', *Process. Polym.*, **4**, 127-134, (2007).
- [42] Vassallo E., Laguardia L., Catellani M., Cremona A., Delleria F., Ghezzi F., 'Characterization of poly(3-methylthiophene)-like films produced by plasma polymerization', *Plasma Process. Polym.*, **4**, S801-S805, (2007).
- [43] Vassallo E., Laguardia L., Cremona A., Mesto E., 'Preparation of plasma -polymerized  $SiO_x$ - like thin films from a mixture of hexamethyldisiloxane and oxygen to improve the corrosion behavior', *Surf. and Coat. Technol.*, **200**, 3035-3040, (2006).

- [44] Clergereaux R., Calafat M., Benitez F., Escaich D., Larclause I. S. D., Raynaud P., Esteve J., 'Comparison between continuous and microwave oxygen plasma post-treatment on organosilicon plasma deposited layers: Effects on structure and properties', *Thin Solid Films*, **515**, 3452-3460, (2007).
- [45] Cech V., Studynka J., Conte N, Perina V., 'Physico-chemical properties of plasma – polymerized tetravinylsilane', *Surf. & Coat. Technol.*, **201**, 5512-5517, (2007).
- [46] Luo H. L., Sheng J. Wan Y. Z., 'Plasma polymerization of styrene with carbon dioxide under glow discharge conditions', *Appl. Surf. Sci.*, **253**, 5203-5207, (2007).
- [47] Jafari R., Tatoulian M., Morscheidt W., Arefi-Khonsari F., 'Stable plasma polymerized acrylic acid coating deposited on polyethylene (PE) films in a low frequency discharge', *Reactive and Functional Polymers*, **66**, 1757-1765, (2006).

## **CHAPTER 2**

### **FUNDAMENTAL ASPECTS OF PLASMA, POLYMER, AND PLASMA POLYMERIZATION**

#### **2.1. Introduction**

#### **2.2. Plasma**

#### **2.3. Polymers**

2.3.1. Classification based upon different factors related to polymers

2.3.2. Crystalline and amorphous states of polymer

2.3.3. Classification based upon polymerization mechanism

2.3.4. Cross-link in polymers

#### **2.4. Plasma Polymerization**

2.4.1. Control parameters of plasma polymer thin film properties

#### **2.5. Overall reactions and growth mechanism in plasma polymerization**

#### **2.6. Glow Discharge**

2.6.1. DC glow discharges

2.6.2. AC and RF Glow Discharges

2.6.3. Different variants to glow discharge plasmas

2.7. Some characteristic differences of Plasma Polymer from the  
Conventional Polymer

References

## 2.1 Introduction

Fundamental aspects of plasma, polymer and plasma polymerization are discussed in this chapter. The details of plasma, Classification of polymers, reaction and growth mechanism in plasma polymerization glow discharge plasma, difference between plasma polymer and conventional polymer are illustrated in this chapter.

### 2.1. Plasma

The term plasma was first applied to ionized gas by Dr. Irving Langmuir an American physicist and chemist in 1929. Plasma is a partially ionized gas composed of freely moving electrons, ions and neutral species, there being approximately the same density of positive charges as of negative. In point of fact it is not necessary for both groups of charge carriers to be mobile for the system to display plasma characteristics; one group can be stationary, as for example, are the positive lattice ions of a metallic solid. For plasma to display plasma characteristics, however the average distances, between the plasma charged particles must be very much smaller than the physical dimensions of the total plasma.

The term "Fourth state of matter" often used to describe the plasma state was coined by W. Crooke in 1879 to describe the ionized medium created in a gas discharge. The term fourth state of matter follows from the idea that as heat is added to a solid, it under goes a phase transition usually to a liquid. If heat is added to a liquid the kinetic energy of the molecules becomes large and it becomes gaseous. The addition of still more energy to the gas, results in the ionization of some of the atoms. At a temperature above 100,000 K most matter exists in an ionized state and this state of matter is called the fourth state of matter.

In analysis plasmas are far harder to model than solids, liquids and gasses because they act in a self-consistent manner. The separation of electrons and ions produce electric fields and the motion of electrons and ions produce both electric and magnetic fields. The electric fields than tend to accelerate plasmas to very high energies while the magnetic fields tend to guide the electrons.

Although 99.9% of the apparent universe exists in a plasma state, there is very little in the way of natural plasma here on earth because the low temperature and high density of the earth and its near atmosphere preclude the existence of plasma. This means that plasma must be created by experimental means to study its properties.

Plasma can be created by various techniques such as combustion flames, Electrical discharges, controlled nuclear reactions, shocks and other means. The technique of most interest is the glow discharge. Plasmas produced by this technique are called non-

equilibrium or cold plasmas in contradistinction to equilibrium plasmas created by arcs or plasma jets. The term non-equilibrium means that there is no thermal equilibrium between electrons and other neutral species and ions. The ambient temperature of plasma in a plasma polymerization reaction however is generally in the vicinity of 380 to 400 K and remains reasonably constant after a steady-state condition is established.

Plasma properties are strongly dependent on the bulk parameters. Some of the most important plasma parameters are—

I. The degree of ionization, II. The plasma temperature III. The density, IV. The magnetic field in the plasma region.

Based on the relative temperatures of the electrons ions and neutrals, plasmas are classified as thermal or non-thermal. Thermal plasmas have electrons and the heavy particles at the same temperature i.e. they are in thermal equilibrium with each other. Non-thermal plasmas on the other hand have the ions and neutrals at a much lower temperature (ambient temperature) whereas electrons are much 'hotter'. Plasma is sometime referred to as being hot if it is nearly fully ionized or cold if only a small fraction (for example 1 %) of the gas molecules is ionized. Even in 'cold' plasma the electron temperature is still typically several thousand degrees. Plasmas utilized in plasma technology (technological plasmas) are usually cold in this sense.

### 2.3. Polymers

The word polymer was derived from the classical Greek words "poly" meaning "many" and "mers" meaning "parts". Simply stated, a polymer is a material whose molecules contain a very large number of atoms linked by covalent bonds, which makes polymers macromolecules. Certain polymers available in nature are protein cellulose, silk etc. while many others including polystyrene, polyethylene and nylon are produced only by synthetic routes.

#### 2.3.1. Classification based upon different factors related to polymers

Thermal processing behavior	Thermoplastic, Thermosets.
Polymerization mechanism	Addition (step growth), Condensation (chain growth)
Chemical structure	Homochain (single, double, Triple bonds along their backbone), Heterochain
Monomer arrangement	Copolymers (two different repeating units in their chain), Ter polymers (three chemically different repeating units)
Tacticity	Isotactic, Syndiotactic, Atactic



### 2.3.2. Crystalline and amorphous states of polymer

Usually the biggest in polymer properties result from how the atoms and chains are linked together in space. Polymers that have a 1D structure will have different properties than those that have either a 2D or 3D structure. Thus polymers can also be classified in the following way.

Form of network		Form of molecule		
		One dimensional	Two dimensional	Three dimensional
Amorphous irregular	Flexible chain	Rubbers (natural synthetic)		
	Rigid chain	Glassy plastics e.g. Polystyrene		Thermoset plastics e.g. Polyester
Crystalline regular	Partial unoriented	Tough plastics e.g. Nylon		
	Partial oriented	Fibers and films (natural man made)	e.g. Carbon fibre	
	Perfect	Single crystals e.g. Polyethylene	e.g. Graphite	

The morphology of most polymers is semi-crystalline. That is, they form mixtures of small crystals and amorphous material and melt over a range of temperature instead of at a single melting point. The crystalline material shows a high degree of order formed by folding and stacking of the polymer chains. The amorphous or glass-like structure shows no long range order, and the chains are tangled as illustrated below.

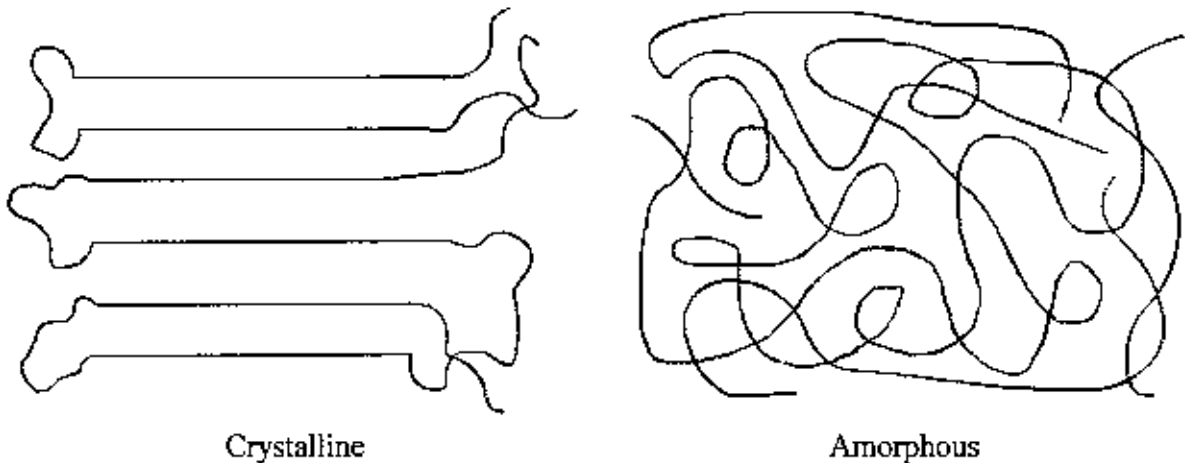


Fig. 2.1. Crystalline and amorphous states of polymer

There are some polymers that are completely amorphous, but most are a combination with the tangled and disordered regions surrounding the crystalline areas. Such a combination is shown in the following diagram.



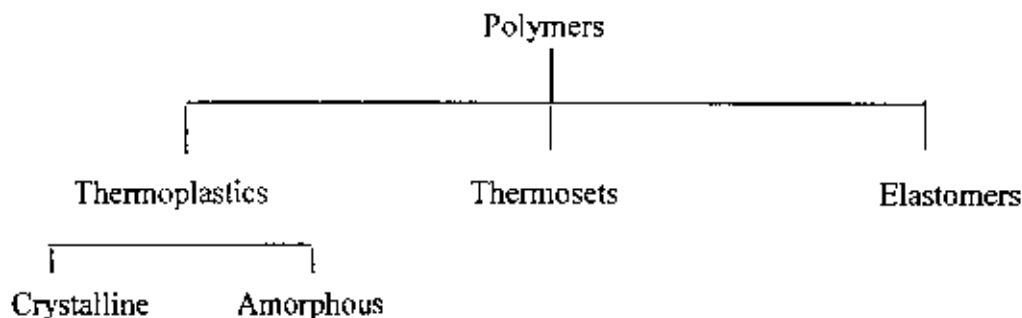
Fig.2.2. Disordered region in amorphous polymer

An amorphous solid is formed when the chains have little orientation throughout the bulk polymer. The glass transition temperature is the point at which the polymer hardens into an amorphous solid. This term is used because the amorphous solid has properties similar to glass.

In the crystallization process, it has been observed that relatively short chains organize themselves into crystalline structures more readily than longer molecules. Therefore, the degree of polymerization (DP) is an important factor in determining the crystallinity of a polymer. Polymers with a high DP have difficulty organizing into layers because they tend to become tangled.

The cooling rate also influences the amount of crystallinity. Slow cooling provides time for greater amounts of crystallization to occur. Fast rates, on the other hand, such as rapid quenches, yield highly amorphous materials.

However, the most common way of classifying polymers is to separate them into three groups



### i. Thermoplastics:

Molecules in a thermoplastic are held together by relatively weak intermolecular forces so that the material softens when exposed to heat and then return to its original condition when cooled. Thermoplastic polymers can be repeatedly softened by heating and then solidified by cooling. Most linear and slightly branched polymers are thermoplastic as shown in Fig.2.3(a). All the major thermoplastics are produced by chain polymerization.

### ii. Thermosets:

A thermosetting plastic or thermoset, solidifies or sets irreversibly when heated. Thermosets cannot be reshaped by heating. Thermosets usually are 3-dimensional networked polymers as shown in Fig.2.3(b) and are formed by the condensation polymerization process. These polymers possess a high degree of cross-linking between polymer chain, which restrict the motion of the chain and lead to a rigid material.

### iii. Elastomers:

Elastomers are rubbery polymer that can be stretched easily to several times their unstretched length and which rapidly returns to their original dimensions when the applied stress is released. Elastomers are cross-linked but have a low cross-link density as shown in Fig.2.3(c). The polymer chain still have some freedom to move, but are prevented from permanently moving relative to each other by the cross-links. To stretch, the polymer chain must not be part of a rigid solid either a glass or a crystal. An Elastomer must be above its glass transition temperature  $T_g$  and have a low degree of crystallinity.

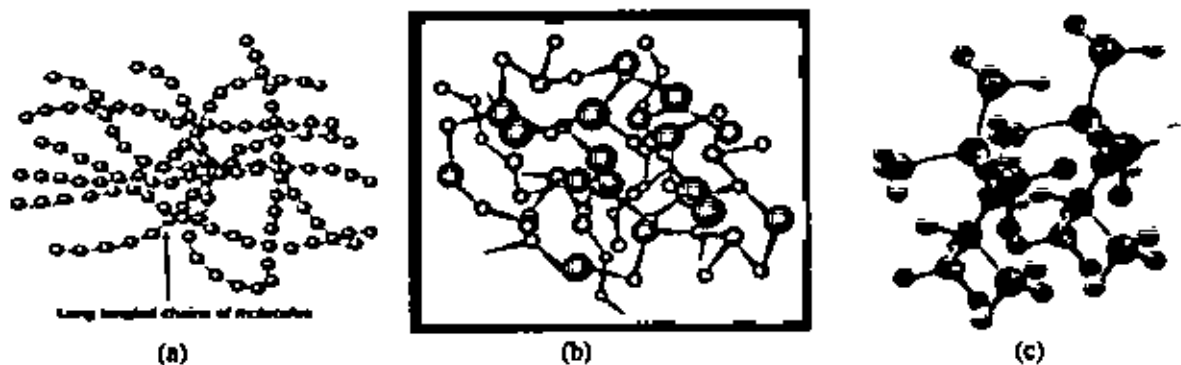


Fig.2.3. Network structure of (a) thermoplastic, (b) thermoset, (c) elastomer

### 2.3.3. Classification based upon polymerization mechanism

On the basis of processing characteristics, polymers can be classified according to the mechanism of polymerization.

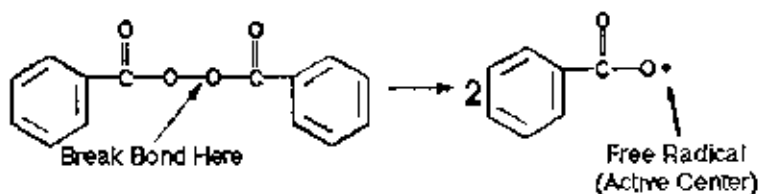
1. Addition
2. Condensation

**Addition:**

A chemical reaction in which simple molecules (monomers) are added to each other to form long-chain molecules (polymers) involving some sort of active centers and forms no by-products. The molecules of the monomer join together to form a polymeric product in which the molecular formula of the repeating unit is identical with that of the monomer.

The most common type of addition polymerization is *free radical polymerization*.

The following diagram shows the formation of a radical from its initiator, in this case benzoyl peroxide.

**Condensation:**

The monomers for condensation polymerization have two main characteristics.

- ⇒ Instead of double bonds, these monomers have functional groups (like alcohol, amine, or carboxylic acid groups)
- ⇒ Each monomer has at least two reactive sites, which usually means two functional groups.

Condensation polymers are usually formed by the stepwise intermolecular condensation of reactive groups.

An example of condensation polymerization is the synthesis of nylon -6,6 by condensation of adipic acid and hexamethylene diamine, as shown below

This polymerization is accompanied by the liberation of two molecules of water which means condensation polymerization produces by-products.

Depending on polymerization kinetics another classification adopted over the addition and condensation categories.

**Step growth polymerization:**

The step growth polymerization is a polymerization process that involves a chemical reaction between multifunctional monomer molecules. In a step growth reaction, the growing chains may react with each other to form even larger chains. Thus a monomer or dimer may react in just the same way as a chain hundreds of monomer units long.

In step growth polymerization a linear chain of monomer residues is obtained by the stepwise intermolecular condensation or addition of the reactive groups in monomers.

For example to make a polyester; two monomers, terephthoyl chloride and ethylene glycol will react to form a dimer.

The dimer can react with a molecule of terephthoyl chloride or it may react with another dimer to form a tetramer and continuing like this in every step it can form a large chain.

The characteristics of step growth polymerization are as follows:

- ⇒ Any two molecular species in the mixture can react.
- ⇒ The monomer is almost all incorporated in a chain molecule in the early stages of the reaction i. e. about 1 per cent of monomer remains untreated when chain length,  $x_n=10$ . Hence polymer yield is independent of the reaction time in the later stages.
- ⇒ At any stage all molecular species are present in a calculable distribution.
- ⇒ Long reaction times and high conversions are necessary for the production of a polymer with large  $x_n$  and high molecular weights.

#### **Chain growth polymerization:**

In a chain growth polymerization, monomers become part of the polymer one at a time.

The characteristics of chain growth polymerization are as follows:

- ⇒ Only growth reaction adds repeating units one at a time to the chain.
- ⇒ Monomer concentration decreases steadily throughout reaction.
- ⇒ High polymer is formed at once and polymer molecular weight changes little throughout reaction.
- ⇒ Long reaction times give high yields but affect molecular weight little.

Polymers can be classified according to the type and arrangement of monomer/monomers in a macromolecule.

#### **Homopolymer:**

When a polymer is made by linking only one type of small molecule or monomer together, it is called a homopolymer.

-A-A-A-A-A-

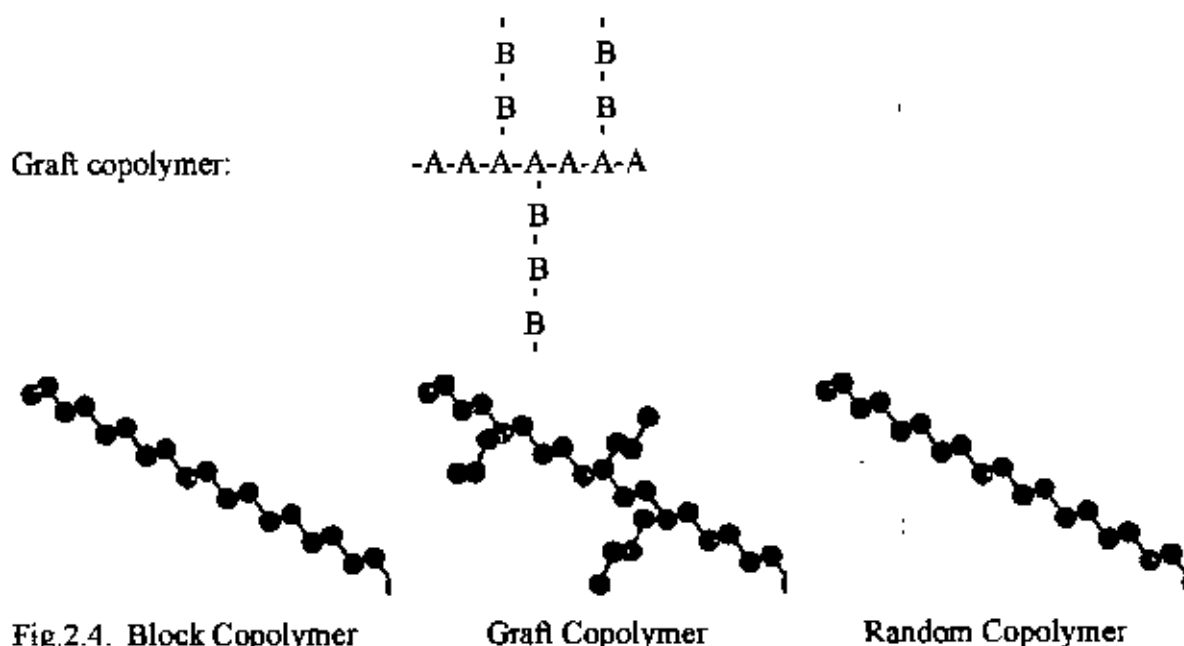
#### **Copolymer:**

When two different types of monomers are joined in the same polymer chain, the polymer is called a copolymer.

Alternating copolymer:      -A-B-A-B-A-B-

Random copolymer:          -A-A-B-A-B-B-B-A-

Block copolymer:            -A-A-A-B-B-B-



### 2.3.4. Cross-link in polymers

Highly cross-linked structure is the most significant property of plasma polymers to distinguish it from the conventional polymers. Cross linking in polymer means, in addition to the bonds which hold monomers together in a polymer chain, many polymers form bonds between neighboring chains. These bonds can be formed directly between the neighboring chains, or two chains may bond to a third common molecule. Though not as strong or rigid as the bonds within the chain, these cross-links have an important effect on the polymer. Polymers with a high enough degree of cross-linking have "memory." When the polymer is stretched, the cross-links prevent the individual chains from sliding past each other. The chains may straighten out, but once the stress is removed they return to their original position and the object returns to its original shape.

### 2.4. Plasma Polymerization

Plasma polymerization is a procedure, in which gaseous monomers, simulated through plasma, condense on freely selectable substrates, as high cross-linked layers. Condition for this process is the presence of chain producing atoms, such as carbon, silicon or sulfur in the working gas. In this process monomer gas is pumped into a vacuum chamber where it is polymerized by plasma to form a thin, clear coating. The monomer starts out as a liquid. It is converted to a gas in an evaporator and is pumped into a vacuum chamber. A glow discharge initiates polymerization. Plasma polymerization occurs due to the dissociation of covalent bonds in gas phase molecules, and subsequent reactions between gas phase

species and surfaces result in the deposition of polymeric materials. Dissociation results from interactions between monomer and energetic species, such as ions, electrons, photons, and excited neutrals created in the glow discharge. The generation of reactive species which take part in the deposition of polymeric films under vacuum can be achieved by the interactions of monomer and energetic species or by thermolysis of monomer. The energetic species can cause considerable fragmentation of the original monomer. The number of different reactive species resulting from monomer-energetic species is interactions limited only by the energy

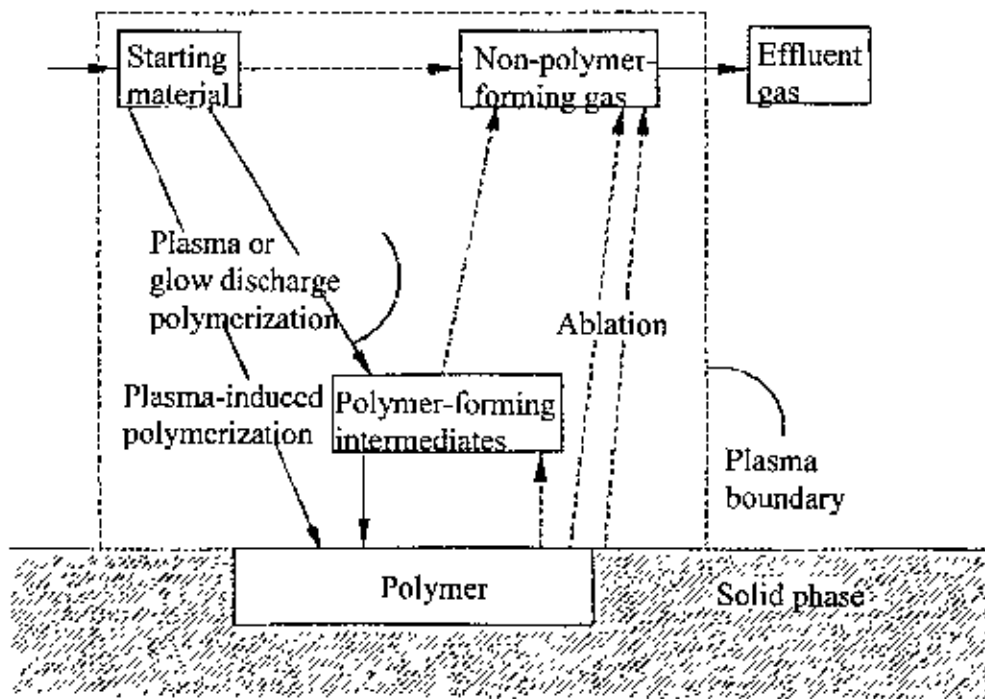


Fig.2.5. Competitive ablation and polymerization, scheme of glow discharge polymerization.

of the energetic species and the number of ways in which the monomer can dissociate. The activated fragments are recombined, sometimes accompanying rearrangement, and the molecules grow to large molecular weight ones in a gas phase or at the surface of the substrate. The process is done in a low pressure, low temperature plasma. This means the temperature in the chamber never really rises above room temperature. Plasma polymerization is essentially a PECVD (Plasma enhanced chemical vapor deposition) process. It refers to the deposition of polymer films through plasma dissociation and to the

excitation of an organic monomer gas and subsequent deposition and polymerization of the excited species on the surface of the substrate.

Plasma polymerization is characterized by several features:

1. Plasma polymers are not characterized by repeating units, as is typical for conventional polymers.
2. The properties of the plasma polymer are not determined by the monomer being used but rather by the plasma parameters.
3. The monomer used for plasma polymerization does not have to contain a functional group, such as a double bond.

#### 2.4.1. Control parameters of plasma polymer thin film properties:

(A). Monomer: The monomer most commonly used for plasma polymerization are;

1. Hydrocarbons: Consisting of triple, double, cyclic structure and saturated monomers. Also the polar group containing hydroca
2. Fluorocarbons
3. Silicon containing monomers
4. Volatile organometallic compounds

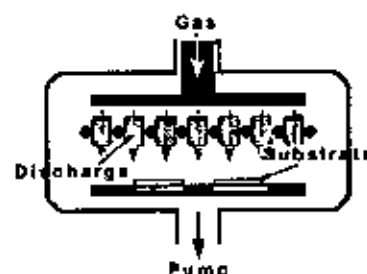


Fig.2.6. Plasma Polymerization reactor

(B). Generation of glow discharge:

1. DC glow discharge
2. DC glow discharge of alternating polarity (at low frequencies e. g. 60 Hz or <500 K Hz).
3. AC glow discharge
4. Radio frequency (13.56 MHz) glow discharge
5. Microwave (300 MHz to 10 GHz) glow discharge
6. Pulsed glow discharge
7. Atmospheric pressure glow discharge
8. Dielectric barrier glow discharge

Depending on the reactor geometry there are several types of discharges;

1. Capacitively coupled (cc) plasmas
2. Inductively coupled plasmas
3. Symmetric and asymmetric reactor glow discharges.

(C). Effect of physical plasma process parameters:

1. Frequency of exciting potential Excitation power,



2. excitation power  $W$ ,
3. monomer(s) flow rate  $F$  [Volume(STP)/unit time],
4. Plasma pressure  $P_g$ ,
5. Geometrical factors, e.g. location of monomer inlet and to exciting electrodes, dimensions of reactor vessel and of electrodes, etc.,
6. Temperature of deposition site.

The effect of these parameters can be understood by considering their effect on basic plasma parameters i.e. electron density  $n_e$ , electron energy distribution  $f(E)$ , gas density  $N$ , residence time for a gas molecule in plasma,  $\tau$ .

Yasuda proposed a controlling parameter of  $W/FM$  which is an apparent input energy per the unit of monomer molecule in J/Kg; therefore, the magnitude of the  $W/FM$  parameter is considered to be proportional to the concentration of activated species in plasma.

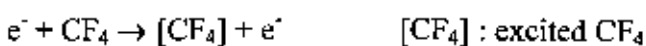
Depending on this parameter, the rate of formation of polymer; increases or decreases under certain conditions [3].

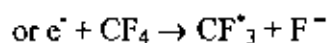
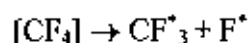
### 2.5. Overall reactions and growth mechanism in plasma polymerization

In plasma monomer molecules gain high energy from electrons, ions, and radicals and are fragmented into activated small fragments, in some cases into atoms. These activated fragments are recombined sometimes accompanying rearrangement, and the molecules grow to large- molecular-weight ones in a gas phase or at the surface of substrates. The repetition of activation, fragmentation, and recombination leads to polymer formation. The chemical structure of polymers formed by plasma polymerization, if the same monomer was used, is never predicted from the structure of the monomer, because the fragmentation and rearrangement of the monomers occur in the plasma.

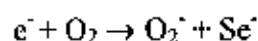
An electron with a high kinetic energy, interacting with atoms, has an approximately equal probability of producing either excitation or ionization (excitation is slightly more probable in the case of interaction with a molecule). The electron passing closely by an atom produces in it an electric field due to coulombic force. This field causes a pulse acting on the 'atom' components. This perturbation of the atom can be theoretically understood as equivalent to the Fourier components of the pulse. The electron interaction with molecules, take place in the same way, as described for atoms. The only difference is that the excitation can result in molecular dissociation.

For example:

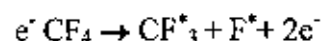




Such reactions are a major source of free radicals and negative ions. These 'electron impact dissociations' require less energy than the direct ionization events where only the electrons in the high energy tail of the electron energy distribution take part. As an example of simple ionization,



Also dissociation ionization can happen:



However, molecular species (e.g. radicals) make a coupling reaction easy because the dissociation energy can be distributed entirely through a large number of degrees of freedom. An example is:

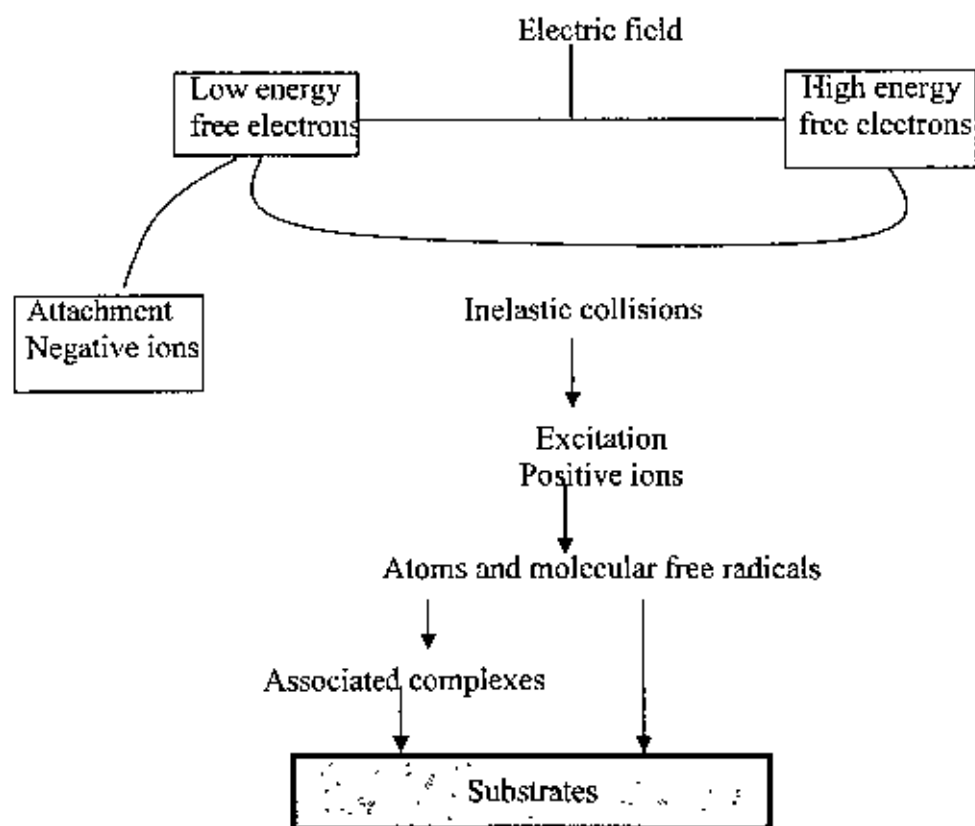
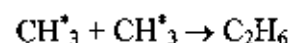
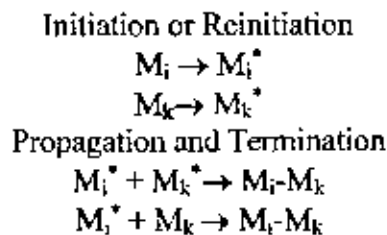


Fig.2.7. General hierarchy for the production of active species in molecular gas plasma.

A comment on metastable species explains that a metastable atom (molecule) can transfer its energy through a collision with another particle and, if this is of lower ionization potential, the result may be an ionization or desiccative ionization event. Such processes are known as Penning ionization process. The general hierarchy for the production of active species in a molecular gas volume is shown in Fig2.7.

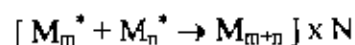
Plasma polymerization consists of several reaction steps:

At first, *generation* of free radicals and atoms are occurred by collisions of electrons and ions with monomer molecules, or by dissociation of monomers absorbed on the surface of the sample. Secondly, *propagation* of the formation of polymeric chain which can take place both in the gas phase (by adding radical atoms to other radicals or molecules) and on the deposited polymer film (by interaction of the surface free radicals with either gas phase or absorbed monomers). Finally, *termination* can also take place in the gas phase or at the polymer surface, by similar process as in the propagation step, but ending either with the final product or with a closed polymer chain. The individual steps and reaction that occur in plasma polymerization generally depends on the system. This type of polymerization can be represented by the following statements.



In which i and k are the numbers of repeating units ( i.e., i=k=1 for the starting material), and  $M^*$  represents a reactive species, which can be ion of either charge, an excited molecule, or a free radical produced by M but not necessarily retaining the molecular structure of the starting material. In plasma state polymerization the polymer is formed by the repeated stepwise reaction.

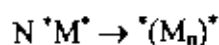
Yasuda suggested that the growth mechanism of plasma polymerization would vary likely be the rapid step growth reaction,



Where  $M^*$  is the mono functional reactive species such as a free radical  $R^*$ , N is the number of repetitions of similar reactions and m and n represents different reactive species.

In case of monofunctional reactive species, a single elementary step is indeed a termination process and does not contribute without additional elementary step.

For a difunctional reactive species, such as a diradical, the polymerization can be represented by



It shows that as polymerized polymers contain a measurable quantity of free radicals.

The overall polymerization mechanism based on the rapid step growth principle is shown in Fig 2.8.

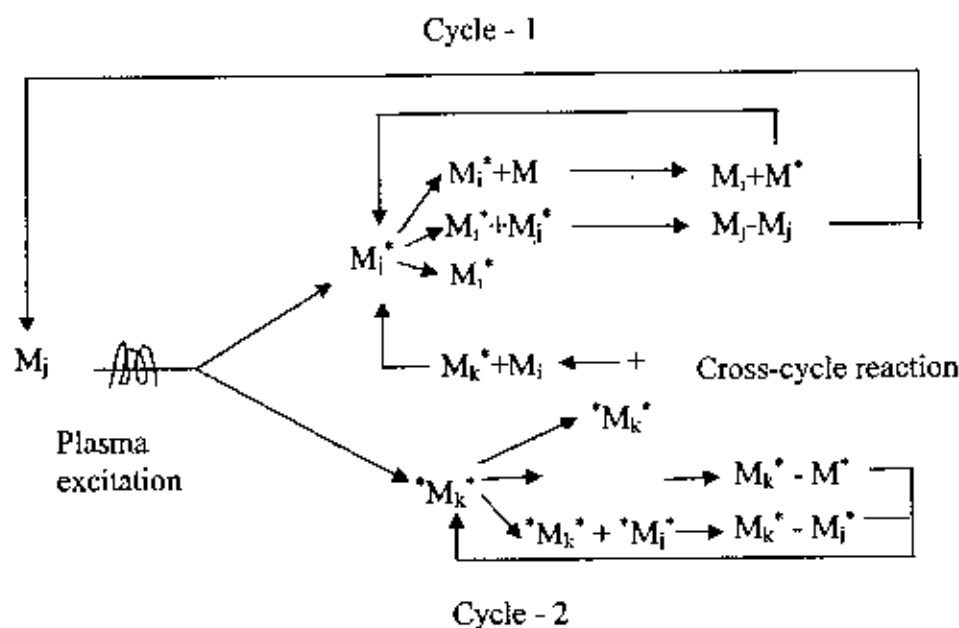


Fig.2.8. Schematic representation of bicyclic step-growth mechanism in plasma polymerization.

Where  $M_x$  refers to a neutral species,  $M^*$  is the monofunctional activated species and  ${}^*M^*$  is the difunctional. The subscripts  $i, j, k$  indicate the difference in the size of species involved. Cycle I is via the repeated activation of the reaction products from monofunctional activated species, and cycle II is that of difunctional.

The species participating in the rapid step growth polymerization can be mono- or multifunctional (radical, cation, cation-radical, diradical, etc.) [1,8, 23].

## 2.6. Glow Discharge

A glow discharge is a kind of plasma. It is an ionized gas consisting of equal concentrations of positive and negative charges and a large number of neutral species i.e. a plasma. In the simplest case, it is formed by applying a potential difference (of a few 100 V to a few kV) between two electrodes that are inserted in a cell (or that form the walls of the cell). The cell is filled with a gas (an inert gas or a reactive gas) at a pressure ranging from a few m Torr to atmospheric pressure. Due to the potential difference, electrons that are emitted from the cathode, give rise to collisions with the gas atoms or molecules (excitation, ionization,

dissociation). The excitation collisions give rise to excited species, which can decay to lower levels by the emission of light. This process is responsible for the characteristic name of the "glow discharge". The ionisation collisions create ion-electron pairs. The ions are accelerated

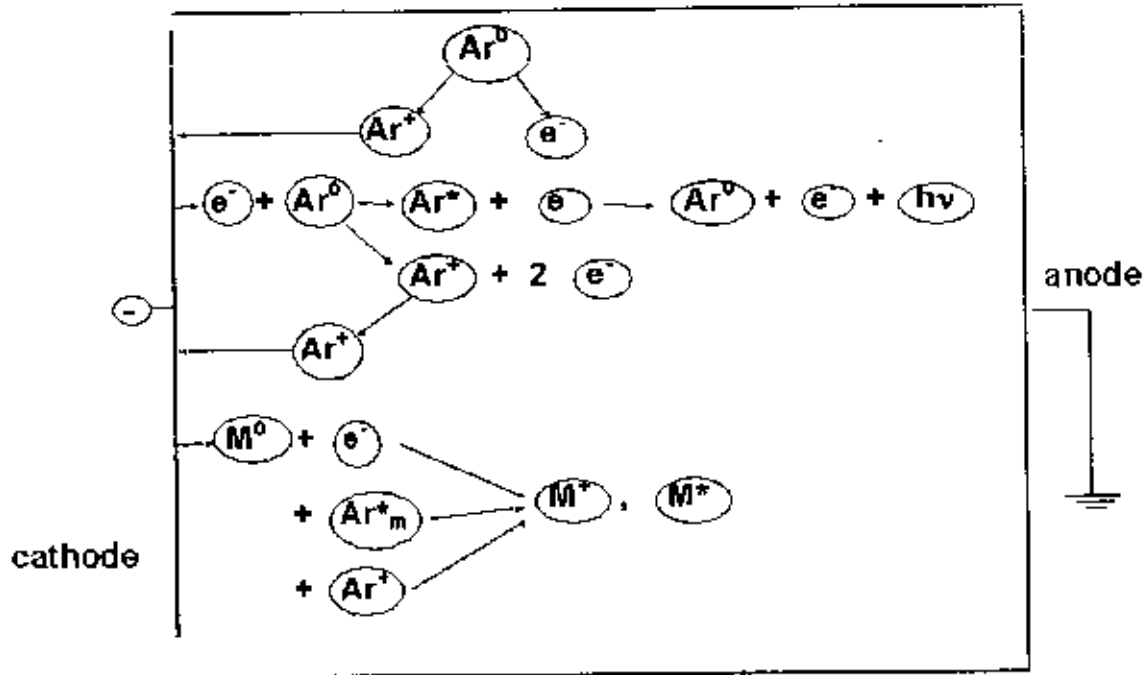


Fig.2.9. Schematic representation of the basic processes in a glow discharge.

toward the cathode, where they release secondary electrons. These electrons are accelerated away from the cathode and can give rise to more ionization collisions. In its simplest way, the combination of secondary electron emission at the cathode and ionization in the gas, gives rise to self-sustained plasma. The character of the gas discharge critically depends on the frequency or modulation of the current.

### 2.6.1. DC glow discharges

For a DC glow discharge, the mechanism involves the bombardment of the cathode with positive ions, resulting in the generation of the secondary electrons which in turn accelerated from the cathode until they have gained enough energy to ionize a molecule (atom) by inelastic collision. A DC glow discharge is observed to have four distinguishable lighter and darker zones which are shown in Fig.2.10.

1. Cathode region: Aston dark space, cathodic (Crooke/Hittorf) dark space.
2. Negative glow region: negative glow, Faraday dark space.

3. Positive column region: positive column.

4. Anode region: anode dark space, anode glow layer.

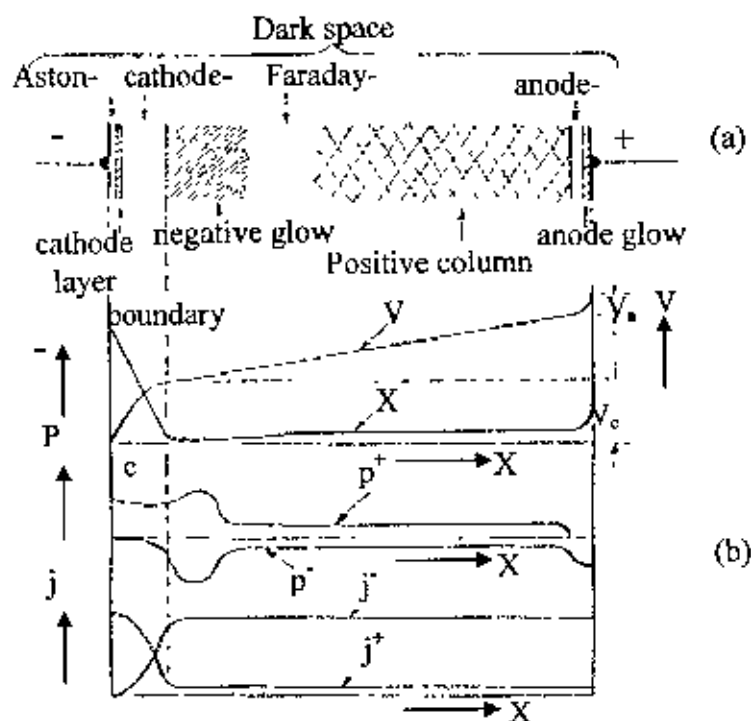


Fig.2.10 Normal glow discharge; (a) the shaded areas are luminous, (b) distribution of potential among luminous zones.

The zone which consists of the Aston dark space, the cathode glow and the Crooke's dark space acceleration of positive ions to the cathode, and electrons away from it, is observed is that between the cathode and negative glow. The thickness of this zone is inversely proportional to pressure and decreases with increasing potential drop between the electrodes because; it is approximately the mean distance travelled by an electron from the cathode before it makes an ionization collision. The negative glow which occurs after the Crooke's dark space is a zone of high concentration of positive ions formed by collision with energetic electrons emerging from the Crooke's dark space. Thus the operation of the glow discharge depends critically on the role of the cathode dark space. In addition to ions, molecules in excited states are formed in the negative glow (thereby giving rise to bright glow by relaxation to lower states) as well as negative ions (combination of neutral and electron) and free radicals (combination of positive ion and electron). The positive column may be considered a conduit of current from the negative glow to the anode. This region is the region of plasma because a partially ionized gas consisting of equal numbers of positive and

negative charges, in addition to neutral molecules. The current is carried largely by the more mobile electrons that enter the positive column from the negative glow and Faraday dark space. The role of the anode is to transform current from the glow discharge to the external circuit. When there is no positive column, the anode is usually in the Faraday dark space.

A decrease of pressure of the glow discharge or of length of the reactor simply results in a decrease of the relative volume assigned to the positive column, which may be eliminated altogether without extinguishing the glow discharge. The salient characteristic of the DC glow discharge is that the negative glow contains a higher concentration of ions, electrons and other active species than the positive column and therefore emits a brighter glow [3,8,23].

### 2.6.2. AC and RF glow discharges

If an ac voltage up to (kHz) is used, the discharge is still basically of a dc type and each electrode really acts as cathode and anode alternately. However as the frequency is increased, the motion of ions can no longer follow the periodic changes in field polarity. This results in a significant reduction in the loss of charged particles from the system and a concomitant decrease in the voltage required to maintain the glow discharge. Raising the frequency of the applied voltage, positive ions become immobile and the positive space charge is partially retained from one half-cycle to the next (this helps the discharge to reinitiate). Above 500 kHz, the regeneration of electrons and ions that are lost to the walls and electrodes takes place within the body of the plasma. When the random collisions of electron with gas molecule occur, the electron picks up an increment of energy with each collision. As a free electron in a vacuum under the action of an alternating electric field oscillates with its velocity  $90^\circ$  out of phase with the field, and gains no energy, the electron can get energy from the field only for the elastic collisions with the gas atoms, as the electric field converts the electron's resulting random motion back to ordered oscillatory motion. Thus from the interaction with the oscillating electric field, the electron gains energy on each collision until it acquires enough energy to be able to make an inelastic collision with a gas atom and some fraction of these collisions will result in ionization. An increase of frequency to the MHz region causes that no significant displacement of either electrons or positive ions happens and losses of charged species from diffusion and recombination processes are replaced by electron impact ionization of neutral gas molecules in the discharge volume. This type of discharge is radio frequency (RF) glow

discharge (100 kHz-13.56 MHz) and it does not depend on processes on the electrodes, which can be covered with any material, e.g., an insulator [3,8].

### 2.6.3. Different variants to glow discharge plasmas

An important type of ac glow discharge, operating at atmospheric pressure, is the *dielectric barrier discharge (DBD)*, where the electrodes are typically covered by a dielectric barrier. A variation to the ac discharge is the *pulsed glow discharge*, which also consists of short glow discharges (with lengths typically in the milli - or microsecond range), followed by an afterglow, which is generally characterized by a longer time-period. The advantage is that high peak electrical powers can be reached for a low average power, resulting in high peak efficiencies for various applications.

In addition to applying an electric field (or potential difference), a magnetic field can also be applied to a glow discharge. The most well-known discharge type with crossed magnetic and electric fields is the *magnetron discharge*. The electrons circulate in helices around the magnetic field lines and give rise to more ionisation. Hence, magnetron discharges are typically operated at lower pressures and higher currents than conventional glow discharges.

Recently, some new discharge types have been developed, which are also characterized by low pressure and high plasma densities, and which have their main application in the semiconductor industry and for materials technology. The major difference with the conventional glow discharge is that the electrical power is not applied through a potential difference between two electrodes, but through a dielectric window. The two most important "high-density sources", are the *inductively coupled discharge*, where the rf power is inductively coupled to the plasma, and the *electron cyclotron resonance reactor*, where microwave power and a magnetic field are applied.

Microwave power can also be applied in so-called *microwave induced plasmas*. Various discharge types can be classified under this name, among others the resonance cavity plasmas, free expanding plasma torches and surface wave discharges [21].

## 2.7. Some characteristic differences of Plasma Polymers from the Conventional Polymers

1. Plasma polymers have a higher elastic modulus than the conventional polymers. (May be due to dense cross-linkage of polymer chains).



2. Low water vapour or gas permeability and low decay of watt ability than the conventional polymers. (Due to cross linking).
3. The properties of plasma polymer are much more dependent on the processing factors and morphology than the conventional polymers. For example, properties of plasma polymers are directly or indirectly related to the number of free radicals.
4. Internal stress in a plasma polymer is a characteristic property which is not found in most conventional polymers.
5. Solvent resistance of plasma polymers is generally higher than the conventional polymers.
6. The surface energies of plasma polymers of hydrocarbons are generally higher than those of conventional hydrocarbon polymers due to the presence of oxygen containing groups [8].

### References

- [1] Shen M., Bell A T., 'Plasma Polymerization', American Chemical Society, (1979).
- [2] Krall N. A., Trivelpiece W.A., 'Principles of Plasma Physics', McGraw-Hill Kogakusha, Ltd., Tokyo, Japan, (1973).
- [3] d'Agostino R., 'Plasma Deposition, Treatment and Etching of Polymers', Harcourt Brace Jovanovich, Publishers, NY, (1990).
- [4] Gaur s., Vergason G., 'Plasma Polymerization Theory and Practice', Vergason Technology. Inc. Van Etten, NY.
- [5] Baalman A., 'Plasma Polymerization', Fraunhofer inst.
- [6] Fried J. R., 'Polymer Science and Technology', Prentic Hall of India Pvt. Ltd., New Delhi, (2002).
- [7] Cowie J. M. G., 'Polymers: Chemistry and Physics of Modern Materials', Blackie Academic & Professional, NY, (1993).
- [8] Yasuda H., 'Plasma Polymerization'; Academic Press, Inc, New York (1985).
- [9] Billmeyer W. JR., 'Text Book of Polymer Science', John Wielly & Sons, NY, (1994).
- [10] <http://www.csua.berkeley.edu>, Lisa P., 'Intoduction to polymers', (2005).
- [11] <http://www.whisnantdm@wolfford.edu>.polymer chemistry (2001).
- [12] <http://www.CategoryChemical processes - Wikipedia, the free encyclopedia.htm>
- [13] <http://www.Plasma Properties.htm>

- [14] <http://www.Plasma Science and Technology - Basics - What are Plasmas.htm>
- [15] <http://www.Polymers.htm>
- [16] <http://www.polymers and Plastics.htm>
- [17] <http://www.Thermoplastic - Wikipedia, the free encyclopedia.htm>
- [18] <http://www.Thermosetting plastic - Wikipedia. the free encyclopedia.htm>
- [19] Arcfi F., Andre V., Motjtazer-Rahmati P., Amouroux J., 'Plasma polymerization and surface treatment of Polymers', *Pure & Appl. Chem.*, **64(5)**, 715-723, (1992).
- [20] <http://www. Polymers/Classification.htm>
- [21] Bogaerts A., Neyts E, Gijbels R., Mullen J. V. D., 'Gas discharge plasmas and their applications', *Spectrochim.Acta Part, B* **57**, 609-658, (2002).
- [22] Frank F. Shi., 'Developments in plasma-polymerized organic thin films with novel mechanical, electrical, and optical properties', *Macromol. Chem. Phys.*, **C36(4)**, 795-826, (1996).
- [23] Biederman H, Osada Y., 'Plasma chemistry of polymers', *Polym. Phys.*, **95**, (1990).
- [24] Inagaki N., 'Plasma Surface Modification and Plasma Polymerization', Tecnominc publishing company, Inc. Pennsylvania U.S.A., (1996).

## **CHAPTER 3**

### **EXPERIMENTAL DETAILS**

**3.1. Introduction**

**3.2. The Monomer**

**3.3. Substrate Material and its Cleaning Process**

**3.4. Capacitively Coupled Plasma Polymerization Set-up**

**3.5. Generation of Glow Discharge Plasma in the Laboratory**

**3.6. Deposition of Plasma Polymerized Thin Film**

**3.7. Contact Electrodes for Electrical Measurements**

**3.8. Measurement of Thickness of the Thin Films**

**3.9. Multiple-Beam Interferometry**

References

### 3.1. Introduction

This chapter deals with the plasma polymerization scheme of 2, 6 diethylaniline which includes the details of monomer, substrate, capacitively coupled glow discharge plasma polymerization set up for polymer formation, the thickness measurement method and contact electrode deposition technique for electrical measurement of PPDEA thin films.

### 3.2. The Monomer

The monomer 2,6 diethylaniline is manufactured by Aldrich Co and is collected from local market. The chemical structure of the monomer is shown in Fig 1 and its typical properties are stated below:

Table 3.1 General properties of 2,6 diethylaniline.

Form	Clear liquid
Color	Yellow to red
Chemical formula	$(C_2H_5)_2C_6H_3NH_2$
Molecular weight	149.20
Freezing point, °C	3
Vapor pressure at 20 °C, mm	0.02
Boiling point, °C	243
Density at 20 °Cg/ml	0.959
Flash point(TCC), °C	104
Viscosity at 20°C	4.60

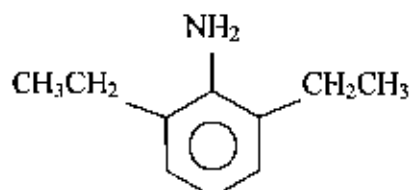


Fig.3.1 The structure of 2,6 diethylaniline

2,6 diethylaniline possesses two ethyl groups and one amine group. It is miscible in iso-octane, toluene, ethyl alcohol and 12% in water.

### 3.3. Substrate Materials and its Cleaning Process

The substrates used were pre-cleaned glass slides (25.4 mm X 76.2 mm X 1.2 mm) of Sail Brand, China, purchased from local market. The samples were prepared by depositing the PPDEA thin film and electrodes onto them.

To get a homogeneous, smooth and flawless thin polymer film, which is a common property of plasma polymers, it is essential to make the substrate as clean as possible. The substrates were chemically cleaned by acetone and thoroughly rinsed with distilled water then dried in hot air.

### 3.4. Capacitively Coupled Plasma Polymerization Set-up

A glow discharge is a kind of plasma and the plasma polymerization setup has been used enormously in recent years to form various kinds of plasma polymers. Different configuration of polymerization set up varies the properties of plasma polymers i.e. the geometry of the reaction chamber, position of the electrodes, nature of input power etc.

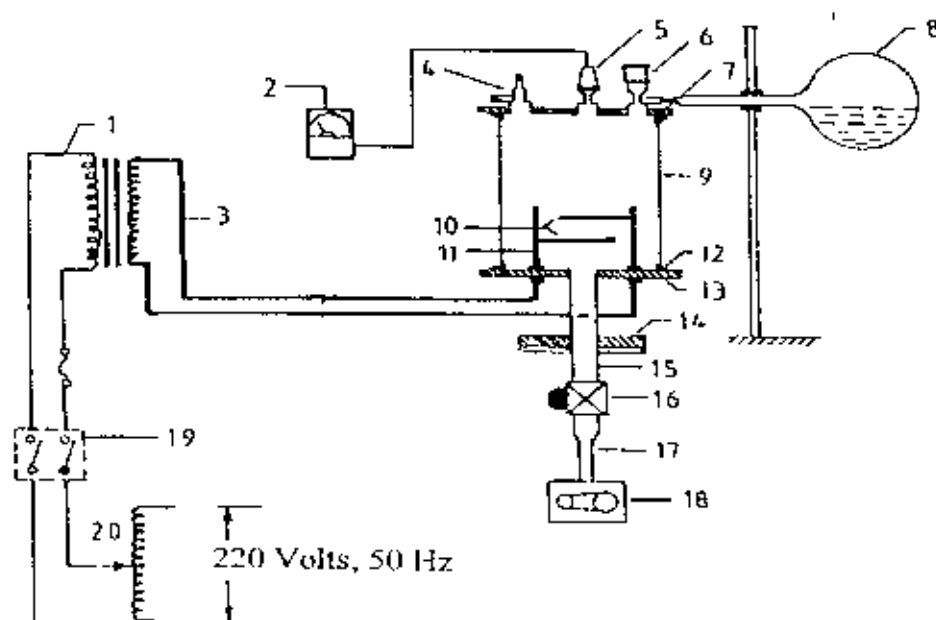


Fig.3.2. Schematic diagram of the plasma polymerization set-up.

1 high voltage power supply, 2 pirani gage, 3 high tension leads, 4 gas inlet valve, 5 gauge head, 6 monomer injection valve, 7 flowmeter, 8 monomer container, 9 Pyrex glass dome, 10 metal electrodes, 11 electrode stands, 12 gasket, 13, lower flange, 14 bottom flange, 15 brass tube, 16 valve, 17 liquid nitrogen trap, 18 rotary pump. 19 switch and 20 variac.

The glow discharge plasma polymerization setup which was used to deposit the PPDEA thin films consists of the following components is shown in Fig.3.2.

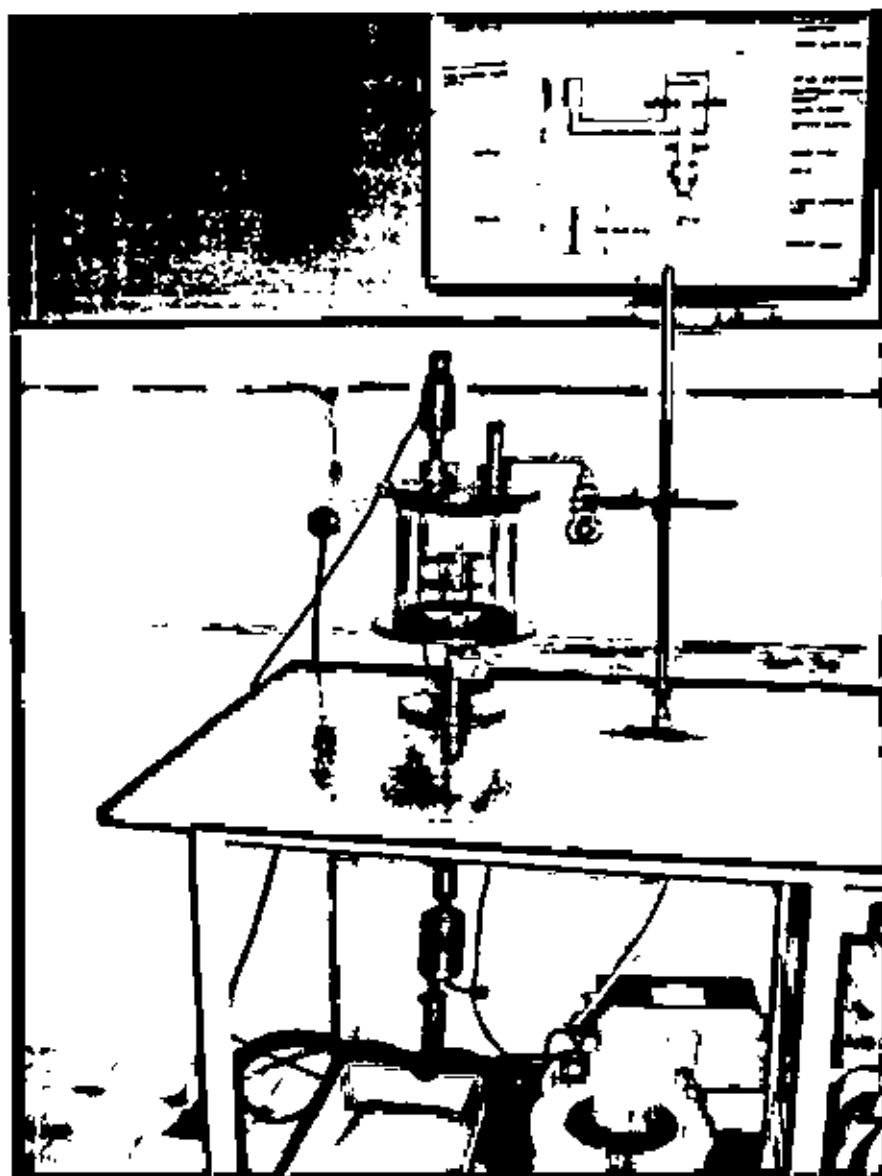


Fig.3.3. Plasma polymerization set-up

#### i. Plasma reaction chamber

The glow discharge reactor is made up of a cylindrical Pyrex glass bell-jar having 0.15 m in inner diameter and 0.18 m in length. The top and bottom edges of the glass bell-jar are covered with two rubber L-shaped (height and base 0.015m, thickness, 0.001 m) gaskets. The cylindrical glass bell jar was placed on the lower flange. The lower flange is well fitted with the diffusion pump by an I joint. The upper flange is placed on the top edge of the bell-jar.

The flange is made up of brass having 0.01 m in thickness and 0.25 m in diameter. On the upper flange a laybold pressure gauge head, Edwards high vacuum gas inlet valve and a monomer injection valve are fitted. In the lower flange two highly insulated high voltage feed-through are attached housing screwed copper connectors of 0.01m high and 0.004 m in diameter via Teflon<sup>TM</sup> insulation.

#### **ii. Electrode system**

A capacitively coupled electrode system is used in the system. Two circular stainless steel plates of diameter 0.09 m and thickness of 0.001m are connected to the high voltage copper connectors. The inter-electrode separation can be changed by moving the electrodes through the electrode stands. After adjusting the distance between the electrodes they are fixed with the stands by means of screws. The substrates were kept on the lower electrode for plasma deposition.

#### **iii. Pumping unit**

For creating laboratory plasma, first step is pumping out the air/gas from the plasma chamber. In this system a rotary pump of vacuubrand (Vacuubrand GMBH & Co; Germany) is used.

#### **iv. Vacuum pressure gauge**

A vacuum pressure gauge head (Laybold AG, Germany) and a gauge meter (Thermotron<sup>TM</sup> 120) are used to measure inside pressure of the plasma deposition chamber.

#### **v. Input power for plasma generation**

The input power supply for plasma excitation comprises of a step-up high-tension transformer and a variac. The voltage ratio at the output of the high-tension transformer is about 16 times that of the output of the variac. The maximum output of the variac is 220V and that of the transformer is about 3.5 KV with a maximum current of 100 mA. The deposition rate increases with power at first and then becomes independent of power at high power values at constant pressure and flow rate.

#### **vi. Monomer injecting system**

The monomer injecting system consists of a conical flask of 25 ml capacity and a Pyrex glass tube with capillarity at the end portion. The capillary portion is well fitted with metallic tube of the nozzle of the high vacuum needle valve. The conical flask with its components is fixed by stand-clamp arrangement.

#### **vii. Supporting frame**

A metal frame of dimension 1.15mX0.76mX0.09m is fabricated with iron angle rods, which can hold the components described above. The upper and lower bases of the frame are made with polished wooden sheets. The wooden parts of the frame are varnished and the metallic parts are painted to keep it rust free. The pumping unit is placed on the lower base of the frame. On the upper base a suitable hole is made in the wooden sheet so that the bottom flange can be fitted with nut and bolts.

#### viii. Flowmeter

The system pressure of a gas flow is determined by the feed in rate of a gas and the pumping out rate of a vacuum system. The monomer flow rate is determined by a flowmeter. In the plasma polymerization set up a flowmeter (Glass Precision Engineering LTD, Meterate, England) is attached between the needle valve and the monomer bottle.

#### ix. Liquid nitrogen trap

Cold trap, particularly a liquid N<sub>2</sub> trap, acts as a trap pump for different type gas. The liquid N<sub>2</sub> trap system is placed in the fore line of the reactor chamber before the pumping unit in the plasma deposition system. It consists of a cylindrical shape chamber having 6.4 cm diameter and 11.5 cm in length using brass material.

### 3.5. Generation of Glow Discharge Plasma in the Laboratory

Glow discharges are produced by an applied static or oscillating electric field where energy is

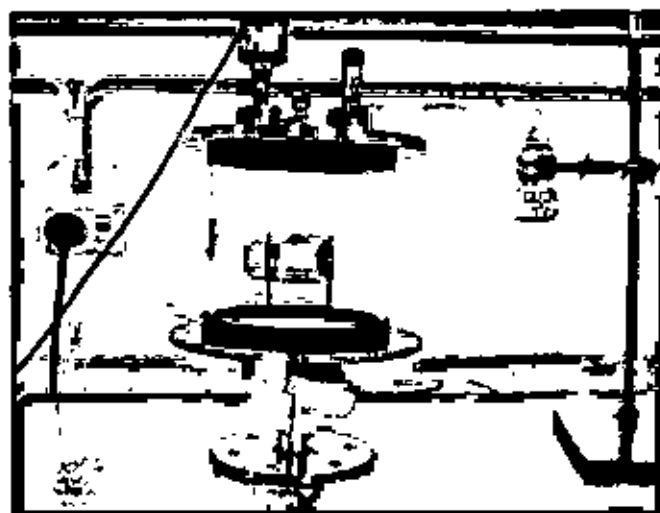


Fig.3.4. Plasma polymerization set-up.



transferred to free electrons in vacuum. Inelastic collisions of the energetic free electrons with the gas molecules generate free radicals, ions, and species in electronically excited states. This process also generates more free electrons, which is necessary for a self-sustaining glow. The excited species produced are very active and can react with the surfaces of the reactors as well as themselves in the gas phase.

The chamber of the glow discharge reactor is evacuated to about 0.01 mbar. A high-tension transformer along with a variac is connected to the feed-through attached to the lower flange. While increasing the applied voltage, the plasma is produced across the electrodes at around 0.15-mbar-chamber pressure. Fig 3.4 shows the photograph of glow discharge plasma across the electrodes in the capacitively coupled parallel plate discharge chamber.

### 3.6. Deposition of Plasma Polymerized Thin Film

The important feature of glow discharge plasma is the non-equilibrium state of the overall system. In the plasmas considered for the purpose of plasma polymerization, most of the negative charges are electrons and most of the positive charges are ions. Due to large mass difference between electrons and ions, the electrons are very mobile as compared to the nearly stationary positive ions and carry most of the current. Energetic electrons as well as ions, free radicals, and vacuum ultraviolet light can possess energies well in excess of the energy sufficient to break the bonds of typical organic monomer molecules which range from approximately 3 to 10 eV. Some typical energy of plasma species available in glow discharge as well as bond energies encountered at pressure of approximately 0.01 mbar.

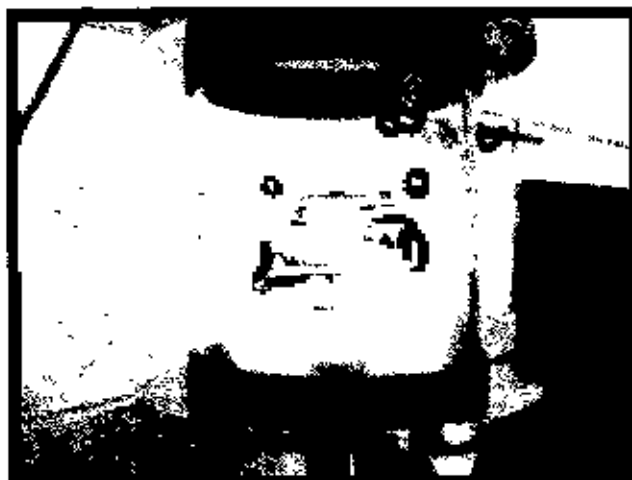


Fig.3.5. Glow discharge plasma during deposition

After finding the desired plasma glow in the reactor the monomer vapor is injected downstream to the primary air glow plasma for some time. Incorporation of monomer vapor changed the usual color of plasma into a light bluish color. Fig3.5 is the photograph of light bluish color monomer plasma in the plasma reactor. The deposition time was varied from 50-115 minute to get the PPDEA thin films of different thicknesses. The optimized conditions of thin film formation for the present study are:

Separation between two electrodes	4 cm
Position of the substrate	Lower electrode
Deposition voltage	15 W
Pressure in the reactor	$10^{-2}$ Torr
Maximum deposition time	1 hr 15 min

### 3.7. Contact Electrodes for Electrical Measurements

#### i. Electrode material

Aluminium (Al) (purity of 4N British Chemical Standard) was used for electrode deposition. Al has been reported to have good adhesion with glass slides. Al film has advantage of easy self-healing burn out of flaws in sandwich structure.

#### ii. Electrode deposition

Electrodes were deposited using an Edward coating unit E-306A(Edward, UK). The system was evacuated by an oil diffusion pump backed by an oil rotary pump. The chamber could be evacuated to a pressure less than  $10^{-5}$  Torr. The glass substrates with mask were supported by a metal rod 0.1 m above the tungsten filament. For the electrode deposition Al was kept on the tungsten filament. The filament was heated by low-tension power supply of the coating unit. The low-tension power supply was able to produce 100 A current at a potential drop of 10 V. During evacuation of the chamber by diffusion pump, the diffusion unit was cooled by the flow of chilled water and its outlet temperature was not allowed to rise above 305K. When the penning gauge reads about  $10^{-5}$  Torr, the Al on tungsten filament was heated by low-tension power supply until it was melted.

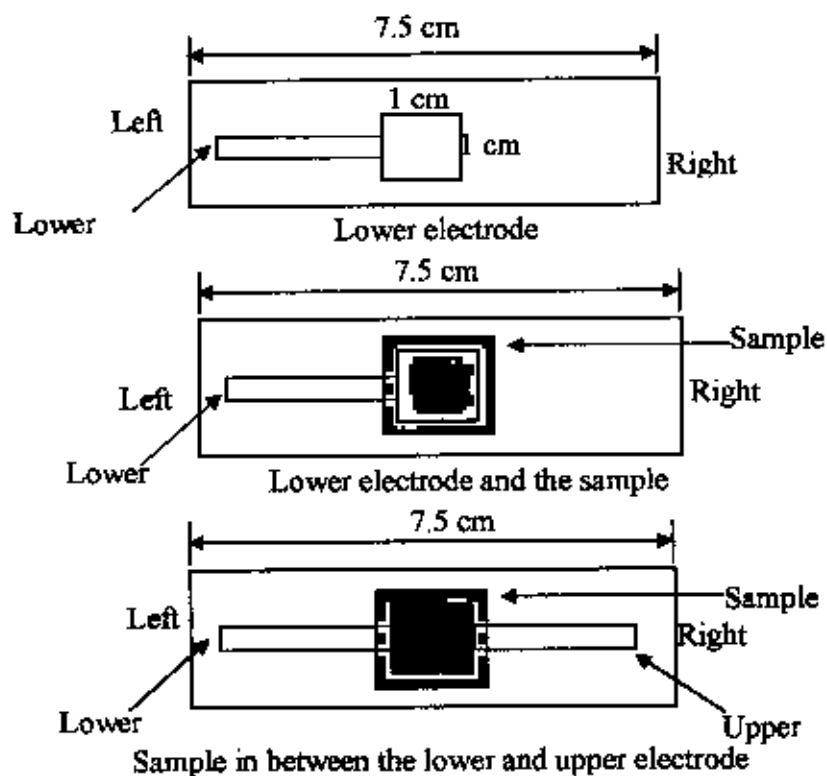


Fig 3.6. Electrode assembly

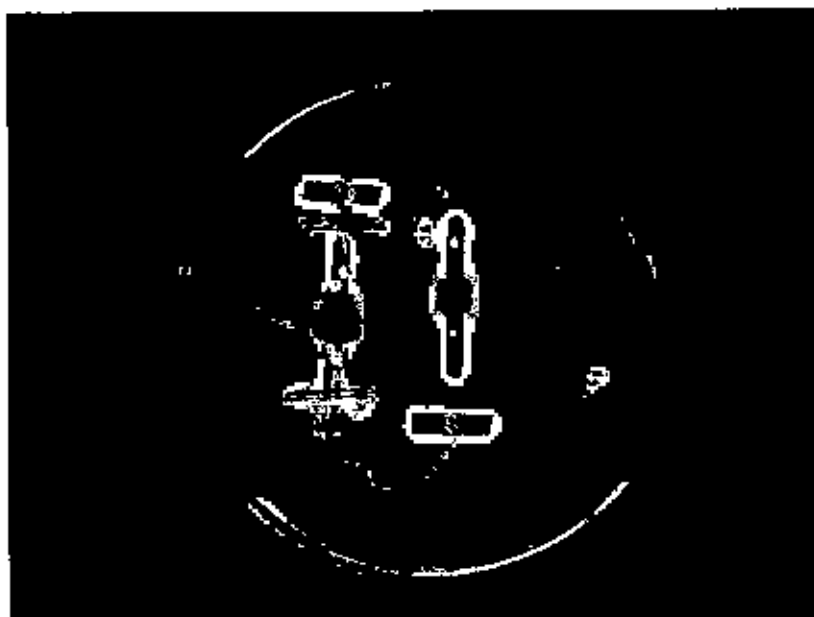


Fig.3.7. Samples for electrical measurement (2 samples from left) and for thickness measurement (sample on right).

### 3.8. Measurement of Thickness of the Thin Films

Thickness is the single most significant film parameter. Any physical quantity related to film thickness can in principle be used to measure the film thickness. It may be measured either by several methods with varying degrees of accuracy. The methods are chosen on the basis of their convenience, simplicity and reliability. Since the film thicknesses are generally of the order of a wavelength of light, various types of optical interference phenomena have been found to be most useful for measurement of film thicknesses. Several of the common methods are i) During Evaporation, ii) Multiple-Beam Interferometry, (Tolansky Fezeau fringes method, Fringes of equal chromatic order, Donaldson method etc.) iii) Michelson interferometer iv) Using a Hysteresis graph and other methods used in film-thickness determination with particular reference to their relative merits and accuracies. Multiple-Beam Interferometry technique was employed for the measurement of thickness of the PPDEA thin films. This technique is described below.

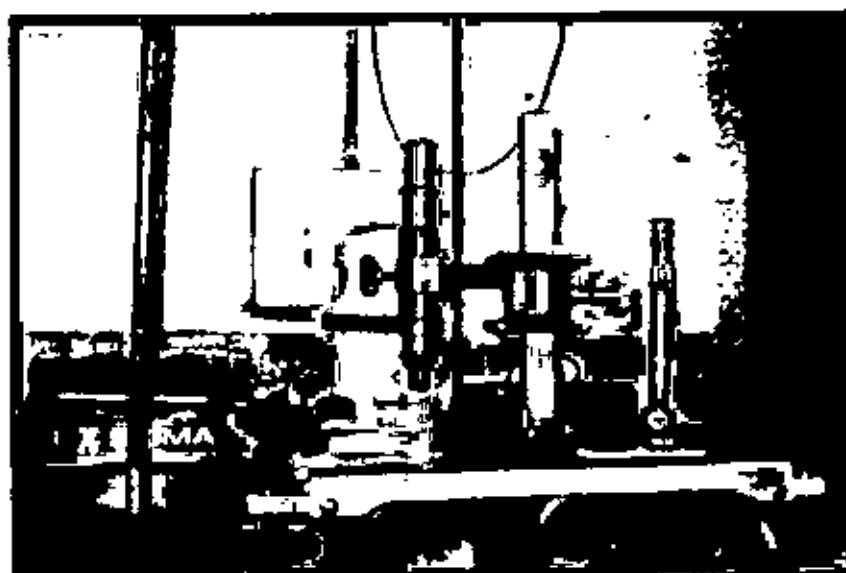


Fig.3.8. Multiple Beam Interferometric set-up in laboratory

### 3.9. Multiple-Beam Interferometry

This method utilizes the resulting interference effects when two silvered surfaces are brought close together and are subjected to optical radiation. This interference technique, which is of great value in studying surface topology in general, may be applied simply and directly to film-thickness determination. When a wedge of small angle is formed between unsilvered

glass plates, which are illuminated by monochromatic light, broad fringes are seen arising from interference between the light beams reflected from the glass on the two sides of the air wedge. At points along the wedge where the path difference is an integral and odd number of wavelengths, bright and dark fringes occur respectively. If the glass surfaces of the plates are coated with highly reflecting layers, one of which is partially transparent, then the reflected fringe system consists of very fine dark lines against a bright background. A schematic diagram of the multiple-beam interferometer along with a typical pattern of Fizeau fringes from a film step is shown in Fig.3.9. As shown in this figure, the film whose thickness is to be

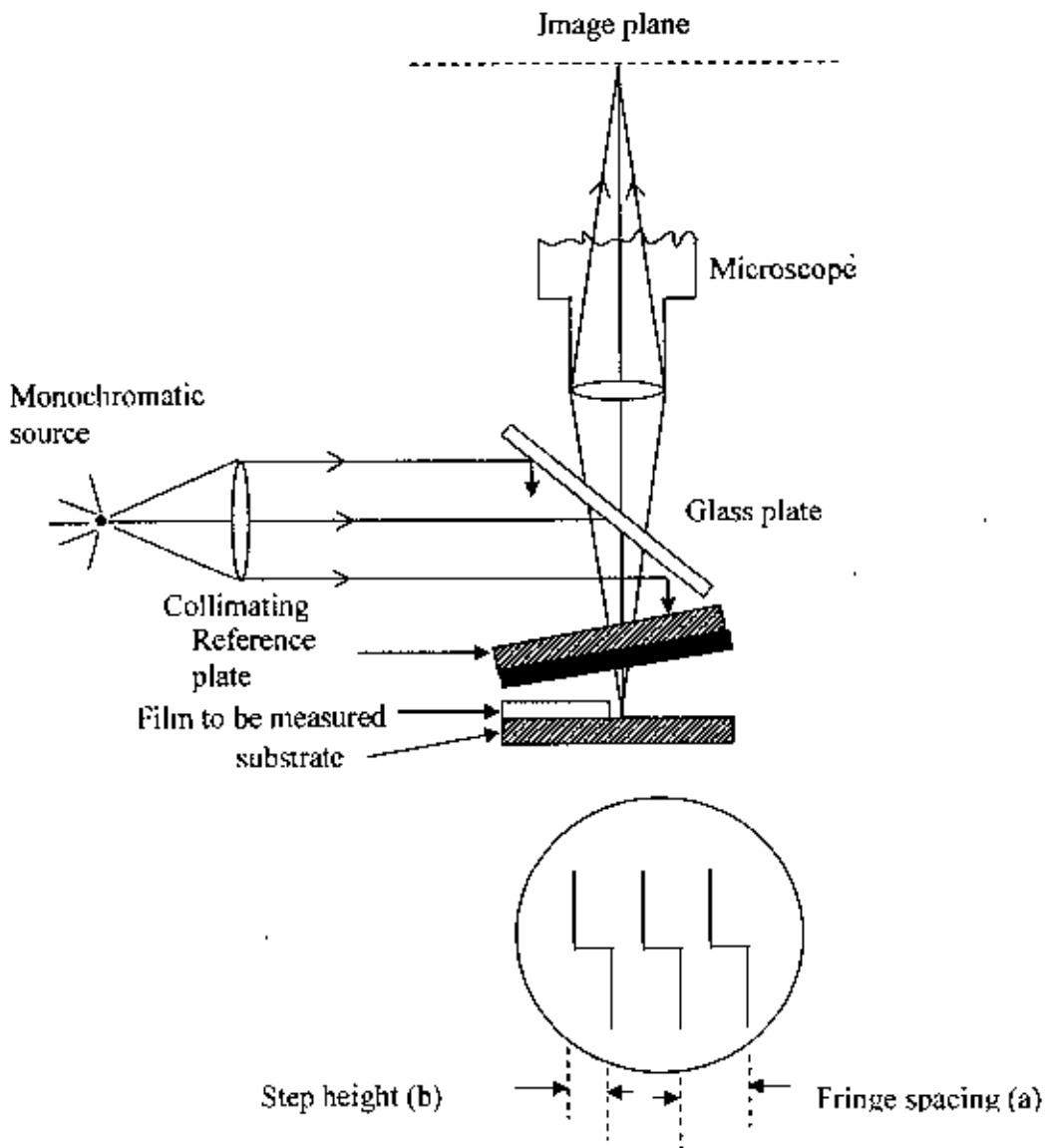


Fig. 3.9. Interferometer arrangement for producing reflection Fizeau fringes of equal thickness.

measured is over coated with a silver layer to give a good reflecting surface and a half-silvered microscope slide is laid on top of the film whose thickness is to be determined. A wedge is formed by the two microscope slides, and light multiply reflected between the two silvered surfaces forms an interference pattern with a discontinuity at the film edge as shown in Fig.3.9. The thickness of the film  $d$  can then be determined by the relation,

$$d = \frac{\lambda b}{2 a}$$

where,  $\lambda$  is the wavelength and  $b/a$  is the fractional discontinuity identified in the figure. In general, the sodium light is used, for which  $\lambda = 5893 \text{ \AA}$ . In measurement one half silvered glass slide is selected for maximum resolution. A resolution of about  $20 \text{ \AA}$  may be obtained in a careful measurement. In conclusion, it might be mentioned that the Tolansky method of film-thickness measurement is the most widely used and in many respects also the most accurate and satisfactory one [5].

### References

- [1] Yasuda H., "Plasma Polymerization" Academic Press, Inc, Tokyo (1985).
- [2] Chowdhury F.-U.-Z., A.B.M.O. Islam, A.H. Bhuiyan, " Chemical analysis of plasma-polymerized diphenyl thin films", *Vacuum*. 57 (2000) 43-50.
- [3] Inagaki N., "Plasma Surface Modification and Plasma Polymerization", Technomic Publishing Co. Inc., New York (1996).
- [4] Chen F.F., "Introduction to Plasma Physics", Plenum Press, New York (1974).
- [5] Tolansky S., "Multiple Beam Interferometry of Surfaces and Films", Clarendon Press, Oxford (1948).

## **CHAPTER 4**

### **STRUCTURAL ANALYSES OF PPDEA**

#### **4.1. Introduction**

#### **4.2. Scanning Electron Microscopy (SEM)**

##### 4.2.1. Theoretical background

##### 4.2.2. Energy Dispersive X-ray (EDX) analysis

##### 4.2.3. Experimental procedure

##### 4.2.4. Results and discussion

#### **4.3. Infrared spectroscopy**

##### 4.3.1. Molecular rotations

##### 4.3.2. Molecular vibrations

##### 4.3.3. Vibrational coupling

##### 4.3.4. Theory of Infrared Absorption

##### 4.3.5. Summary of absorptions of bonds in organic molecules

##### 4.3.6. Infrared activity

##### 4.3.7. Sample Preparation

##### 4.3.10. Results and Discussion

#### References

#### 4.1. Introduction

This chapter includes the study of surface structure, elemental analysis and chemical characterization of PPDEA by means of SEM, EDX and IR analysis.

The use of SEM can be found in numerous investigations dealing with the surface morphology of different polymer materials. In the case of plasma polymer the main interest is to find a homogeneous, dense, without pinhole thin films which are useful as corrosion protective coatings for microelectronic devices and selective layers in sensors [1-5]

It is rarely, if ever, possible to identify an unknown compound by using IR spectroscopy alone. Its principal strengths are: (i) it is a quick and relatively cheap spectroscopic technique, (ii) it is useful for identifying certain functional groups in molecules and (iii) an IR spectrum of a given compound is unique and can therefore serve as a fingerprint for this compound. Researchers apply this technique enormously because it involves collecting absorption information and analyzing it in the form of a spectrum.[1, 6-17]

#### 4.2. Scanning Electron Microscopy (SEM)

In SEM a beam of electrons is generated in the electron gun, located at the top of the column, which is pictured to the left. This beam is attracted through the anode, condensed by a condenser lens, and focused as a very fine point on the sample by the objective lens.

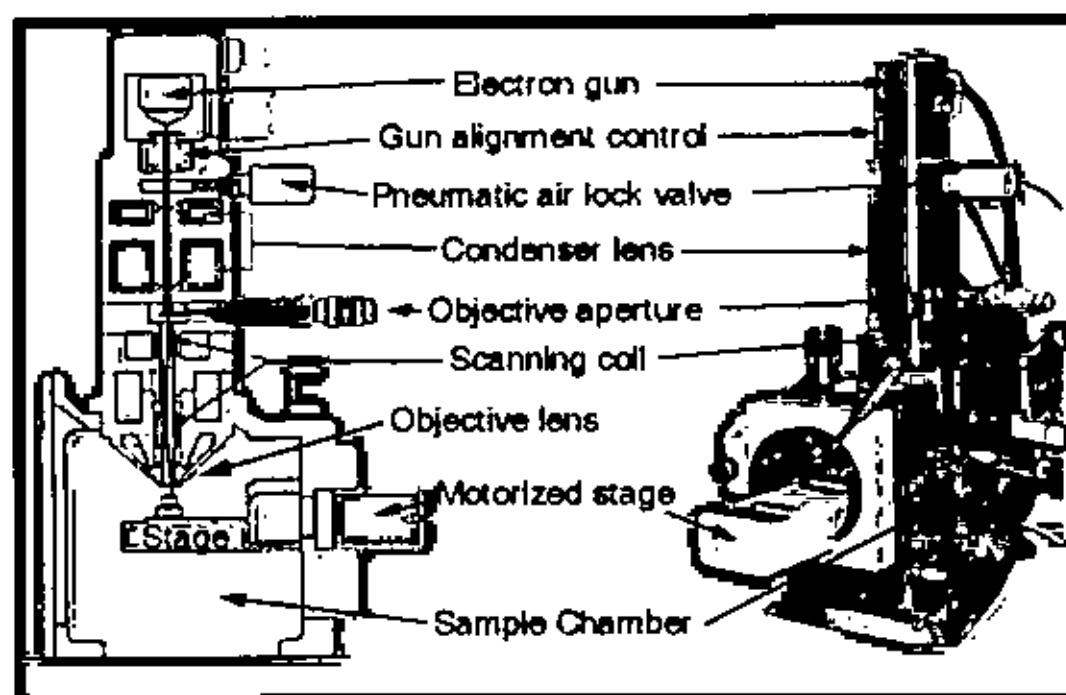


Fig 4.1. Schematic diagram of a scanning electron microscope



The scan coils are energized (by varying the voltage produced by the scan generator) and create a magnetic field which deflects the beam back and forth in a controlled pattern. The varying voltage is also applied to the coils around the neck of the Cathode-ray tube (CRT) which produces a pattern of light deflected back and forth on the surface of the CRT. The pattern of deflection of the electron beam is the same as the pattern of deflection of the spot of light on the CRT. The electron beam hits the sample, producing secondary electrons and backscattered electrons from the sample. These electrons are collected by a secondary detector or a backscatter detector, converted to a voltage, and amplified. The amplified voltage is applied to the grid of the CRT and causes the intensity of the spot of light to change. The image consists of thousands of spots of varying intensity on the face of a CRT that correspond to the topography of the sample.

#### 4.2.1. Theoretical background

At any given moment, the specimen is bombarded with electrons over a very small area; several things may happen to these electrons. They may be elastically reflected from the specimen, with no loss of energy or absorbed by the specimen and give rise to secondary electrons of very low energy, together with X-rays. They may be absorbed and give rise to the emission of visible light (an effect known as cathodoluminescence). And they may give rise to electric currents within the specimen. All these effects can be used to produce an image.

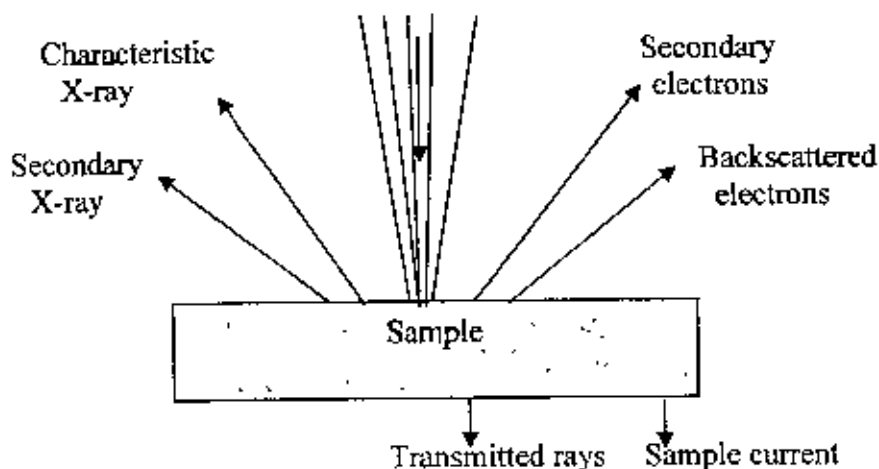


Fig 4.2. Phenomena occurring in scanning electron microscope.

Secondary electron imaging is the most common because it can be used with almost any specimen. Moving electrons are not only moving particles, but also behave as waves; this

is called in quantum mechanics “particle/wave duality”. Therefore, electrons obey all the optical laws of diffraction. If there are two small slits beside each other, on one side of the slit a small electron source and at the other side of the slit a fluorescent screen, if the electron were only particles, two illuminated lines would be seen on the screen. However, in reality the screen will show a large number of black and white lines, which is only due to the wave like nature of electrons. The wavelength of an electron is much smaller than that of visible light. Therefore, the electron microscope has a possibility of showing much smaller details.

Small samples up to several millimeters and sometimes even larger can be investigated directly in the SEM if the sample material has a sufficiently high electric conductivity to prevent charging produced. For insulating samples, it needs to be coated with an extremely thin layer of an electrically conducting material (Ag, Au etc).

#### 4.2.2. Energy Dispersive X-ray (EDX) analysis

EDX Analysis stands for Energy Dispersive X-ray analysis. It is sometimes referred to also as EDS or EDAX analysis. It is a technique used for identifying the elemental composition of the specimen, or an area of interest thereof. The EDX analysis system works as an integrated feature of a scanning electron microscope (SEM), and can not operate on its own without the latter.

During EDX analysis, the specimen is bombarded with an electron beam inside the scanning electron microscope. The bombarding electrons collide with the specimen atoms' own electrons, knocking some of them off in the process. A position vacated by an ejected inner shell electron is eventually occupied by a higher-energy electron from an outer shell. To be able to do so, however, the transferring outer electron must give up some of its energy by emitting an X-ray.

The amount of energy released by the transferring electron depends on which shell it is transferring from, as well as which shell it is transferring to. Furthermore, the atom of every element releases X-rays with unique amounts of energy during the transferring process. Thus, by measuring the amounts of energy present in the X-rays being released by a specimen during electron beam bombardment, the identity of the atom from which the X-ray was emitted can be established.

The EDX spectrum is just a plot of how frequently an X-ray is received for each energy level. An EDX spectrum normally displays peaks corresponding to the energy levels for

which the most X-rays had been received. Each of these peaks is unique to an atom, and therefore corresponds to a single element. The higher a peak in a spectrum, the more concentrated the element is in the specimen.

### 4.2.3. Experimental procedure

The PPDEA thin films were deposited onto small pieces of chemically cleaned glass substrates. Two samples of different thicknesses were sorted out for the analysis. To avoid the charging effect the PPDEA films were coated with a thin layer of gold by gold sputtering (AGAR Auto Sputter Coater). The SEM and EDX were performed by a scanning electron microscope (S-3400 N Hitachi, Japan).

### 4.2.4. Results and discussion

The SEM micrographs of thin films of PPDEA were taken in various magnifications (0.5, 1, 6, 8, 12, 35 K) and various accelerating voltages (10, 15 KV), which are shown in Fig.4.3 to 4.5. Smooth, flawless and pinhole free surfaces are observed for PPDEA thin films. No significant change is observed in PPDEA thin films of different thicknesses.

The compositional analysis was taken for the same samples by EDX, which is attached to the SEM. The EDX spectra and weight percentages of the samples are shown in Fig 4.6. The weight percentage of DEA monomer is shown in Table 4.1. The observations indicate the presence of C, N and O in the samples. The main obstacle of EDX is that it cannot detect the presence of H. The presence of O in PPDEA implies incorporation of carbonyl and hydroxyl groups through the reaction of the free radicals or from the chamber during plasma polymerization and these two phenomena are common in plasma polymer. It is also predicted that the PPDEA films are deficient in carbon and nitrogen with respect to monomer, which may be due to the breakdown of bonds owing to the complex reaction during plasma polymerization.

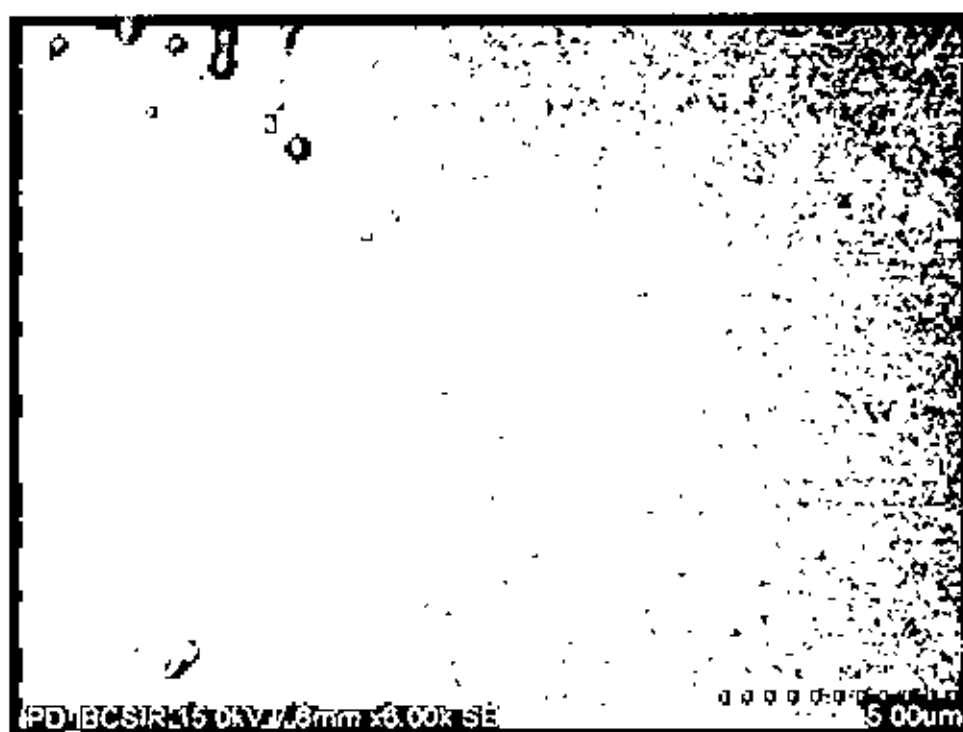


(a)

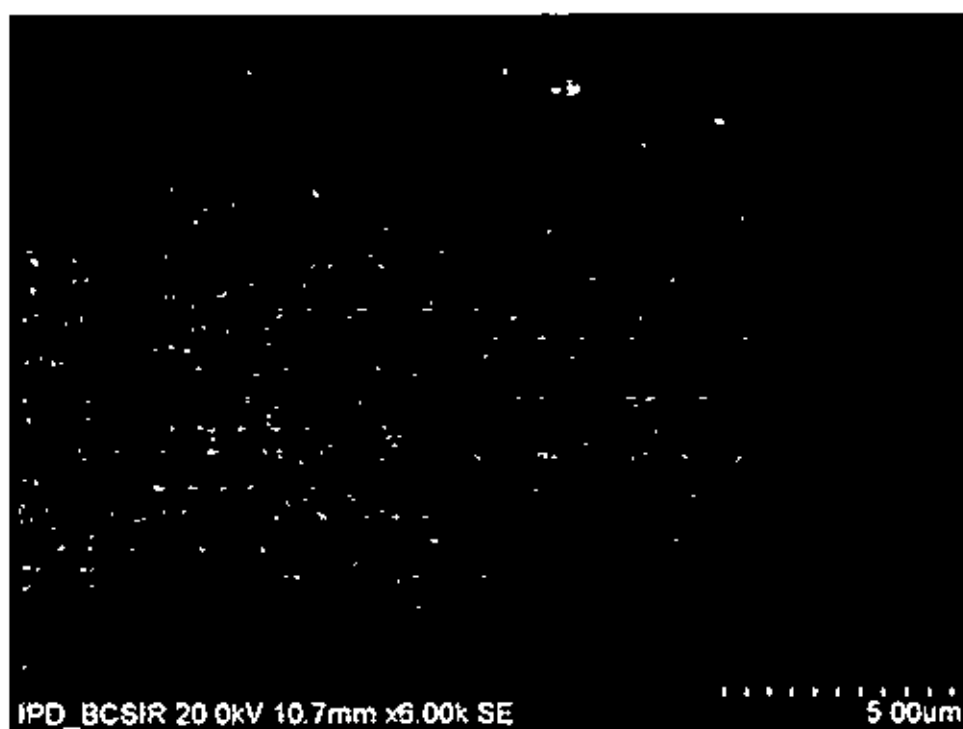


(b)

Fig. 4.3 Micrographs of PPDEA thin films onto glass substrate (magnification 500x) (a)  $d = 250$  nm (b)  $d = 350$  nm

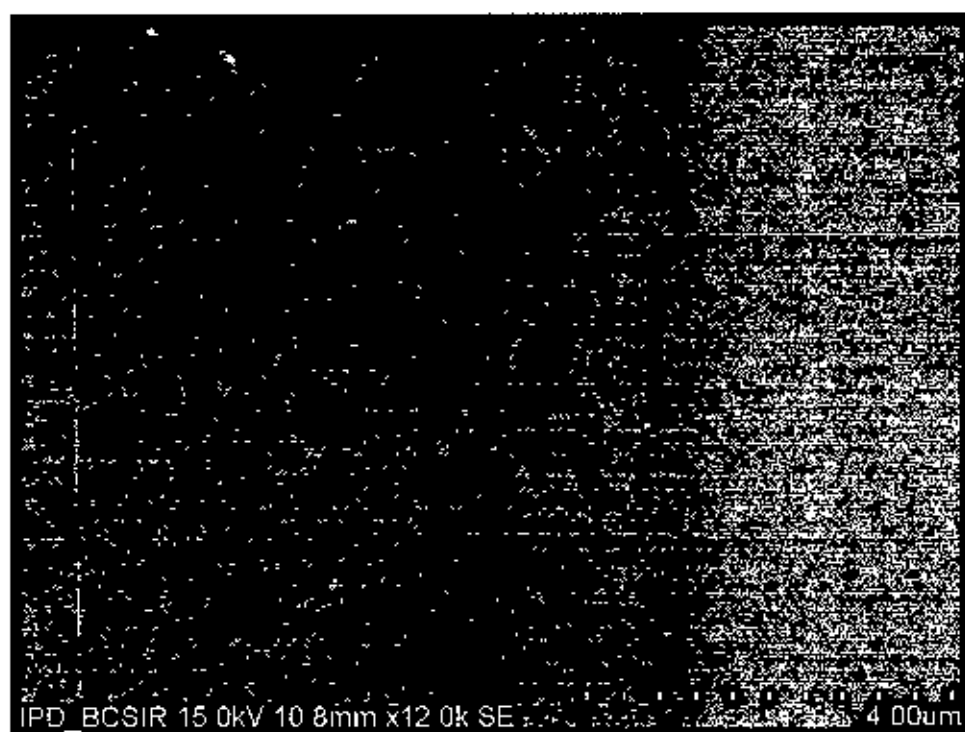


(a)

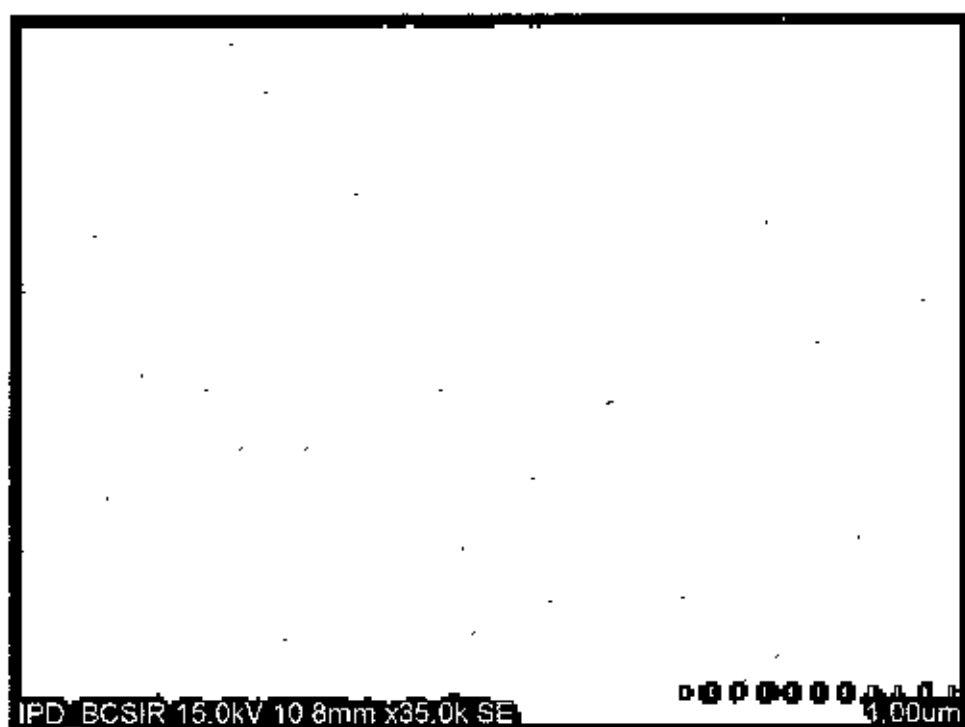


(b)

Fig. 4.4 Micrographs of PPDEA thin films onto glass substrate (magnification 6.00Kx) (a)  $d = 250$  nm (b)  $d = 350$  nm



(a)



(b)

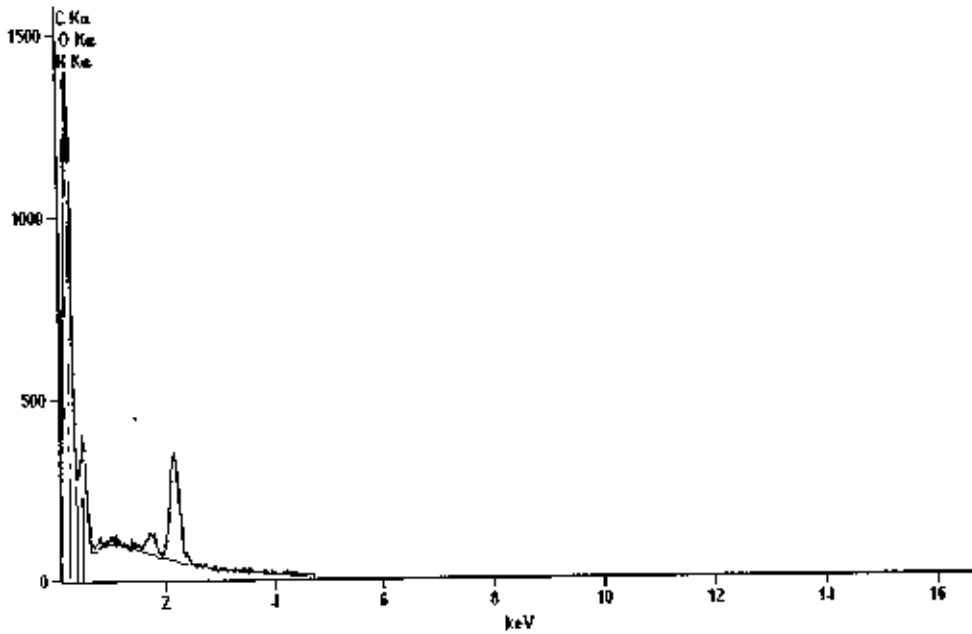
Fig. 4.5 Micrographs of PPDEA thin film ( $d=350$  nm) onto glass substrate  
(a)magnification 12.0 Kx (b) magnification 35.0 Kx

Table 4.1 Weight % of monomer (DEA)

	C	N	H
<i>Monomer (DEA)</i>	80.5	9.5	10

Full scale counts: 1399

■ Thin Film 3  
 □ Synthetic Spectrum



## Net Counts

	C	N	O
<i>Thin Film 3</i>	15414	671	2790

## Weight %

	C	N	O
<i>Thin Film 3</i>	79.27	8.51	12.22

## Weight % Error

	C	N	O
<i>Thin Film 3</i>	+/-1.58	+/-3.21	+/-0.65

Fig 4.6 EDX spectrum and weight percentages of PPDEA thin films.

### 4.3. Infrared Spectroscopy

The term "infrared" covers the range of the electromagnetic spectrum between 0.78 and 1000  $\mu\text{m}$ . In the context of infra red spectroscopy, wavelength is measured in "wavenumbers", which have the unit  $\text{cm}^{-1}$ .

wavenumber = 1 / wavelength in centimeters

It can also take the wavenumber as being a unit of energy, thus  $1 \text{ cm}^{-1}$  corresponds to  $1.9855 \times 10^{-16}$  erg/molecule, or  $11.959 \times 10^{-7}$  ergs/mole.

It is useful to divide the infra red region into three sections; near, mid and far infra red.

Region	Wavelength range ( $\mu\text{m}$ )	Wavenumber range ( $\text{cm}^{-1}$ )
Near	0.78 - 2.5	12800 - 4000
Middle	2.5 - 50	4000 - 200
Far	50 - 1000	200 - 10

The most useful IR region lies between 4000 and  $670 \text{ cm}^{-1}$ .

#### 4.3.1. Molecular rotations

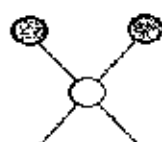
Rotational transitions are of little use to the spectroscopist. Rotational levels are quantized, and absorption of IR by gases yields line spectra. However, in liquids or solids, these lines broaden into a continuum due to molecular collisions and other interactions.

#### 4.3.2. Molecular vibrations

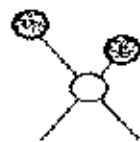
The positions of atoms in a molecule are not fixed; they are subject to a number of different vibrations. Vibrations fall into the two main categories of stretching and bending.

**Stretching:** Change in inter-atomic distance along bond axis.

##### Stretching vibrations



Symmetric



Asymmetric

**Bending:** Change in angle between two bonds. There are four types of bend:

Rocking, Scissoring, Wagging, Twisting



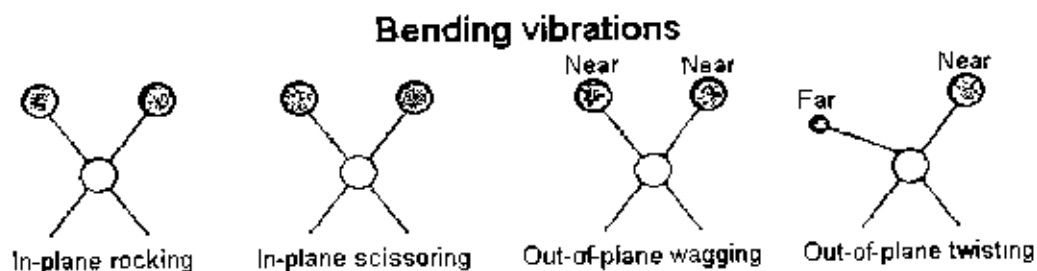


Fig 4.7. Different vibrational modes

### 4.3.3. Vibrational coupling

In addition to the vibrations mentioned above, interaction between vibrations can occur (coupling) if the vibrating bonds are joined to a single, central atom. Vibrational coupling is influenced by a number of factors;

- The vibration must be of the same symmetry species if interaction is to occur.
- Strong coupling of stretching vibrations occurs when there is a common atom between the two vibrating bonds.
- Coupling of bending vibrations occurs when there is a common bond between vibrating groups.
- Coupling between a stretching vibration and a bending vibration occurs if the stretching bond is one side of an angle varied by bending vibration.
- Coupling is greatest when the coupled groups have approximately equal energies.
- No coupling is seen between groups separated by two or more bonds.[2]

### 4.3.4. Theory of infrared absorption

IR radiation does not have enough energy to induce electronic transitions as seen with UV. Absorption of IR is restricted to compounds with small energy differences in the possible vibrational and rotational states. For a molecule to absorb IR, the vibrations or rotations within a molecule must cause a net change in the dipole moment of the molecule. The alternating electrical field of the radiation (electromagnetic radiation consists of an oscillating electrical field and an oscillating magnetic field, perpendicular to each other) interacts with fluctuations in the dipole moment of the molecule. If the frequency of the radiation matches the vibrational frequency of the molecule then radiation will be absorbed, causing a change in the amplitude of molecular vibration. The bonds that hold a molecule together and the masses of the constituents are so related that the molecule exerts radiation of a frequency, corresponding to one of its normal vibrating frequencies, for the

incident beam. Therefore, the absorption bands in an infrared spectrum are at frequencies corresponding to the frequencies of vibration of the molecule concerned [3].

Each atom has three degrees of freedom, corresponding to motions along any of the three Cartesian coordinate axes ( $x$ ,  $y$ ,  $z$ ). A polyatomic molecule of  $n$  atoms has  $3n$  total degrees of freedom. However, 3 degrees of freedom are required to describe translation, the motion of the entire molecule through space. Additionally, 3 degrees of freedom correspond to rotation of the entire molecule. Therefore, the remaining  $3n - 6$  degrees of freedom are true, fundamental vibrations for nonlinear molecules. Linear molecules possess  $3n - 5$  fundamental vibrational modes because only 2 degrees of freedom are sufficient to describe rotation. Among the  $3n - 6$  or  $3n - 5$  fundamental vibrations (also known as normal modes of vibration), those that produce a net change in the dipole moment may result in an IR activity.

#### 4.3.5. Summary of absorptions of bonds in organic molecules

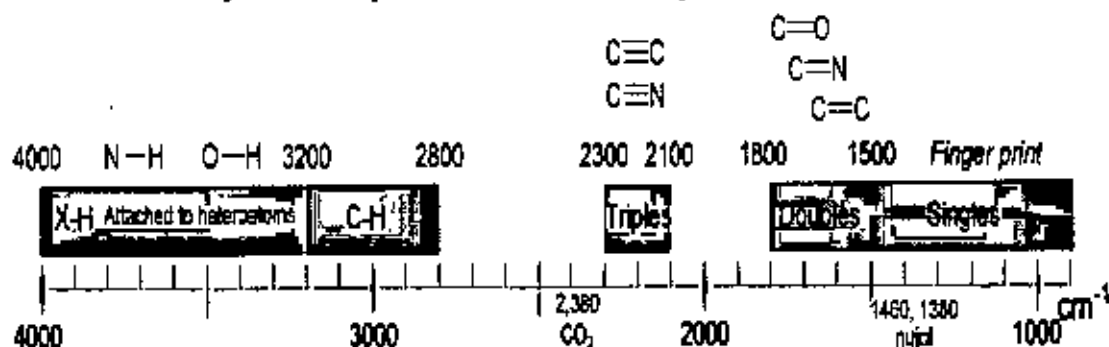


Fig.4.8. Infrared Spectroscopy Correlation Table

#### 4.3.6. Infrared activity

Not all possible vibrations within a molecule will result in an absorption band in the infrared region. To be infrared active the vibration must result in a change of dipole moment during the vibration. This means that for homonuclear diatomic molecules such as Hydrogen ( $\text{H}_2$ ), Nitrogen ( $\text{N}_2$ ) and Oxygen ( $\text{O}_2$ ) no infrared absorption is observed, as these molecules have zero dipole moment and stretching of the bonds will not produce one. For heteronuclear diatomic molecules such as Carbon Monoxide ( $\text{CO}$ ) and Hydrogen Chloride ( $\text{HCl}$ ), which do possess a permanent dipole moment, infrared activity occurs because stretching of this bond leads to a change in dipole moment (since Dipole Moment = Charge  $\times$  Distance). It is important to remember that it is not necessary for a compound to have a permanent dipole moment to be infrared active. In the case of Carbon Dioxide

(CO<sub>2</sub>) the molecule is linear and centrosymmetric and therefore, does not have a permanent dipole moment. This means that the symmetric stretch will not be infrared active. However, in the case of the asymmetric stretch a dipole moment will be periodically produced and destroyed resulting in a changing dipole moment and therefore infrared active.

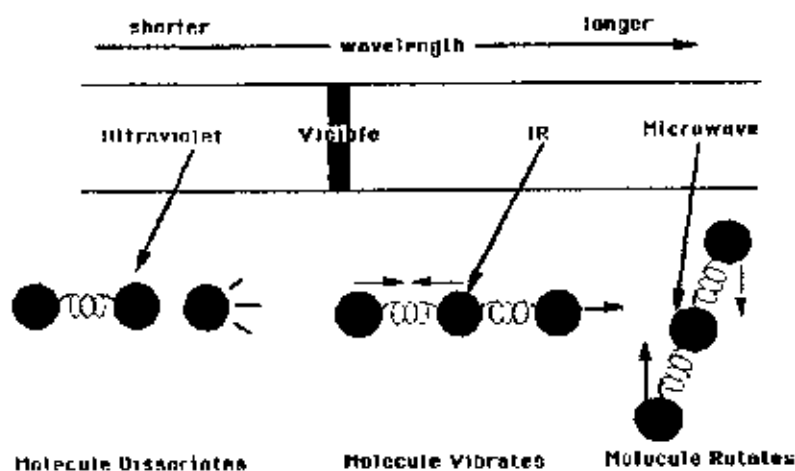


Fig.4.9. Molecular responses to radiation

Assignments for stretching vibrations can be approximated by the application of Hook's law. In the application of the law, 2 atoms and their connecting bond are treated as a simple harmonic oscillator composed of 2 masses joined by a spring. The following equation, derived from Hook's law, states that, the vibrational frequency

$$\bar{\nu} = \frac{1}{2\pi c} \left( \frac{f}{\frac{M_x M_y}{M_x + M_y}} \right)^{\frac{1}{2}}$$

Where  $c$  = velocity of light (cm/sec),  $F$  = Force constant of bond (dynes/cm),  $M_x$  and  $M_y$  = mass (g) of atom  $x$  and atom  $y$ , respectively.

#### i. Factors Influencing Number of Absorption Bands

Infrared absorption occurs as a result of vibrational and rotational transitions within the molecule. Because only a few compounds exhibit pure rotational bands, the vibrational absorption bands are of more practical interest. There are other factors influencing the number of absorption bands.

\* Overtone bands: Absorption at frequencies representing the fundamental frequencies at the multiples of the fundamentals.

\* Combination bands: Two fundamental vibrations interact and are influenced by radiation at the combined frequency.

\* **Vibrational-Rotational bands:** The single vibrational band is accompanied by a series of subsidiary bands both at lower and higher frequencies. Gas spectra are commonly characterized by very complex vibration-rotation systems.

\* **Harmonic coupling bands:** Interaction from adjacent groups of nearly identical oscillation frequencies produces a series of bands quite apart from those normally expected. This phenomenon is relatively uncommon.

## ii. Factors limiting the number of absorption bands

The total number of observed absorption bands is generally different from the total number of fundamental vibrations. It is reduced because some modes are not IR active and a single frequency can cause more than one mode of motion to occur. Conversely, additional bands are generated by the appearance of overtones (integral multiples of the fundamental absorption frequencies), combinations of fundamental frequencies, differences of fundamental frequencies, coupling interactions of two fundamental absorption frequencies, and coupling interactions between fundamental vibrations and overtones or combination bands (Fermi resonance). The intensities of overtone, combination, and different bands are less than those of the fundamental bands. The combination and blending of all the factors thus create a unique IR spectrum for each compound.

Infrared radiation is absorbed and the associated energy is converted into these types of motions. The absorption involves discrete, quantized energy levels. However, the individual vibrational motion is usually accompanied by other rotational motions.

\* No change in dipole moment due to symmetry.

\* Degeneracy: Vibrational frequencies located too closely.

\* Weak absorptions.

### 4.3.7. Sample Preparation

There are a variety of techniques for sample preparation dependent on the physical form of the sample to be analyzed.

#### i. Solids

There are two main methods for sample preparation involving the use of Nujol mull or potassium bromide disks. However there is also a third option of preparing a solution in a suitable solvent (not infrared active in the region of interest).

#### ii. Nujol Mull

The sample is ground using an agate mortar and pestle to give a very fine powder. A small amount is then mixed with nujol to give a paste and several drops of this paste are then applied between two sodium chloride plates (these do not absorb infrared in the region of interest). The plates are then placed in the instrument sample holder ready for scanning.

### iii. Potassium Bromide disk

A very small amount of the solid (approximately 1–2 mg) is added to pure potassium bromide powder (approximately 200 mg) and ground up as fine as possible. This is then placed in a small die and put under pressure mechanically. The pressure is maintained for several minutes before removing the die and the KBr disk formed. The disk is then placed in a sample holder ready for scanning. The success of this technique is dependent on the powder being ground as fine as possible to minimize infrared light scattering off the surface of the particles. It is also important that the sample be dry before preparation. KBr has no infrared absorption in the region 4000 – 650  $\text{cm}^{-1}$ .

### iv. Thin Films

The infrared spectrum of a thin film can be easily obtained by placing a sample in a suitable holder, such as a card with a slot cut for the sample window. This method is often used for checking the calibration of an instrument with a polystyrene sample as the bands produced by this material are accurately known.

### v. Liquids

This is possibly the simplest and most common method of sample preparation. A drop of the sample is placed between two potassium bromide or sodium chloride circular plates to produce a thin capillary film. The plates are then placed in a holder ready for analysis.

### vi. Gases

To obtain an infrared spectrum of a gas requires the use of a cylindrical gas cell with windows at each end composed of an infrared inactive material such as KBr, NaCl or  $\text{CaF}_2$ . The cell usually has an inlet and outlet port with a tap to enable the cell to be easily filled with the gas to be analyzed.

## 4.3.8. Instrumentation

In simple terms, IR spectra are obtained by detecting changes in transmittance (or absorption) intensity as a function of frequency. This instrument uses a source of infrared radiation such as a nichrome wire or cooled rod of silicon carbide to produce a range of frequencies which are then separated into individual frequencies using a monochromator diffraction grating. The beam produced is then split into two; and one passes through the

sample whilst the other is used as a reference beam. The two beams then converge on the detector which measures the difference in intensity and then sends a proportional signal to the recorder. The resulting plot is a measure of transmission against frequency which is usually plotted as wavenumber ( $\text{cm}^{-1}$ ). Most commercial instruments separate and measure IR radiation using dispersive spectrometers or Fourier transform spectrometers. This method has some obvious advantages. Firstly, it is much quicker, taking seconds instead of minutes to record a complete spectrum. A further advantage is that it is possible to get a spectrum from very small or very dilute samples by performing multiple scans and adding the data to improve the signal-to-noise ratio. Slow scans using diffraction gratings are inefficient. Almost all modern IR spectrometers use a different approach, the Fourier transform method, to scan the full spectral range at the same time.

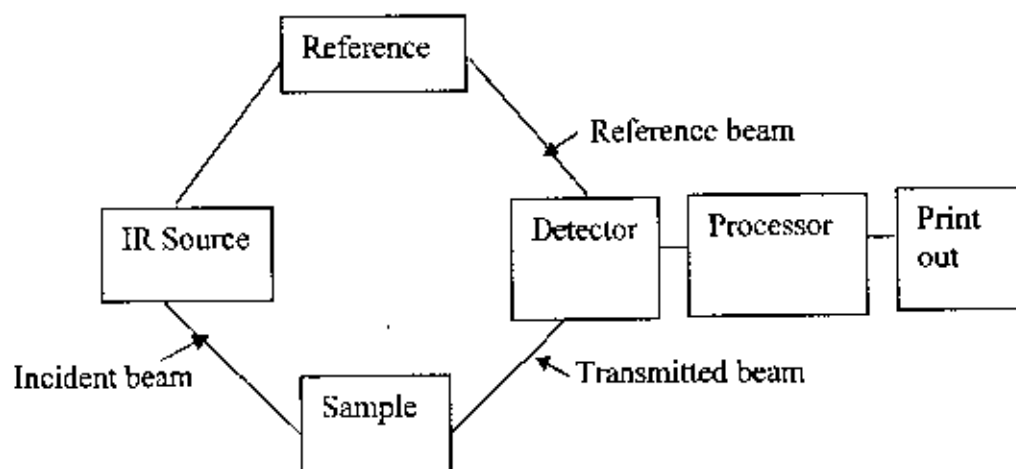


Fig.4.10. Schematic Diagram of a double beam Infrared Spectrometer

#### 4.3.9. Experimental procedure

The IR spectroscopic analysis was carried out by a double beam SHIMADZU FTIR-8900 spectrophotometer. The PPDEA sample was collected from the electrode surface by scrapping method. The sample for IR measurement was prepared by above mentioned KBr technique. All the spectra were recorded in transmittance mode and the wave number range was from  $4000$  to  $500 \text{ cm}^{-1}$ . The IR spectrum of DEA liquid monomer was also recorded by placing the liquid between two thin KBr pellets.

#### 4.3.10. Results and Discussion

Reflecting the various extent of fragmentation and rearrangement of atoms and legends during the process of polymer formation in plasma, IR spectra also vary with the

conditions of the plasma polymerization. In general the IR spectrum of the plasma polymer in comparison with the conventional polymer of the monomer may contain most major peaks characteristic of the conventional polymer, but not always nor in a quantitative manner. Sharp peaks in the spectrum of the conventional polymer generally become less resolved broader bands and some peaks are significantly reduced. The FTIR spectra of DEA monomer and as deposited PPDEA are shown in Fig 4.11 as curves M and P respectively. In spectrum M the weak absorption peak at about  $3550\text{-}3420\text{ cm}^{-1}$  in fig indicates N-H asymmetric stretching and that at about  $3395\text{ cm}^{-1}$  represents N-H symmetric stretching. These frequencies are normally related to the non-hydrogen bonded  $\text{-NH}_2$

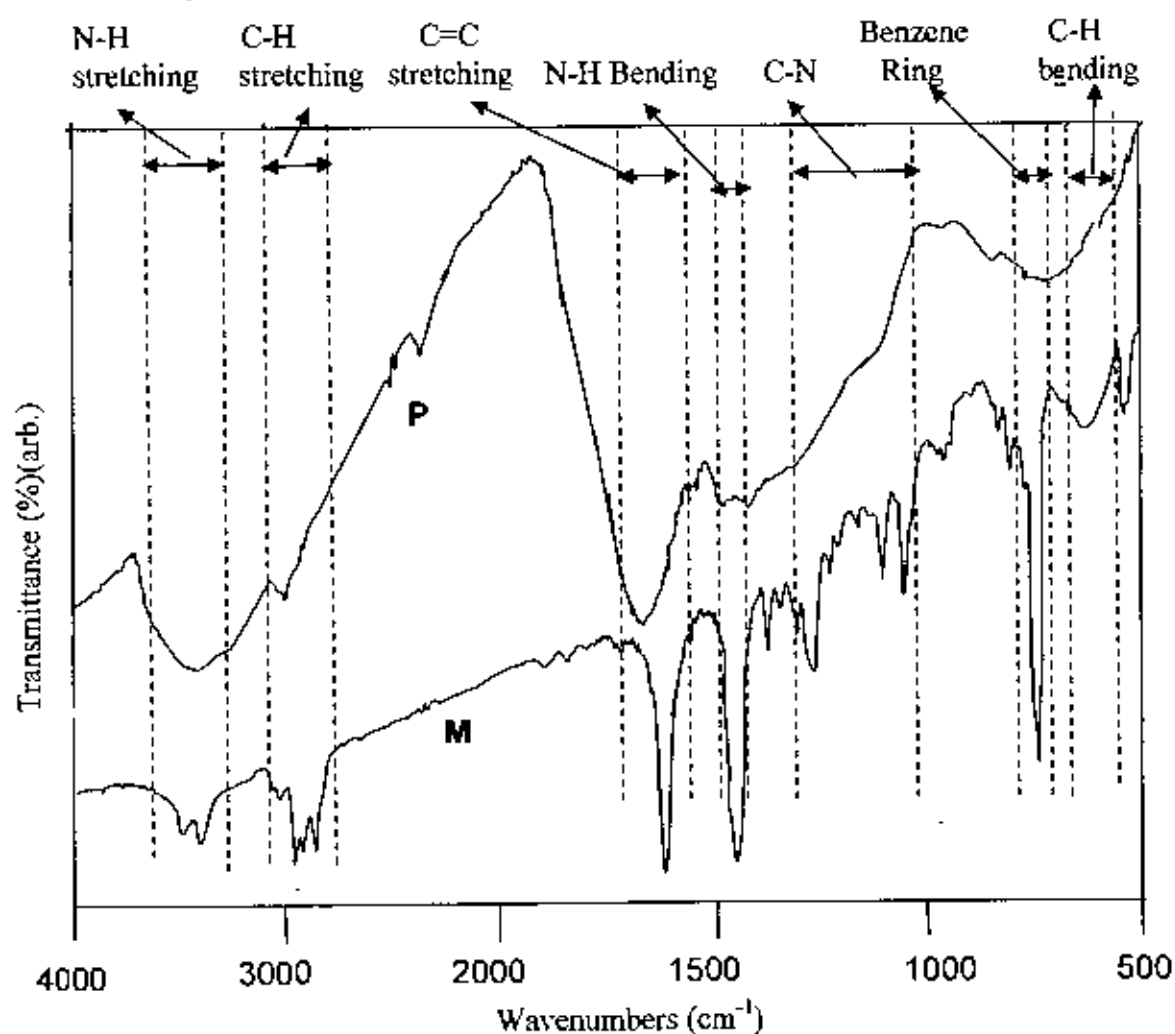


Fig .4.11. The IR spectra of DEA monomer, spectrum M and PPDEA, spectrum P. group and show similarities to the changes observed in hydroxyl absorption accompanying changes in concentration, solvent and environment. But in spectrum P a wide absorption band is found at about  $3364\text{ cm}^{-1}$ , which can originate from a primary amine, a secondary amine or an imine as well and the asymmetric stretching band is merged in the broad band.

Multiple bands at  $2964\text{ cm}^{-1}$  and  $2934\text{ cm}^{-1}$ ,  $2871\text{ cm}^{-1}$  in spectrum M, correspond to the C-H stretching vibration and retained in reduced form at  $2926\text{ cm}^{-1}$  in spectrum P. This is indicative of monomer fragmentation during the plasma polymerization. A weak absorption at  $1844\text{ cm}^{-1}$  of C=O asymmetric stretching is identified in spectrum M and is also detected in spectrum P. This indicates that there are trapped free radicals in the PPDEA which reacts with the atmospheric oxygen. Clearly, there appears a considerably stronger absorption band at  $1620\text{ cm}^{-1}$  in spectrum M, which became stronger and broader in P spectrum, which may be attributed to the conjugated C=C stretching vibration indicating presence of conjugation during plasma polymerization of DEA. It can be seen from curve P that the intensity of absorption band corresponding to aromatic ring N-H bending vibrations ( $1545, 1456\text{ cm}^{-1}$ ) is diminished in PPDEA which is significantly present in the DEA. This is indicative of monomer (aromatic ring) fragmentation during the plasma polymerization. In curve M the C-N (saturated carbon) stretching vibration is observed at  $1213\text{ cm}^{-1}$  and  $1167\text{ cm}^{-1}$ , which is found to be merged in the broad band in curve P. This vibration is usually a doublet due to asymmetric and symmetric vibrational possibilities. When an aromatic ring is present, two bands are observed at high frequency band due to conjugation of electron pair of the nitrogen atom with the ring, imparting double-bond

Table 4.2. Assignments of IR absorption peaks for DEA and PPDEA

Type of vibration	Wavenumber $\text{cm}^{-1}$	
	DEA monomer	PPDEA
N-H asymmetric stretching	3490	Marged in broad band 3600-3400
N-H symmetric stretching	3395	3363
C-H stretching	2964, 2934, 2871	2926
C=O asymmetric stretching	1627	1620
C=C stretching	1620	1628
N-H bending	1545, 1456	1558
C-N stretching	1213, 1167	Marged in broad band 1200-1000
Tetrasubstituted Benzene stretching	837, 812	Broad band 850-800
N-H Out of plane bending	744	Broad band 750-600

to the C-N bond ( $1232\text{ cm}^{-1}$ ) and a lower frequency band ( $1213, 1165, 1107, 1059\text{ cm}^{-1}$ ) due to aliphatic C-N band was present in curve M, which was obtained in reduced form in



spectrum P. Tetrasubstituted benzene bands ( $837, 812, 745 \text{ cm}^{-1}$ ) present in the DEA spectrum are found as a broad band in PPDEA spectrum [3].

From the IR spectra in Fig 4.11. it is depicted that the peaks in the PPDEA are not sharp when compared with those in DEA and most of the IR absorption features of DEA are noticeable in the spectrum of PPDEA with the shift in wavenumbers. Thus the IR analysis reveals that the PPDEA thin film deposited by plasma polymerization technique does not exactly resemble to that of the 2, 6 diethylaniline monomer i.e. the plasma technique affects the chemical structure of the deposited films. The presence of C=O indicates that there are trapped free radicals in the PPDEA which reacts with the atmospheric oxygen.

### References

- [1] Yasuda H., 'Plasma Polymerization', Academic Press, Inc, New York (1985).
- [2] Silverstein R. M., Bassler G. C., 'Spectroscopic Identification of Organic Compounds', John Wiley & Sons, NY (1981).
- [3] Conley R. T., 'Infrared Spectroscopy', Allyn and Bacon, Inc., Boston, (1972).
- [4] Radeva E., 'SEM study of plasma polymerized hexamethyldisiloxane thin films', PII, S0042-207X, 00212-6, (1996).
- [5] Kumar. S., Nakamura K., Nishiyama S., Ishii S., Noguchi H., Kashiwagi K., Yoshida Y., 'Optical and electrical characterization of plasma polymerized pyrrole films', J. Appl. Phys. **93**, 205-2711, (2003).
- [6] Valaski R., Ayoub S., Micaroni L., Hummelgen I.A., 'Influence of thin thickness on charge transport of electrodeposited polypyrrole thin films', Thin Solid Films **415**, 206-210,(2002).
- [7] Sarvanan S, Mathai C. J., 'Low K thin films based on rf plasma polymerized aniline', New J. Phys., **6**, 64, (2004).
- [8] Akther H. and Bhuiyan A. H., 'Infrared and ultra violet- visible spectroscopic investigation of plasma polymerized N, N, 3, 5,-tetramethylaniline thin films', Thin Solid Films, **474**, 14-18,(2005).
- [9] Zaman M., Bhuiyan A.H., 'Elemental analysis and infrared investigation of plasma polymerized Tetraethylthosilicate thin films', J. of Appl. Sci. and Tech., **03(02)**, 133-137, (2003).
- [10] Kim Jinmo, Jung Donggeun, Park Yongsup, Kim Yongki, Won Moon Dae, Geol Lee Tae, 'Quantitative analysis of surface amine groups on plasma-polymerized ethylenediamine films using UV-visible spectroscopy compared to chemical

- derivatization with FT-IR spectroscopy, XPS and TOF-SIMS', *Appl. Surf. Sci.* **253**, 4112-4118, (2007).
- [11] Vassillo E., Cremona A., Laguardia L., Mesto E., 'Preparation of plasma polymerized  $\text{SiO}_x$  like thin films from mixture of hexaethyldisiloxane an oxygen to improve the corrosion behavior', *Surf. and Coat. Technol.*, **200**, 3035-3040, (2006).
- [12] Sajeev U. S., Mathai, C. J., Saravanan S., Ashokan R., Venkatachalam S., Anantharaman M. R., 'On the optical and electrical properties of rf and a.c. plasma polymerized aniline thin films', *Bull. Mater. Sci.*, **29**, No.2 (2006).
- [13] Wu L., Zhu C., Liu M., 'Study on plasma polymerization of 1.1.1-trifluoroethene: deposition and structure of plasma polymer films'. *Desalination*, **192**, 234-240, (2006).
- [14] Jafari R., Tatoulian M., Morscheidt W., Arefi-Khonsari F., 'Stable plasma polymerized acrylic acid coating deposited on polyethylene (PE) films in a low frequency discharge', *Reactive and Functional Polymers*, **66**, 1757-1765, (2006).
- [15] Zhao X. Wang, M. Xiao, J. 'Deposition of plasma conjugated polynitrile thin films and their optical properties'. *Euro. Polym. J.*, **42**, 2161-2167, (2006).
- [16] Zhao Xion-Yan, Wang Ming-Zhu, Zhang Bing-Zhu, Mao Lei, 'Synthesis, Characterization and nonlinear optical properties of plasma-prepared poly (4-biphenylcarbonitrile) thin films', *Polym. Int.*, **56**, 630-634, (2007).
- [17] Zhao Xion-Yan, Wang Ming-Zhu, 'Deposition of plasma polymerized 1-Cyanoisoquinoline thin films and their dielectric properties', *Plasma Process. Polym.*, **4**, 840-846, (2007).
- [18] Yatsuda H., Nara M., Kogai T., Aizawa H., Kurosawa S., 'STW gas sensors using plasma polymerized allylamine', *Thin Solid Films*, **515**, 4105-4110, (2007).
- [19] Asabe M. R., Chate S. D., Garadkar K. M., Mulla I. S., Hankare P. P., 'Synthesis, characterization of chemically deposited indium selenide thin films at room temperature', *J. of Phy. And Chem. of Solids*. **69**, 249-254, (2008).
- [20] <http://www.prenhall.com/settle/chapters/ch15.pdf>
- [21] [http://www.chem.ucla.edu/~pang/chem11cl\\_net/11cl\\_home.html](http://www.chem.ucla.edu/~pang/chem11cl_net/11cl_home.html) -
- [22] <http://www.cem.msu.edu/~reusch/VirtualText/Spectrpy/InfraRed/infrared.htm>

## **CHAPTER 5**

### **UV-vis SPECTROSCOPY OF PPDEA**

#### **5.1 Introduction**

#### **5.2. Ultraviolet Visible Optical Absorption Spectroscopic Analysis**

##### 5.2.1. UV-vis spectrophotometer

##### 5.2.2. The Beer-Lambert law

##### 5.2.3. Electronic transitions

##### 5.2.5. Absorbing species containing $\pi$ , $\sigma$ , and $n$ electrons

##### 5.2.6. Direct and Indirect optical transitions

#### **5.3. Experimental Procedure**

#### **5.4. Results and discussion**

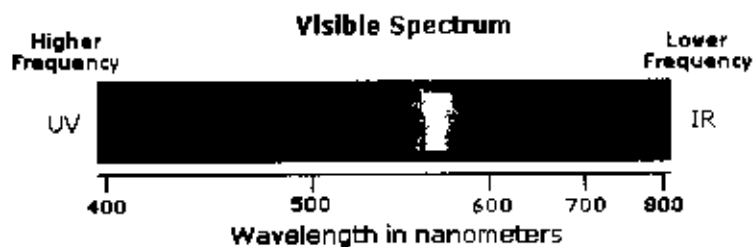
#### References

### 5.1. Introduction

For plasma polymerized thin films, Ultraviolet and visible spectroscopic methods is being widely used by many investigators to determine the presence, nature and extent of conjugation in materials, impurity states, optical energy gaps, direct and indirect transitions, refractive index and extinction coefficients, etc. These properties refers to the potential applications such as light guide materials, optical fibers, photo diodes, optical coating to inhibit corrosion, etc.[2-11]

### 5.2. Ultraviolet Visible Optical Absorption Spectroscopic Analysis

Most materials absorb some light, and the degree to which they absorb light is a function of the wavelength of the light. Because optical absorption in the visible and near-UV portions of the spectrum is generally the result of absorption of light by electrons in atoms, ions or molecules, the absorption characteristics can yield a considerable amount of information regarding their electronic structure.



The visible region of the spectrum comprises photon energies of 36 to 72 kcal/mole, and the near ultraviolet region, out to 200 nm, extends this energy range to 143 kcal/mole. In the most important region where most investigations are carried out, namely between 200 and 600 nm, there are electronic transitions of double bonds. Whereas, nonaromatic polymers show no specific absorption in the near UV and usually none in the visible region either.

The energies noted above are sufficient to promote or excite a molecular electron to a higher energy orbital. Consequently, absorption spectroscopy carried out in this region is sometimes called "electronic spectroscopy". An incident photon can also be absorbed by a molecule and then the photon energy is converted into an excitation of that molecule's electron cloud. This type of interaction is sensitive to the internal structure of the molecule, since the laws of

quantum mechanics only allow for the existence of a limited number of excited states of the electron cloud of any given chemical species. Each of these excited states has a defined energy; the absorption of the photon has to bridge the energy gap between the ground state (lowest energy state) and an allowed excited state of the electron cloud. Molecules can therefore be identified by their absorption spectrum. [12]

### 5.2.1. UV-vis spectrophotometer

A spectrophotometer is an instrument that measures the amount of optical absorption in a material, as a function of wavelength.

There are four main components of a spectrophotometer:

**A light source:** This is usually a tungsten-filament or gas-discharge lamp. Different light sources are used in different regions of the spectrum.

**A monochromator:** The input to the monochromator is the broadband light from the light source; the output is tunable, highly monochromatic light.

**A sample chamber:** The material under investigation is placed here.

**A detector:** The detector measures the amount of light that passes through the sample. Typically, detectors are either solid-state photodiodes (silicon, germanium, etc.) or photomultiplier tubes.

In Fig 5.1. Light of intensity  $I_0$  incident upon a sample of thickness  $t$  undergoes a loss in intensity upon passing through the sample. The intensity measured after passing through a sample of thickness,  $t'$  is  $I$ .

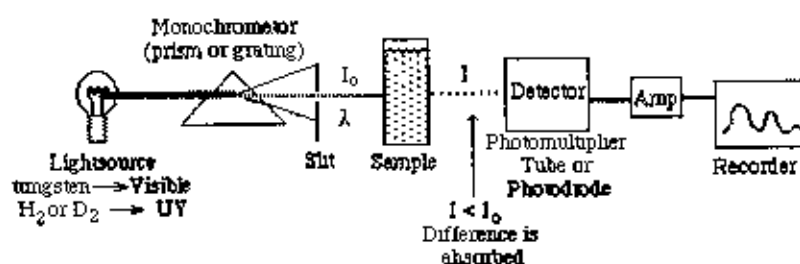


Fig. 5.1. Schematic of a uv-vis spectrophotometer

The basic setup of measuring the absorption or transmission of light through a sample is shown in Figure 5.1. Light of some wavelength  $\lambda$  having reference intensity  $I_0$  is incident normally on some sample of interest. Upon passing through the sample the intensity of the light is reduced to some value  $I$ , perhaps due to absorption within the sample and reflection at

the surfaces of the sample. A measurement of  $I_0$  and  $I$  can then be used to determine the transmission of the sample at wavelength  $\lambda$ .

There are two basic types of spectrophotometers, single-beam and dual-beam. In a single-beam spectrophotometer the reference intensity  $I_0$  and the intensity of the light,  $I$ , after passing through the sample are obtained sequentially. The dual-beam design greatly simplifies this process by simultaneously measuring  $I$  and  $I_0$  of the sample and reference cells, respectively. Most spectrometers use a mirrored rotating chopper wheel to alternately direct the light beam through the sample and reference cells. The detection electronics or software program can then manipulate the  $I$  and  $I_0$  values as the wavelength scans to produce the spectrum of absorbance or transmittance as a function of wavelength.

The advantage of the dual beam instrument is that any time-dependent variations in the intensity of the light emitted by the source can be compensated thus improving sensitivity and reducing uncertainty.

In addition to transmission, another useful way to report the optical absorption is in units of optical absorbance or optical density. Absorbance is a dimensionless quantity defined as the negative of the base-10 logarithm of the transmission:

$$A = -\log_{10}(I/I_0) \quad 5.1$$

An absorbance of 1 corresponds to a transmission of 0.1; an absorbance of 2 corresponds to a transmission of 0.01, and so on. Most spectrometers, after measuring  $T$ , use internal circuitry or, common nowadays, operating software to obtain the absorbance.

Absorbance units are useful when working with Beer's Law, which states that the absorbance of a solution is proportional to the concentration,  $C$ , of the absorber in that solution:

$$A = k C \quad 5.2$$

Most simple molecules obey Beer's Law, particularly at low concentration. Others, such as organic dyes, often exhibit a significant departure from Beer's Law at high concentration. This occurs because at higher concentrations, the molecules begin to interact with each other, and can no longer be treated as independent absorbers.

Another quantity that can be measured is the absorption coefficient. The absorption coefficient is a useful quantity when comparing samples of varying thickness. The absorption coefficient is typically the only value reported when discussing the absorption characteristics

of absorbing media. To determine the absorption coefficient we first start with Bouguer's Law which relates  $I$  to  $I_0$  via the equation

$$I = I_0 e^{-\alpha d} \quad 5.3$$

In this expression "d" is the thickness of the sample in units of centimeters (cm) and, consequently, the absorption coefficient  $\alpha$  is to be reported in units of  $\text{cm}^{-1}$ .

### 5.2.2. The Beer-Lambert law

The Beer-Lambert law can be derived from an approximation for the absorption coefficient for a molecule by approximating the molecule by an opaque disk whose cross-sectional area,  $\sigma$  represents the effective area seen by a photon of frequency  $\nu$ . If the frequency of the light is far from resonance, the area is approximately 0, and if  $\nu$  is close to resonance the area is a maximum. Taking an infinitesimal slab,  $dz$  of sample:

$I_0$  is the intensity entering the sample at  $z=0$ ,  $I_z$  is the intensity entering the infinitesimal slab at  $z$ ,  $dI$  is the intensity absorbed in the slab, and  $I$  is the intensity of light leaving the sample. Then, the total opaque area on the slab due to the absorbers is  $\sigma N A dz$ . Then, the fraction of photons absorbed will be  $\sigma N A dz / A$  so,

$$\frac{dI}{I} = -\sigma N dz \quad 5.4$$

Integrating this equation from  $z = 0$  to  $z = b$  gives and  $I = I_0$  to  $I = I$

$$\ln(I) - \ln(I_0) = -\sigma N b \quad 5.5$$

Or

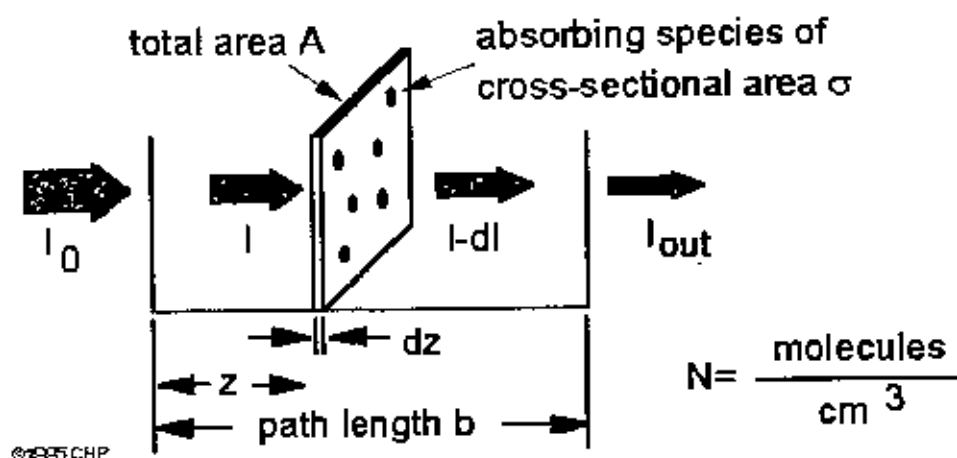
$$-\ln\left(\frac{I}{I_0}\right) = -\sigma N b \quad 5.6$$

Since  $N$  (molecules/ $\text{cm}^3$ ) ( $1 \text{ mole} / 6.023 \times 10^{23} \text{ molecules}$ )  $1000 \text{ cm}^3 / \text{liter} = c$  (moles/liter) i.e. concentration, and  $2.303 \log(x) = \ln(x)$ , then

$$-\log\left(\frac{I}{I_0}\right) = -\sigma \left(\frac{6.023 \times 10^{20}}{2.303}\right) c b \quad 5.7$$

or

$$\log\left(\frac{I_0}{I}\right) = A = \alpha b$$



5.8

Where  $\epsilon = \sigma(6.023 \times 10^{20} / 2.303) = \sigma(2.61 \times 10^{20})$ , and  $\epsilon$  is a constant of proportionality, called the *absorbivity*.

This equation can be written as

$$\alpha = \frac{2.303 A}{d} \quad 5.9$$

where  $\alpha$  is the absorption co-efficient,  $A$  is the absorbance, and  $d$  is the thickness of the material.

Thus the Beer Lambert law states that. "When a beam of monochromatic radiation passes through a homogeneous absorbing medium; the rate of decrease in intensity of electromagnetic radiation in UV-vis region with thickness of the absorbing medium is proportional to the intensity of the incident radiation".

The relation of extinction co-efficient  $k$  with  $\alpha$  is

$$\alpha = \frac{4\pi k}{\lambda} \quad 5.10$$

where  $\lambda$  is the wavelength.

### 5.2.3. Electronic transitions

The absorption of UV or visible radiation corresponds to the excitation of outer electrons. There are three types of electronic transition which can be considered;

- Transitions involving  $\pi$ ,  $\sigma$ , and  $n$  electrons
- Transitions involving charge-transfer electrons
- Transitions involving  $d$  and  $f$  electrons



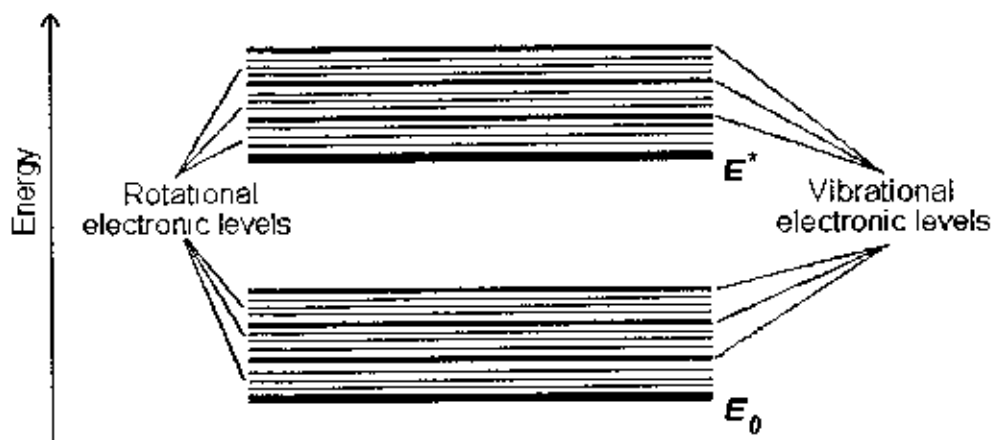


Fig.5.2. Vibrational and rotational energy levels of absorbing materials.

When an atom or molecule absorbs energy, electrons are promoted from their ground state to an excited state. In a molecule, the atoms can rotate and vibrate with respect to each other. These vibrations and rotations also have discrete energy levels, which can be considered as being packed on top of each electronic level.[11]

### 5.2.5. Absorbing species containing $\pi$ , $\sigma$ , and $n$ electrons

Absorption of ultraviolet and visible radiation in organic molecules is restricted to certain functional groups (*chromophores*) that contain valence electrons of low excitation energy.

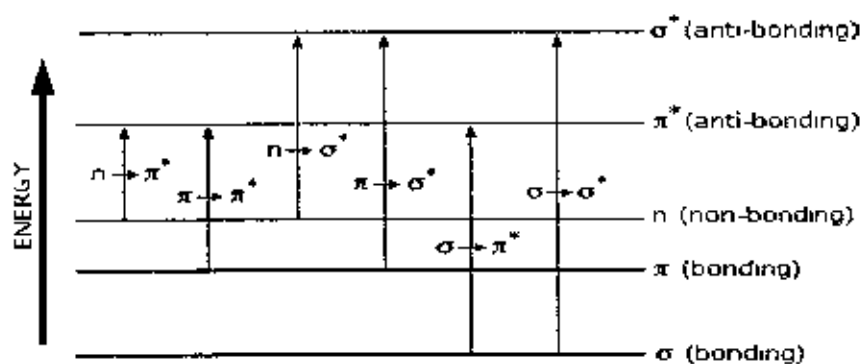


Fig.5.3. Electronic transitions in different energy level

The spectrum of a molecule containing these chromophores is complex. This is because the superposition of rotational and vibrational transitions on the electronic transitions gives a combination of overlapping lines. This appears as a continuous absorption band. Possible *electronic* transitions of  $\pi$ ,  $\sigma$ , and  $n$  electrons are;

$\sigma \rightarrow \sigma^*$  Transitions

An electron in a bonding  $\sigma$  orbital is excited to the corresponding antibonding orbital. The energy required is large. For example, methane (which has only C-H bonds, and can only undergo  $\sigma \rightarrow \sigma^*$  transitions) shows an absorbance maximum at 125 nm. Absorption maxima due to  $\sigma \rightarrow \sigma^*$  transitions are not seen in typical UV-Vis. spectra (200 - 700 nm)

#### $n \rightarrow \sigma^*$ Transitions

Saturated compounds containing atoms with lone pairs (non-bonding electrons) are capable of  $n \rightarrow \sigma^*$  transitions. These transitions usually need less energy than  $\sigma \rightarrow \sigma^*$  transitions. They can be initiated by light whose wavelength is in the range 150 - 250 nm. The number of organic functional groups with  $n \rightarrow \sigma^*$  peaks in the UV region is small.

#### $n \rightarrow \pi^*$ and $\pi \rightarrow \pi^*$ Transitions

Most absorption spectroscopy of organic compounds is based on transitions of  $n$  or  $\pi$  electrons to the  $\pi^*$  excited state. This is because the absorption peaks for these transitions fall in an experimentally convenient region of the spectrum (200 - 700 nm). These transitions need an unsaturated group in the molecule to provide the  $\pi$  electrons.

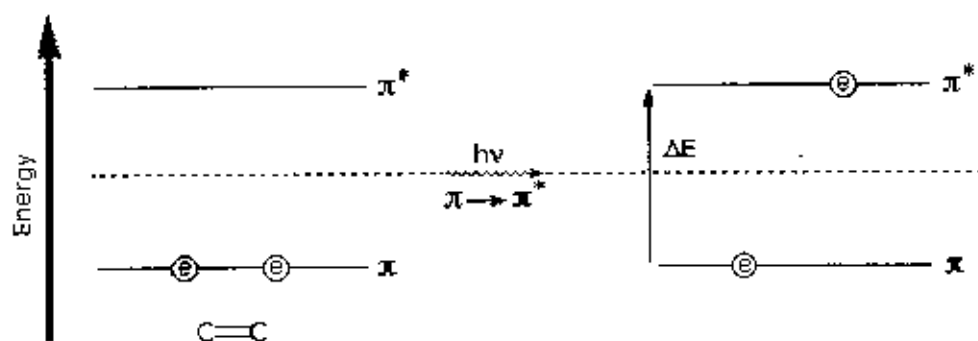


Fig.5.4. Examples of  $\pi \rightarrow \pi^*$  Excitation

Molar absorptivities from  $n \rightarrow \pi^*$  transitions are relatively low, and range from 10 to 100  $\text{L mol}^{-1} \text{cm}^{-1}$ .  $\pi \rightarrow \pi^*$  transitions normally give molar absorptivities between 1000 and 10,000  $\text{L mol}^{-1} \text{cm}^{-1}$ .

The solvent in which the absorbing species is dissolved also has an effect on the spectrum of the species. Peaks resulting from  $n \rightarrow \pi^*$  transitions are shifted to shorter wavelengths (*blue shift*) with increasing solvent polarity. This arises from increased solvation of the lone pair, which lowers the energy of the  $n$  orbital. Often (but *not* always), the reverse (i.e. *red shift*) is seen for  $\pi \rightarrow \pi^*$  transitions. This is caused by attractive polarization forces between the

solvent and the absorber, which lower the energy levels of both the excited and unexcited states. This effect is greater for the excited state, and so the energy difference between the excited and unexcited states is slightly reduced - resulting in a small red shift. This effect also influences  $n \rightarrow \pi^*$  transitions but is overshadowed by the blue shift resulting from solvation of lone pairs [14].

### 5.2.6. Direct and indirect optical transitions

For a direct gap material if it absorbs light and the light source is then removed, the optically generated electrons and holes recombine. Since the minimum in the conduction band has the same  $\mathbf{k}$  value as the maximum in the valance band. The electron can drop back easily into the hole in the valance band and the energy lost in the process is emitted as radiation of wavelength  $\lambda_c = hc/E_g$ , where  $E_g$  is the band gap. i.e. the total energy and the momentum of the electron-photon system must be conserved.

For the indirect gap material the momentum has to be adjusted by a cooperative process involving a phonon (quantized lattice vibration). Such a process does not emit radiation at the band gap wavelength and the energy lost during a recombination process is effectively dissipated as heat i.e. indirect transition involves the absorption or emission of a phonon to converse momentum. Thus in this case the top of the valance band and the bottom of the conduction band take place at different wave vectors in the Brillouin zone. In this respect it is unfortunate therefore that  $\mathbf{k}$  is not effectively a good quantum number in amorphous non-crystalline materials and such materials are usually regarded as indirect gap materials.

To estimate the nature of absorption a random phase model is used where the  $\mathbf{k}$  momentum selection rate is completely relaxed. The integrated density of states  $N(E)$  has been used and defined by

$$N(E) = \int_{-\infty}^{+\infty} g(E) dE$$

The density of states per unit energy interval may be represented by

$$g(E) = \frac{1}{V} \sum \delta(E - E_n)$$

where  $V$  is the volume,  $E$  is the energy at which  $g(E)$  is to be evaluated and  $E_n$  is the energy of the  $n$ th state.

If  $g_v \propto E^p$  and  $g_c \propto (E - E_{opt})$ , where energies are measured from the valance band mobility edge in the conduction band (mobility gap), and substituting these values into an expression for the random phase approximation, the relationship obtained

$\nu^2 I_2(\nu) \propto (\hbar\nu - E_0)^{p-q+1}$ , where  $I_2(\nu)$  is the imaginary part of the complex permittivity. If the density of states of both band edges is parabolic, then the photon energy dependence of the absorption becomes

$$\alpha\nu \propto \nu^2 I_2(\nu) \propto (\hbar\nu - E_{opt})^n.$$

So for higher photon energies the simplified general equation, known as Tauc relation is,

$$\alpha h\nu = B(\hbar\nu - E_{opt})^n$$

where,  $h\nu$  is the energy of absorbed light,  $n$  is the parameter connected with distribution of the density of states and  $B$ , a constant or Tauc parameter and here  $n = 1/2$  for direct and  $n = 2$  for indirect transitions.[1]

The above equation can be written as

$$\frac{d[\ln(\alpha h\nu)]}{d[h\nu]} = \frac{n}{\hbar\nu - E_{opt}}$$

when finding the  $n$ , type of transition can be obtained from the absorption spectrum. A discontinuity in the  $d[\ln(\alpha h\nu)]/d(h\nu)$  versus  $h\nu$  plot at the band gap energy ( $E_{opt}$  or  $E_g$ ), i.e. at  $h\nu = E_g$  can be observed. The discontinuity at a particular energy value gives the band gap  $E_g$ .

### 5.3. Experimental Procedure

The PPDEA thin films of different thickness for UV-vis spectroscopy were prepared in a glow discharge reactor onto chemically cleaned glass substrates. The optical absorption measurements were made in the wavelength range 190-1100 nm by using a dual beam Shimadzu UV-1601 (UV-visible spectrophotometer) at room temperature. The spectrum of DEA monomer was also recorded with the same spectrophotometer. An identical, uncoated glass substrate in the reference beam made a substrate absorption correction.

### 5.4. Results and Discussion

The UV-Vis spectra of PPDEA thin films of different thicknesses are presented in Fig 5.5. From this figure it is observed that the absorption peak intensity increases and broadens with increasing thickness of the PPDEA thin films. It is found that the maximum peak value of the

wavelength of PPDEA thin films is about 290nm whereas, for DEA monomer is 320nm. The absorption edge shifts to the lower wavelength by about 30nm and absorption intensity also became much weaker than that of DEA monomer. This phenomenon indicates a lower conjugation in the polymer. This can occur due to the plasma polymerization where the aromatic rings of monomers may be dissociated and fragmented, which results in more non conjugated polymers being formed in the plasma polymerized films [8]. The absorption coefficient,  $\alpha$  at various wavelengths were also calculated using the eqn 5.9. Plot of absorption co-efficient,  $\alpha$ , as a function of photon energy,  $h\nu$ , for PPDEA thin films are shown in fig 5.6. The figure shows exponential falling edges, which may either be due to the lack of long-range order or due to the presence of defects in the thin films. Thus, the optical band gap  $E_g$  of the film can be obtained by using absorption co-efficient. The plot of  $(\alpha h\nu)^{1/2}$  as a function of  $h\nu$  for indirect transition and the plot of  $(\alpha h\nu)^2$  as a function of  $h\nu$  for direct transition of the films of different thicknesses are shown in Fig.5.7 and Fig.5.8 respectively. The  $E_g$  values were obtained by extrapolating the linear portion of the plots to intercept the photon energy axis and calculated  $E_g$  values for direct and indirect transition are given in table 5.1.

Table 5.1. The optical parameters of thin films of PPDEA

Film thickness, $d$ (nm)	Direct transition energy gap, $E_{g(d)}$ (eV)	Indirect transition energy gap, $E_{g(i)}$ (eV)
100	3.47	2.30
150	3.61	2.38
200	3.54	2.36
250	3.54	2.20
350	3.63	2.46

From Table 5.1 it is observed that the values of  $E_{g(d)}$  and  $E_{g(i)}$  increased with increasing thickness. The values of allowed direct transition energy gap,  $E_{g(d)}$  is, 3.56 eV and that of allowed indirect transition energy gap,  $E_{g(i)}$  is 2.34 eV. Physical processes that control the behavior of gap states in non-crystalline materials are structural disorder responsible for the tail states and structural defects in deep states.

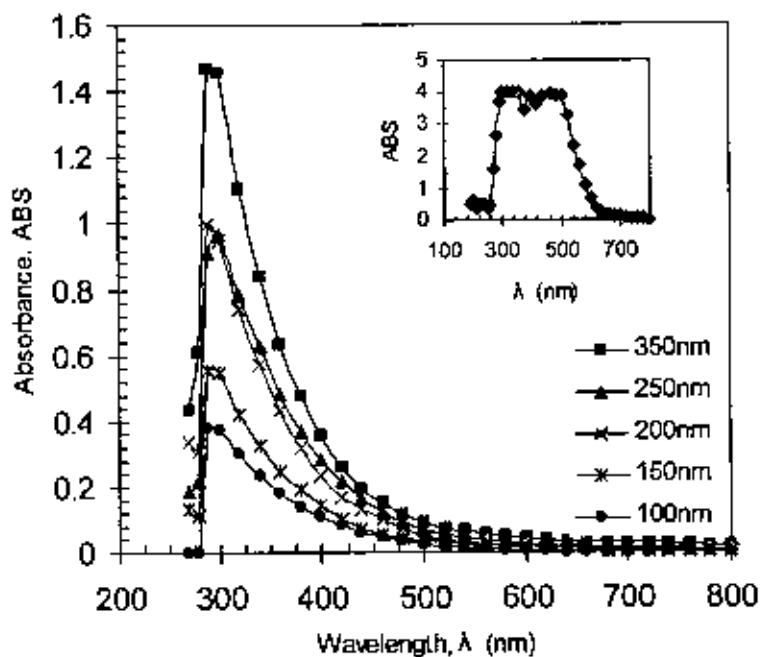


Fig.5.5. Variation of absorbance (ABS) with wavelength,  $\lambda$  for PPDEA thin films of different thicknesses. (inset: DEA monomer).

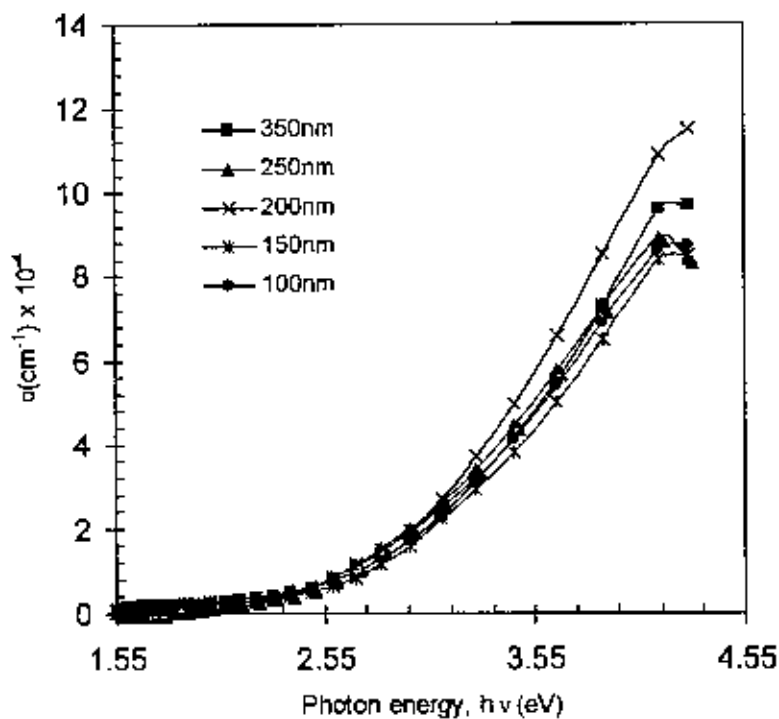


Fig.5.6. Plot of absorption co-efficient,  $\alpha$ , as a function of photon energy,  $h\nu$ , for PPDEA thin films of different thicknesses.

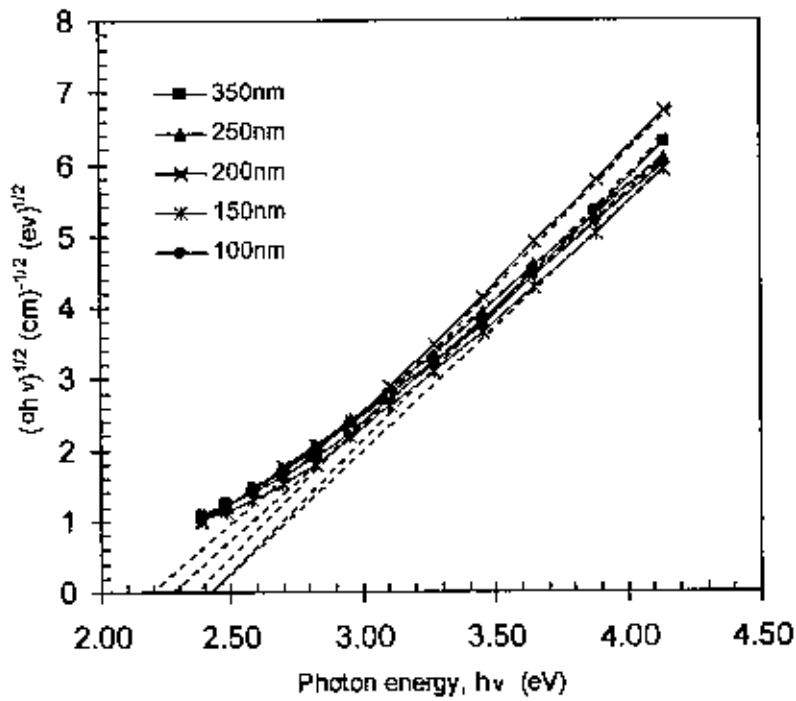


Fig.5.7.  $(\alpha hv)^{1/2}$  vs.  $h\nu$  curves for PPDEA thin films of different thickness.

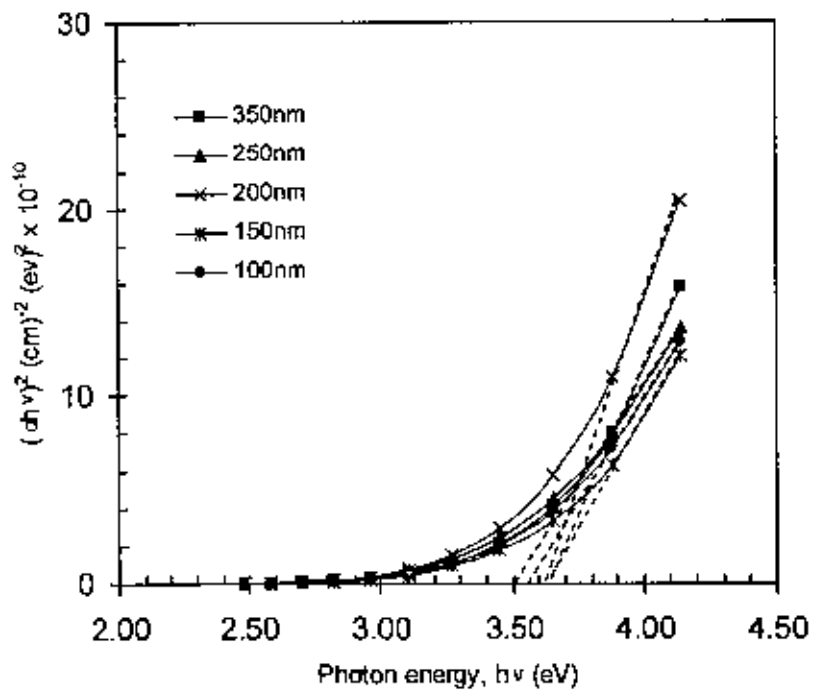


Fig.5.8.  $(\alpha hv)^2$  vs.  $h\nu$  curves for PPDEA thin films of different thickness.

## References

- [1] Hogarth C. A., "The optical properties of amorphous semiconductors", *Condens Mater Phys.*, **1**, (1996).
- [2] Yakuphanoglu F., Arslan M., Kucukislamoglu M., Zengin M., "Temperature dependence of the optical band gap and refractive index of poly (ethylene terephthalate) oligomer- DDQ complex thin film", *Sol. Energy*, **79**, 96-100, (2005).
- [3] Kim J., Jung D., Park Y., Kim Y., Moon D. W., Lee T. G., "Quantitative analysis of surface amine groups on plasma-polymerized ethylenediamine films using UV-visible spectroscopy compared to chemical derivatization with FT-IR spectroscopy, XPS and TOF-SIMS", *Appl. Surf. Sci.* **253**, 4112-4118, (2007).
- [4] Al-Mamun, Islam A.B.M.O, Bhuiyan A.H. 'Structural, electrical and optical properties of copper selenide thin films deposited by chemical bath deposition technique'. *J. Mater. Sci.* **16**,263-268, (2005).
- [5] Akther H. and Bhuiyan A. H., 'Electrical and optical properties of plasma polymerized N, N, 3, 5,-tetramethylaniline thin films', *New J. Phys.* **7**, 173, (2005).
- [6] Yakuphanoglu F., Cukuoali A., Yilmaz I., 'Refractive index and optical absorption properties of the complexes of a cyclobutane containing thiazoyl hydrazone ligand', *Optical Materials*, **27**, 1363-1368, (2005).
- [7] Yakuphanoglu F., Cukuoali A., Yilmaz I., 'Determination and analysis of the dispersive optical constants of some organic films', *Physica B*, **351**, 53-58, (2004).
- [8] Zaman M., Bhuiyan A. H., 'Optical properties of plasma polymerized tetra-ethylorthosilicate thin films', *Bangladesh J. Phys.* **2**(1), 107-113, (2006).
- [9] Hu Xiao, Zhao Xiongyan, Uddin A., Lee C. B. 'Preparation characterization and electronic and optical properties of plasma polymerized nitriles', *Thin Solid Films*, **477**, 81-87, (2005).
- [10] Sajeev U. S., Mathai, C. J., Saravanan S, Ashokan R, Venkatachalam S., Anantharaman M. R. 'On the optical and electrical properties of rf and a.c. plasma polymerized aniline thin films', *Bull. Mater. Sci.*, **29**. No.2 (2006).
- [11] [http://www.chemsoc.org/pdi/LearnNet/rsc/UV\\_txt.pdf](http://www.chemsoc.org/pdi/LearnNet/rsc/UV_txt.pdf)
- [12] <http://www.cem.msu.edu/~reusch/VirtualText/Spectrpy/UV-Vis/spectrum.htm>
- [13] <http://www.monos.leidenuniv.nl/smo/index.html?basics/spectroscopy.htm>
- [14] <http://accept.asu.edu/PiN/rdg/optical/optical.shtml>



## **CHAPTER 6**

### **DC ELECTRICAL PROPERTIES OF PPDEA**

#### **6.1 Introduction**

#### **6.2. DC electrical conduction mechanism**

6.2.1. Schottky Mechanism

6.2.2. Poole-Frenkel mechanism

6.2.3. Space charge limited conduction (SCLC) mechanism

#### **6.3. Thermally activated conduction processes**

#### **6.4. Experimental Procedure**

#### **6.5. Results and Discussion**

6.5.1. Current density-voltage (J-V) characteristics

6.5.2. Temperature dependence of current

References

## 6.1. Introduction

Our modern life style increasingly demands more from the polymers than their traditional role of insulators for heat and electric current. To satisfy this purpose much more attentions have been made in the research activities to investigate the electrical responses of the polymer insulators. This chapter includes the brief description of the existing theories of DC electrical conduction mechanisms which are usually operative in thin insulating polymer and other thin films and the experimental techniques used in the measurements of current density–voltage (J-V) and thermally activated current to ascertain the conduction mechanism operative in the investigated PPDEA thin films.

## 6.2. DC Electrical Conduction Mechanism

Electrical properties of insulating polymers are their responses when an electric field is applied to them. The subject of electrical properties of polymers covers an extremely diverse range of molecular phenomena. In contrast to metals, in which the electrical field response is one of electronic conduction, polymers may respond in a more varied manner, and a whole set of delicate electrical effects may be observed. No known polymer is completely free of conduction processes, however small the quantity of charge carriers it may possess. Low level conduction in insulating polymers can take a variety of forms. Conduction may very often be contributed by impurities that provide a small concentration of charge carriers in the form of electrons or ions. At high fields, the electrodes may inject new carriers (holes and electrons) into polymers. At very high fields, these and other processes will lead to complete breakdown of polymers as insulating materials. The imposition of an electrical field upon a polymer will cause a redistribution of any charges in the polymer, provided they are mobile enough to respond in the time scale in the applied field. If some of the mobile charges are able to diffuse throughout the specimen and charge migration through the electrode sample interface is possible, then the charges will support a dc conductance. It should be mentioned that the vacuum-deposited thin film insulators can contain a large density of both impurity and trapping centers. A well judged study of electrical conduction in vacuum deposited thin films cannot be accomplished without consideration of these possibilities.[1] A power law can express the variation of current density with voltage in a material generally:

$$J \propto V^n$$

6.1

where,  $n$  is a power factor. When  $n$  is unity, the conduction is ohmic. If the value of  $n$  is less or more than unity, then the conduction process is other than ohmic.

Many scientists have investigated three worth-mentioning electrical conduction mechanisms which are operative in the thin films of various organic compounds [2-17]:

- The injection of carriers from the electrode by means of thermal or field assisted emission usually referred to as Schottky emission.
- The other process in which carriers are produced by the dissociation of donor-acceptor centers in the bulk of the material, is called Poole-Frenkel generation.
- If the generation process is slower than transport by the carriers through the material, the conduction is controlled by generation, specifically by either the Schottky, or Poole-Frenkel (PF) mechanism. Conversely, when the transport is slower than generation, it constitutes the rate-determining step, and the conduction is described by the theory of space-charge-limited current (SCLC). The phenomenon is, if a charge is injected at the electrode polymer interface, a large excess carrier density at the injecting electrode will exist and a space-charge-limited current will flow.[1,2]

A brief explanation of these conduction mechanisms is stated below.

### 6.2.1. Schottky mechanism

Charge injected from a metal to an insulator or semiconductor at medium fields may take place by field-assisted thermionic emission, a process known as Richardson-Schottky effect or simply Schottky emission. This is a procedure of image force induced lowering potential energy for charge carrier emission when an electric field is applied. The potential step changes smoothly at the metal insulator interface as a result of the image force. This happens when the metal surface become polarized (positively charged) by an escaping electron, which

in turn exerts an attractive force  $F_m = -\frac{e^2}{16\pi\epsilon_0\epsilon'x^2}$  on the electron. The potential energy of the

electron due to the image force is thus

$$\phi_m = -\frac{e^2}{16\pi\epsilon_0\epsilon'x} \quad 6.1$$

where  $x$  is the distance of electron from the electrode surface.

The potential step at a neutral barrier with attendant image potential as a function of the distance  $x$  from the interface is given by,

$$\phi(x) = \phi_0 + \phi_m = \phi_0 - \frac{e^2}{16\pi\epsilon_0\epsilon'x} \tag{6.2}$$

where  $\phi_0$  = Coulombic barrier height of the electrode-polymer interface in Schottky conduction. The barrier potential  $\phi(x)$  in the presence of image forces is illustrated by the line AB in Fig 6.1. Schottky assumed that the image force holds only for  $x$  greater than some critical distance  $x_0$ . For  $x < x_0$ , he assumes a constant image force, i.e. the potential energy is a linear function of  $x$ , and such that it matches the bottom of the electrode conduction band at the surface.

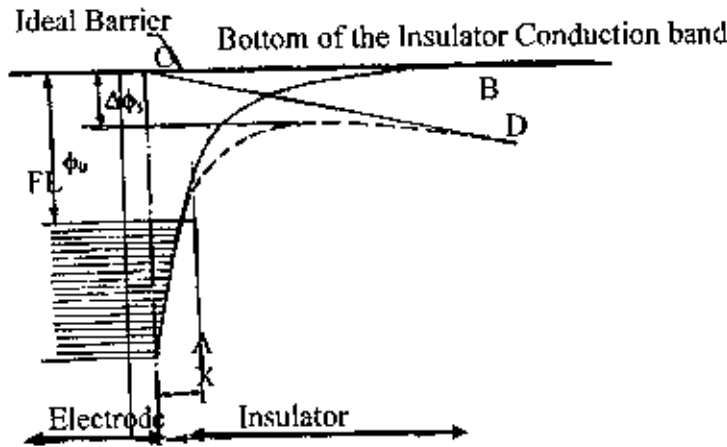


Fig. 6.1. Schottky effect at a neutral contact.

When an electric field exists at a metal-insulator interface, it interacts with the image force and lowers the potential barrier. The line CD represents the potential due to a uniform applied field. The dotted line represents the potential  $\Delta\phi_s$ , when the potential due to a uniform electric field is added to the barrier potential  $\phi(x)$  and thus it is lower than that of without the electric field. Under the influence of the field the potential energy of the barrier with respect to Fermi level of the electrode can be given by

$$\phi(x) = \phi_0 - \frac{e^2}{16\pi\epsilon'\epsilon_0x} - eFx \tag{6.3}$$

This equation has a maximum at  $x_m = \left( \frac{e}{16\pi\epsilon'\epsilon_0F} \right)^{1/2}$

Therefore, the change  $\Delta\phi_s = \phi_0 - \phi(x_m)$  in the barrier height due to the interaction of the applied field with the image potential can be given by

$$\Delta\phi_s = \left( \frac{e^3}{4\pi\epsilon'\epsilon_0} \right)^{1/2} F^{1/2} \equiv \beta_s F^{1/2} \quad 6.4$$

Because of image force lowering of the barrier, the electrode limited current does not saturate according to the Richardson law

$$J = AT^2 \exp\left(-\frac{\phi_0}{kT}\right) \quad 6.5$$

but rather obeys the Richardson-Schottky law

$$J = AT^2 \exp\left(-\frac{\phi_0 - \Delta\phi}{kT}\right) \quad 6.6$$

$$J = AT^2 \exp\left(\frac{\beta_s F^{1/2} - \phi_0}{kT}\right) \quad 6.7$$

where,  $A = 4\pi em(kT)^2 / h^2$  is the Richardson constant,  $F$  = static electric field and is equal to  $V/d$ ,  $V$  = applied voltage,  $d$  = film thickness,  $T$  = Temperature in Kelvin,  $k$  = Boltzmann constant and  $\beta_s$  is the Schottky coefficient which is given by,

$$\beta_s = \left( \frac{e^3}{4\pi\epsilon'\epsilon_0} \right)^{1/2} \quad 6.8$$

where,  $e$  = elementary charge of the electron and  $\epsilon'$  is the high frequency dielectric constant of the material.

The electrode limited Richardson-Schottky effect in insulators appears to have been first observed by Emptage and Tantraporn, who reported a  $\log I$  vs.  $F^{1/2}$  relationship in their samples. It was suggested that the plot should have to be linear in nature for Schottky type conduction mechanism.[18]

### 6.2.2. Poole-Frenkel mechanism

The Poole-Frenkel (PF) conduction mechanism is a field assisted thermal ionization process and is the bulk analogue of the Schottky effect at an interfacial barrier. This effect is lowering of a Coulombic potential barrier when it interacts with an electric field, as shown in fig 6.2.

The PF lowering of a Coulombic barrier  $\Delta\phi_{PF}$  in a uniform electric field is twice that due to the Schottky effect at a neutral barrier, because the potential energy of an electron in a

Coulombic field  $-\frac{e^2}{4\pi\epsilon_0\epsilon r}$  is four times that due to image force effects in Schottky mechanism; i.e.

$$\Delta\phi_{PF} = 2\Delta\phi_s = 2\left(\frac{e^3}{4\pi\epsilon'\epsilon_0}\right)^{1/2} F^{1/2} \equiv \beta_{PF} F^{1/2} \quad 6.9$$

where,  $\beta_{PF}$  is PF coefficient.

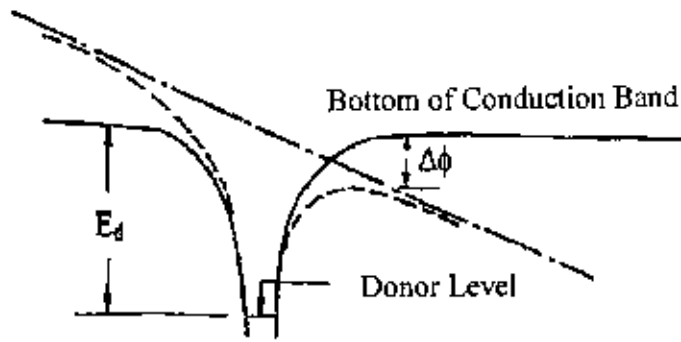


Fig.6.2. Poole-Frenkel effect at a donor center.

From this we can conclude that,

$$\beta_{PF} = 2\left(\frac{e^3}{4\pi\epsilon'\epsilon_0}\right)^{1/2} = 2\beta_s \quad 6.10$$

i.e.  $2\beta_s = \beta_{PF}$

In the bulk limited PF mechanism, the thermal emission of trapped carriers from the bulk material gives rise to conductivity

$$J = \sigma_0 F \exp\left(\frac{\beta_{PF} F^{1/2} - \phi_c}{kT}\right) \quad 6.11$$

where,  $\phi_c$  is the ionization potential of the PF centers.

Consequently, a general expression of the form

$$J = J_0 \exp\left(\frac{\beta F^{1/2} - \phi}{kT}\right) \quad 6.12$$

holds equally well for both Schottky and PF mechanisms. Where, J is the current density at a biased voltage.

By taking natural logarithms of Eqn.. 6.12 we can write,

$$\beta_{exp} = skTd^{1/2} \quad 6.13$$

where,  $\beta_{exp}$  denotes the value of  $\beta$  obtained experimentally and  $s\left(=\frac{\Delta \ln J}{\Delta V^{1/2}}\right)$  is the slope of graph plotted between  $\ln J$  and  $V^{1/2}$ .

### 6.2.3. Space charge limited conduction (SCLC) mechanism

When an Ohmic contact is made to the insulator, the space charge injected into the conduction band of the insulator is capable of carrying current and when the transport is slower than generation, it constitutes the rate-determining step, and the conduction is described by the theory of space-charge-limited current (SCLC) [1].

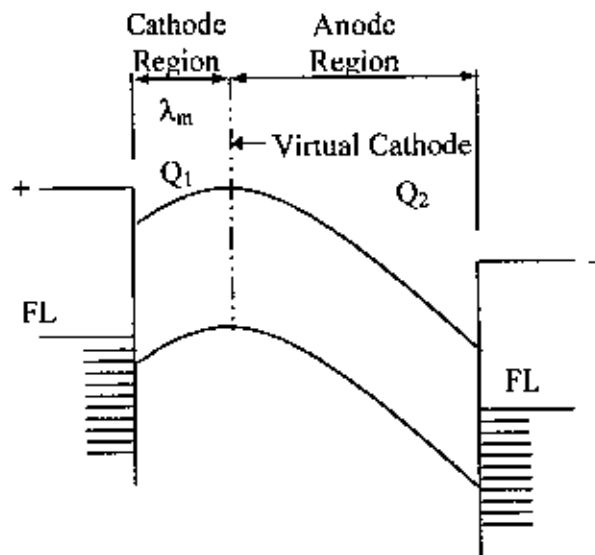


Fig. 6.3. Energy diagram for different regions under space charge limited conduction mechanism.

When a voltage bias is applied to the metal electrodes, this results an addition of positive charge to the anode and negative charge to the cathode. If now the voltage bias increases, the net positive charge on the anode increases and that on the cathode decreases. Assuming that the anode region extends throughout the insulator and neglecting the diffusion effect the current can be interpreted by the Mott and Gurney relation

$$J = \frac{9\mu\epsilon'\epsilon_0 V^2}{8d^3} \quad 6.14$$

Where,  $\mu$  is the mobility of charge carriers,  $\epsilon$  is dielectric constant,  $\epsilon_0$  is the permittivity of free space,  $V$  is the applied voltage and  $d$  is the thickness. If the insulator contains  $N_t$  shallow

traps positioned an energy  $E_t$  below the conduction band then the free component of the space charge

$$\rho_f = eN_c \exp\left(-\frac{E_t}{kT}\right) \quad 6.15$$

and trapped component of space charge

$$\rho_t = eN_t \exp\left(-\frac{E_t}{kT}\right) \quad 6.16$$

thus trapping factor,  $\theta$  is defined as

$$\theta \equiv \frac{\rho_f}{\rho_t} = \frac{N_c}{N_t} \exp\left(-\frac{E_t}{kT}\right) \quad 6.17$$

where  $N_c$  is the effective density of states in the conduction band, and  $N_t$  the density of trapping levels situated at an energy  $E_t$  below the conduction band edge.

The SCLC current density with traps is defined by

$$J = \frac{9\mu\epsilon'\epsilon_0 V^2}{8d^3} \theta \quad 6.18$$

For a shallow trap SCLC and trap-free SCLC,  $\theta = 1$ . According to Eqn. 6.18,  $J$  varies as  $d^{-1}$  in the Ohmic region and as  $d^{-3}$  in the SCLC region for the trap-filled SCLC part. For a fixed  $V$ , the dependence of  $\ln J$  on  $\ln d$  should be linear with slope  $1 \geq -3$ .

Lampert calculated the voltage at which the transition from the Ohmic to shallow trap SCLC region ( $V_{tr}$ ) occurs is given by

$$V_{tr} = \frac{8}{9} n_0 \frac{ed^2}{\epsilon} \quad 6.19$$

Where, volume generated free carrier density,  $n_0$  is independent of both  $\mu$  and  $J$  [18].

According to Fig. 6.4 it was found that the second linear region would extend up to a certain voltage, called as the crossover voltage, and beyond which the current would vary with the voltage as a power law:

$$I \propto V^2 \quad 6.20$$

Which would continue until the current is close to the saturation current, i.e. the maximum current that the electrode could supply. However in real samples which contain several trap sites to capture the electrons that had been injected inside the sample. There are two types of traps; the



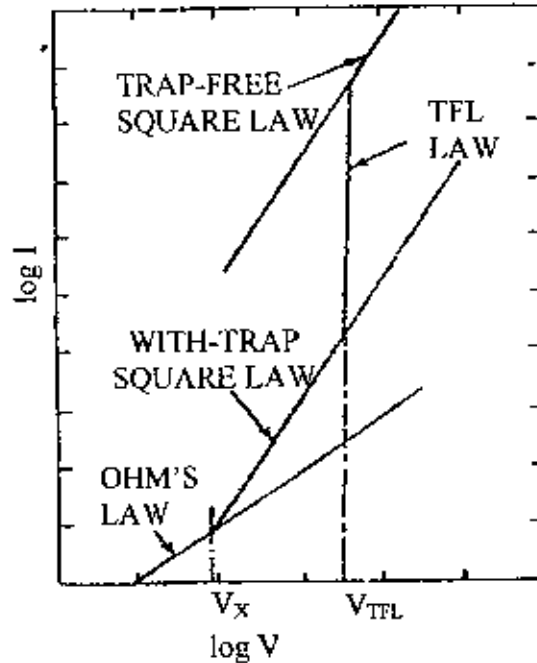


Fig. 6.4 Space charge limited conduction characteristic for an insulator containing shallow traps.

ones above the Fermi level are the shallow traps, and the others below the Fermi level being the deep traps. During trapping both shallow and deep traps would get filled. The voltage at which all the traps would get completely filled is called the trap filled limit (TFL). Beyond  $V_{TFL}$  all the excess charges would be injected into the conduction band and the current would approach the trap free square law as described in Eqn. 6.20 [17, 18].

### 6.3. Thermally Activated Conduction Processes

Electronic conduction in organic, molecular compounds differs in several important ways from the more familiar kind in metals and semiconductors. An important feature of the band system is that electrons are delocalized and spread over the lattice. Some delocalization are naturally expected when an atomic orbital of any atom overlaps appreciably with those of more than one of its neighbors, but delocalization reaches an extreme form in the case of a regular 3 dimensional lattice. The band theory assumes that the electrons are delocalized and can extend over the lattice. When electronic conduction is considered in polymers, band theory is not totally suitable because the atoms are covalently bonded to one another, forming polymeric chains that experience weak intermolecular interactions. But macroscopic

conduction will require electron movement, not only along the chain but also from one chain to another.

If two solids are put in contact, the Fermi levels equalize at the interface, the other energy levels moving to accommodate this. In pure insulator the Fermi level bisects the forbidden band. Impurities may introduce allowed levels into the forbidden band, and this moves the Fermi level up and down.

As the temperature is increased the charge carrier concentration increases strongly with temperature. This dominates the temperature dependence of the conductivity, giving it an Arrhenius - like character.

It is difficult to generalize about the temperature dependence of dc conduction whether it is ionic or electronic since so many processes are possible. Ohmic (low field) conduction whether ionic or electronic, gives exponential temperature dependence, given by

$$J = J_0 \exp \frac{-\Delta E}{kT} \quad 6.21$$

where  $J_0$  is a constant and  $\Delta E$  is the activation energy for carrier generation. Now

$$J = Ne\mu \quad 6.22$$

where  $N$  is the number of charge carriers,  $e$  their charge, and  $\mu$  their mobility. With extrinsic ionic conduction, it is the mobility i.e. the activated process,  $\Delta E$  being the energy for the ion to hop. With extrinsic electronic conduction, the electrons may move by hopping. However, if the electronic conduction is by excitation into the conduction band, the production of free electrons,  $n$  not their mobility,  $\mu$  is activated. Whatever the Ohmic mechanism, a  $\log J$  vs.  $1/T$  plot (Arrhenius plot) will usually exhibit increasing linear slopes (activation energies) as  $T$  is raised.[18]

For variable range hopping the electrical conductivity is given by

$$\sigma = \sigma_0 \exp - \left( \frac{T_0}{T} \right)^{\frac{1}{d+1}} \quad 6.23$$

where "d" is the dimensionality of transport,  $\sigma$  is the conductivity,  $\sigma_0$  is the initial value of conductivity,  $T$  is the absolute temperature and  $T_0$  is the activation energy in terms of temperature.

In bulk material ionic conduction occurs due to the drift of defect under the influence of an applied electric field. The degrees of ionic impurities that may be totally ignored in the

context of other properties may have a significant effect on conductivity. A theoretical expression may

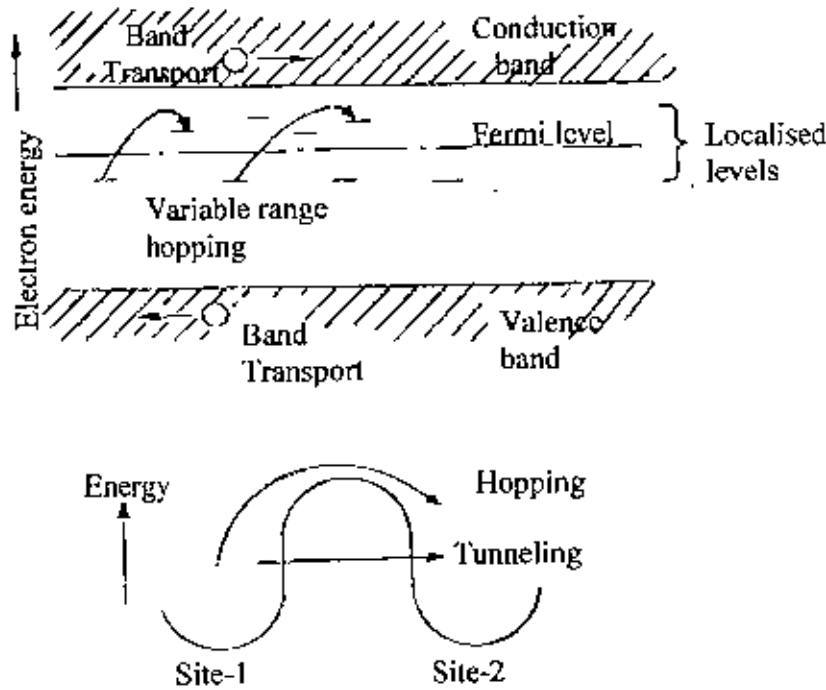


Fig. 6.5. Diagram of electron-transfer mechanisms between adjacent sites separated by a potential-energy barrier.

be derived for the current density,

$$J = \sin h (eaE/2kT) \quad 6.24$$

where  $E$  is the electric field,  $a$  is the distance between neighboring potential wells,

$e$  = electronic charge.

#### 6.4. Experimental Procedure

For electrical measurements, Al electrodes were deposited on the both sides of the sample, i.e. after the lower electrode was deposited, the PPDEA film was deposited onto the electrode and then the upper electrode was deposited on the film in the opposite direction of the lower electrode using an Edward coating unit, E-306A (Edward, UK). The system was evacuated by an oil diffusion pump backed by an oil rotary pump at a pressure of about  $10^{-5}$  Torr. The current across the thin films was measured by a high impedance Keithley 614 electrometer and the dc voltage was applied by an Agilent 6545A stabilized dc power supply. The

measurements were carried out under dynamic vacuum of about  $10^{-2}$  Torr to avoid any ambient effect. The block diagram for dc measurements and dc measurement set up are shown in Fig. 6.6 and Fig. 6.7. The thermally activated current or the temperature dependence of current across the PPDEA thin films was measured at applied voltages of 8 and 14 V using the above mentioned electrometer. The measurements were performed from 298 to 398 K. For these measurements the samples were heated by a heating coil which was wrapped around the specimen chamber. The temperature was measured by a Chromel-Alumel (Cr-Al) thermocouple placed very close to the sample which was connected to a 197 A digital microvolt (DMV) meter.

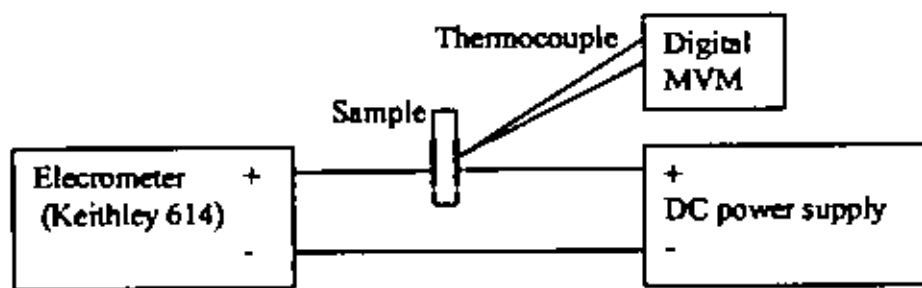


Fig. 6.6. A schematic circuit diagram of DC measurement.

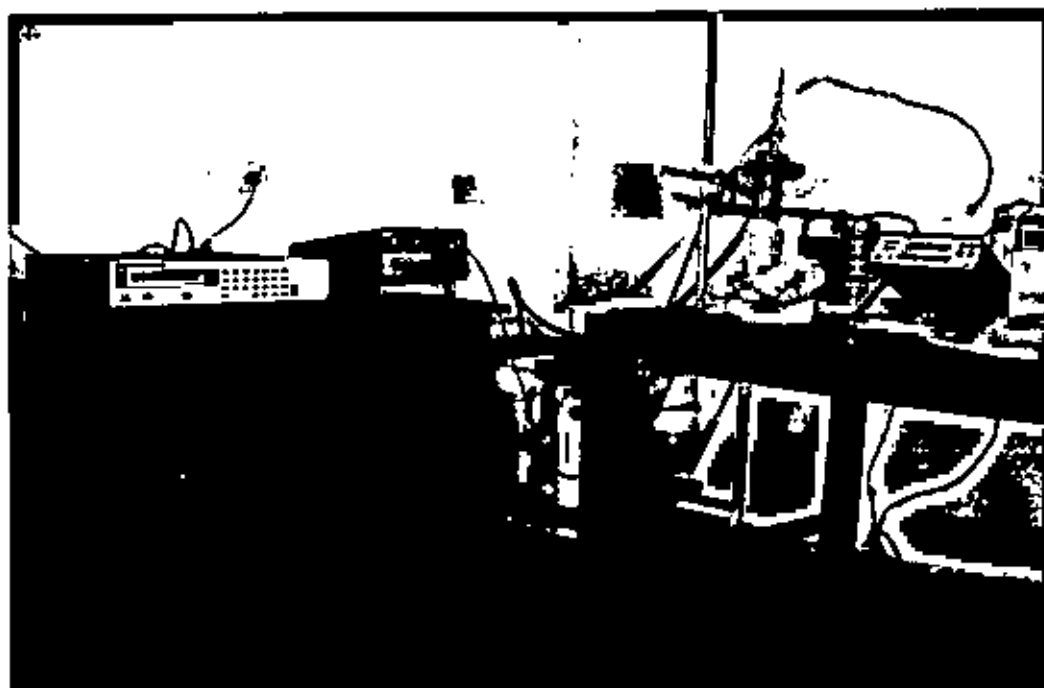


Fig. 6.7. Arrangement for DC measurement

## 6.5. Results and Discussion

### 6.5.1. Current density-voltage (J-V) characteristics

J-V characteristics of thin films of different thicknesses (150, 250, 300, and 400nm) were studied in Al/PPDEA/Al sandwich configuration, in the voltage range 0.1 - 25.0V in the temperatures of 298, 303, 373 and 398 K. The observed J-V characteristics of the films are presented in Fig. 6.8 to Fig. 6.11. Each curve shows two different slopes in the lower and higher voltage regions, corresponding to different conduction processes according to the power law of the form  $J \propto V^n$  where  $n$  is a power index. At lower voltages the slopes of  $0.56 \leq n \leq 1.3$  indicates approximate Ohmic region while at higher voltages the slopes of  $1.72 \leq n \leq 4.00$  represents the non-Ohmic region. The values of the slopes are tabulated in Table. 6.1. The voltage dependence of current density at higher voltage region suggests that the current may be due to Schottky, PF or SCLC mechanism in PPDEA thin films. From the relation  $J \propto d^{-l}$ , where  $l$  is a parameter depending upon the trap distribution, a slope  $l < 3$  at a higher voltage region suggests the possibility of Schottky or PF mechanism and  $l \geq 3$  evaluates the possibility of SCLC mechanism. Fig.6.12 illustrates the dependence of current density on

Table. 6.1 The slopes in the two voltage regions at different temperatures for samples of different thicknesses.

Thickness of PPDEA thin films d (nm)	Measurement temperature (K)	Values of slopes	
		Low voltage region (Ohmic)	High voltage region (non Ohmic)
150	298	1.03	2.13
	303	1.03	2.44
	373	1.30	2.38
	398	1.20	2.83
250	298	0.72	2.36
	303	0.78	3.22
	373	1.00	3.55
	398	1.08	4.00
300	298	0.92	2.36
	303	1.30	2.92
	373	1.20	3.15
	398	1.10	3.51
400	298	0.65	2.34
	303	0.77	1.72
	373	0.88	1.68
	398	0.90	1.73

PPDEA film thicknesses ranging from 150 to 400 nm at higher voltage region of 20 V. The plot has yielded a negative slope with a value of 1.5, which is much smaller than that for SCLC mechanism. These observations ruled out the possibility of SCLC mechanism and it could be predicted that the conduction mechanism operative in these films is probably either Schottky or PF.

According to Eqn. 6.12, for Schottky or Poole-Frenkel mechanism the expression for the current should give rise to a linear graph if  $\ln J$  is plotted against  $V^{1/2}$ . From the plots of  $\ln J$  vs  $V^{1/2}$  for PPDEA films of different thicknesses in Fig. 6.13 and at different temperature in Fig. 6.14 for a PPDEA thin film, which indicate  $\ln J$  is proportional to  $V^{1/2}$  and gives a straight line in the higher voltage region. Thus, the conduction mechanism in these films is of Schottky or PF type.

For Schottky or PF mechanism it is also necessary that a graph plotted between  $\ln J$  vs  $d^{1/2}$  should be a straight line with a negative slope. Fig. 6.15 shows that this is also satisfied in our case.

Using the slope of the straight line of the plot of  $\ln J$  vs  $V^{1/2}$  the experimental value of the  $\beta$  coefficient,  $\beta_{exp}$  can be evaluated by Eqn. 6.13. The theoretical values of  $\beta_S$  and  $\beta_{PF}$  were obtained from Eqns. 6.8 and 6.10 respectively, taking the high frequency dielectric constant, which is about 4.90. The value of  $\beta_{exp}$  is compared with the theoretical values of  $\beta_S$  and  $\beta_{PF}$  in Table 6.2. It is seen that the experimental  $\beta_{exp}$  value coincides with the theoretical  $\beta_S$  value for the Schottky type mechanism. Thus it can be inferred that the conduction mechanism in PPDEA thin films is most probably a Schottky type mechanism.

Table 6.2 : Comparison of experimental and theoretical  $\beta$  coefficients.

Film thickness $d$ , nm	Temperature K	$\beta_{exp}$ ( $eV m^{1/2} V^{-1/2}$ )	$\beta_S$ ( $eV m^{1/2} V^{-1/2}$ )	$\beta_{PF}$ ( $eV m^{1/2} V^{-1/2}$ )
150	298	$0.90 \times 10^{-5}$	$1.71 \times 10^{-5}$	$3.42 \times 10^{-5}$
250		$1.06 \times 10^{-5}$		
300		$1.15 \times 10^{-5}$		
400		$1.16 \times 10^{-5}$		

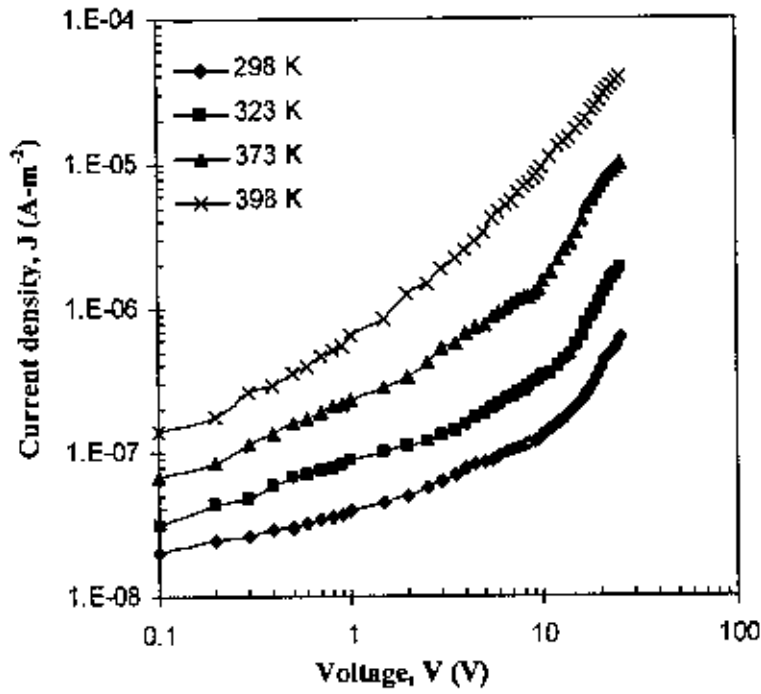


Fig. 6.8. log J-log V plot for PPDEA thin film at different temperatures ( $d = 400$  nm).

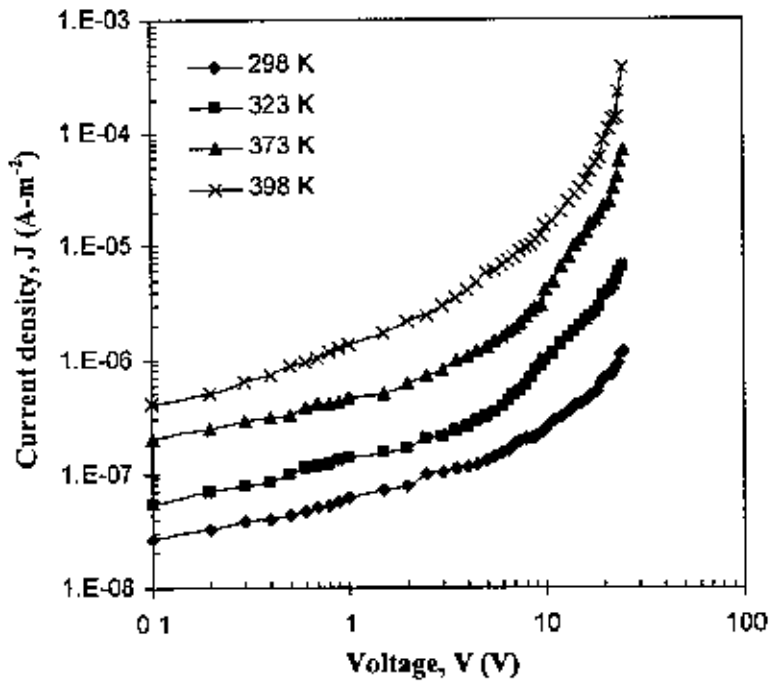
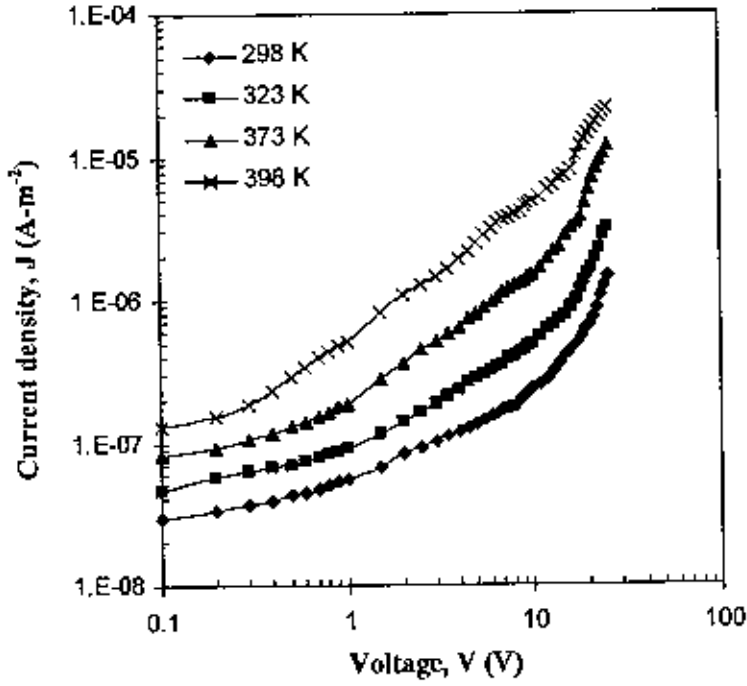
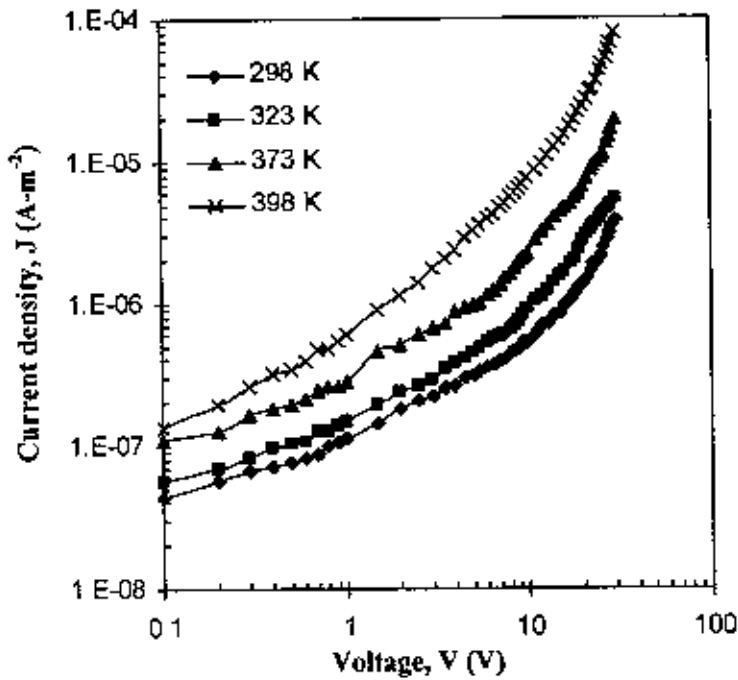


Fig. 6.9. log J-log V plot for PPDEA thin film at different temperatures ( $d = 300$  nm).Fig. 6.10. log J-log V plot for PPDEA thin film at different temperatures ( $d = 250$  nm).Fig. 6.11 log J-log V plot for PPDEA thin film at different temperatures ( $d = 150$  nm).



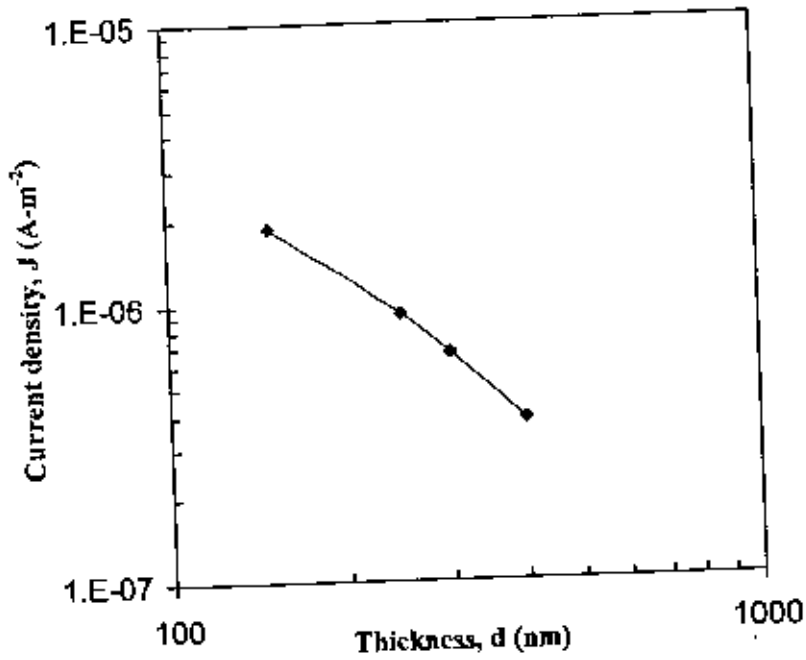


Fig. 6.12. Plots of  $\log J$ - $\log d$  for PPDEA thin films in the non-Ohmic region.

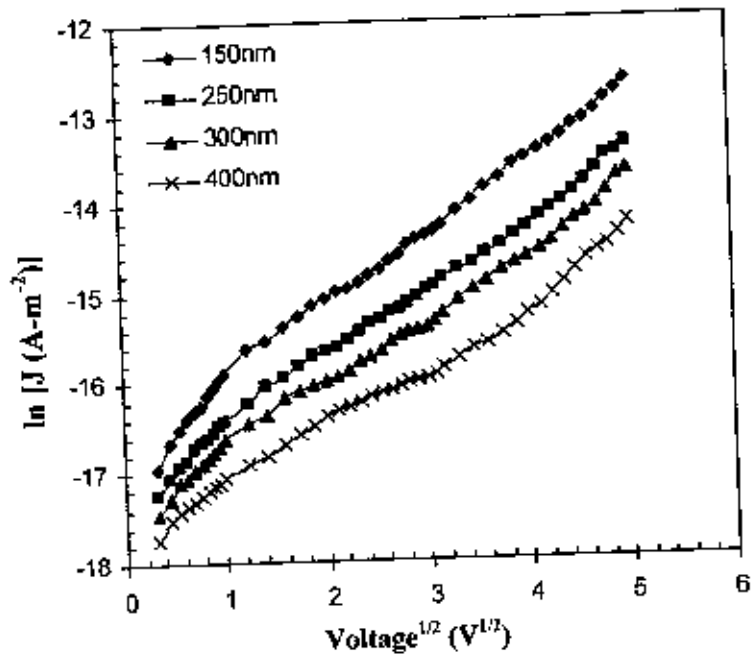


Fig. 6.13.  $\ln J$  vs.  $V^{1/2}$  at room temperature for PPDEA thin films of different thicknesses.

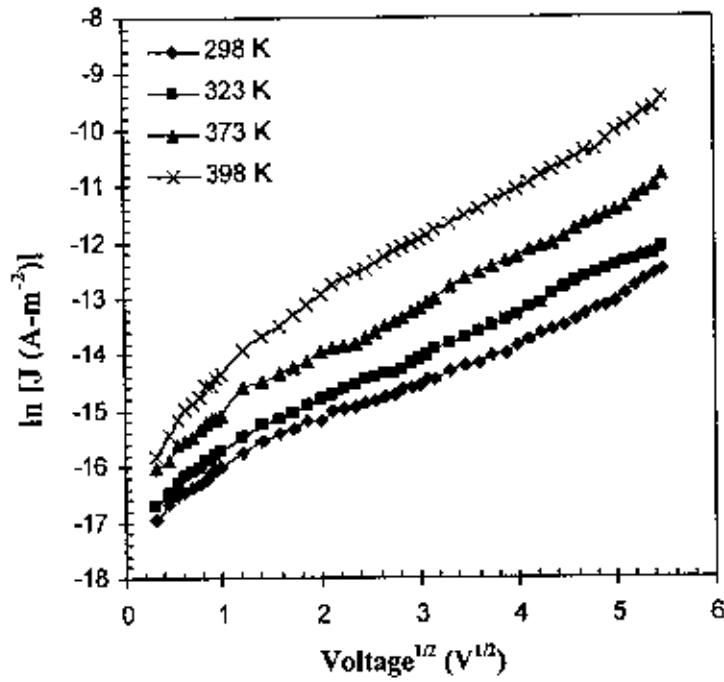


Fig. 6.14.  $\ln J$  vs.  $V^{1/2}$  at different temperatures for a PPDEA thin film ( $d = 150$  nm).

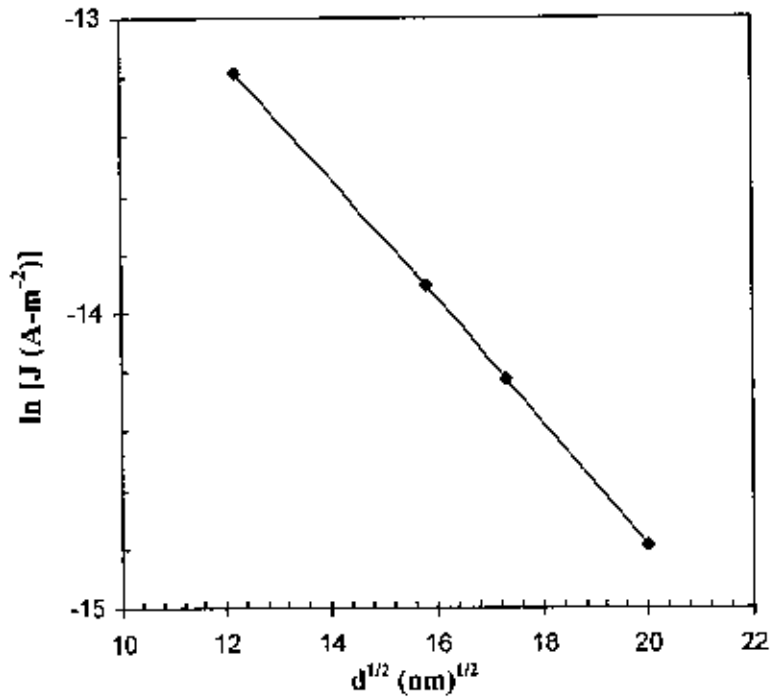


Fig. 6.15. Plots of  $\ln J$  vs  $d^{1/2}$  for PPDEA thin films at the higher voltage region.

### 6.5.2. Temperature dependence of current

Figs.6.16 to 6.19 shows the dependence of  $J$  on inverse absolute temperature,  $1/T$ , for PPDEA thin films of different thicknesses. There are two curves, one in the ohmic region with an applied voltage, 8 V, and the other in the Schottky region with an applied voltage, 14V. Each of the curves has two different slopes in the low temperature and in the higher temperature regions. The activation energies calculated from the slopes of plots of Figs.6.16 to 6.19 for all samples are reported in table 6.3.

Table.6.3: Values of activation energy  $\Delta E$  (eV) for PPDEA thin films of different thicknesses.

Thickness d (nm)	Activation energies $\Delta E$ (eV)			
	8.0 V		14.0 V	
	Temperature		Temperature	
	low	high	low	high
150	0.20	0.76	0.25	0.71
250	0.07	0.68	0.22	0.66
300	0.03	0.63	0.19	0.61
400	0.11	0.68	0.15	0.54

From Table.6.3, for applied voltage 8V (Ohmic), the activation energy is observed to be around  $0.10 \pm 0.03$  eV at the low temperature region and that at the higher temperature region is  $0.69 \pm 0.06$  eV. Whereas for 14V (Schottky) applied voltage, the activation energies were observed to be around  $0.20 \pm 0.05$  eV at the low temperature region and  $0.63 \pm 0.03$  eV at the higher temperature region. The lower activation energies of about  $0.10 \pm 0.03$  eV and  $0.20 \pm 0.05$  eV for 8 and 14 V respectively, at the lower temperature region and the higher activation energies of about  $0.69 \pm 0.06$  eV and  $0.63 \pm 0.03$  eV for 8 and 14 V respectively, at the higher temperature region may be attributed to a transition from a hopping regime to a regime dominated by distinct energy levels. In this kind of transition process, the localized carrier may be bound with the agglomerates itself. As a result the carriers cannot take part in the conduction through out the bulk of the material. As the hopping behavior, which have an activation energy of few in eV, the low temperature activation energy cannot be explained as hopping behavior but the decrease of activation energy with decreasing temperature can be explained as a gradual transition to the hopping regime.

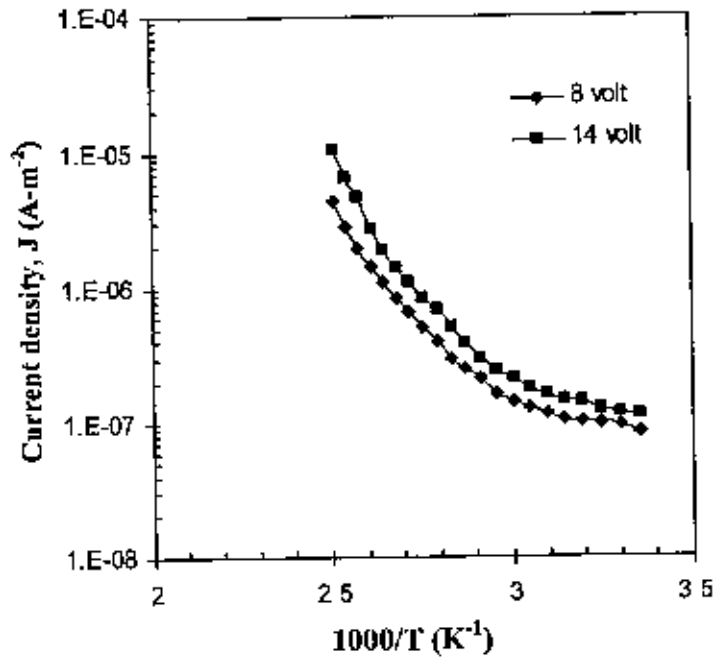


Fig. 6.16 Plots of Current density vs. inverse of absolute temperature for PPDEA thin film in Ohmic and non-Ohmic regions ( $d = 400\text{nm}$ ).

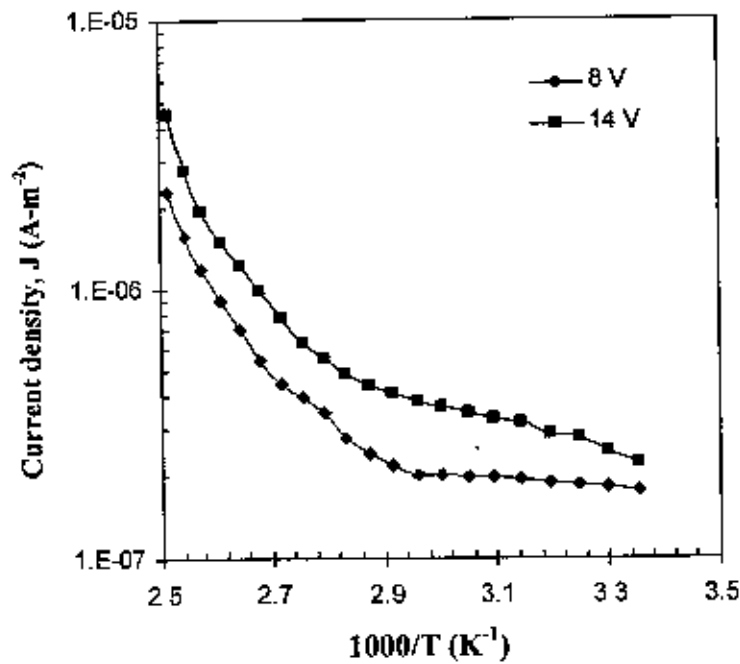


Fig. 6.17 Plots of Current density vs. inverse of absolute temperature for PPDEA thin film in Ohmic and non-Ohmic regions ( $d = 300\text{nm}$ ).

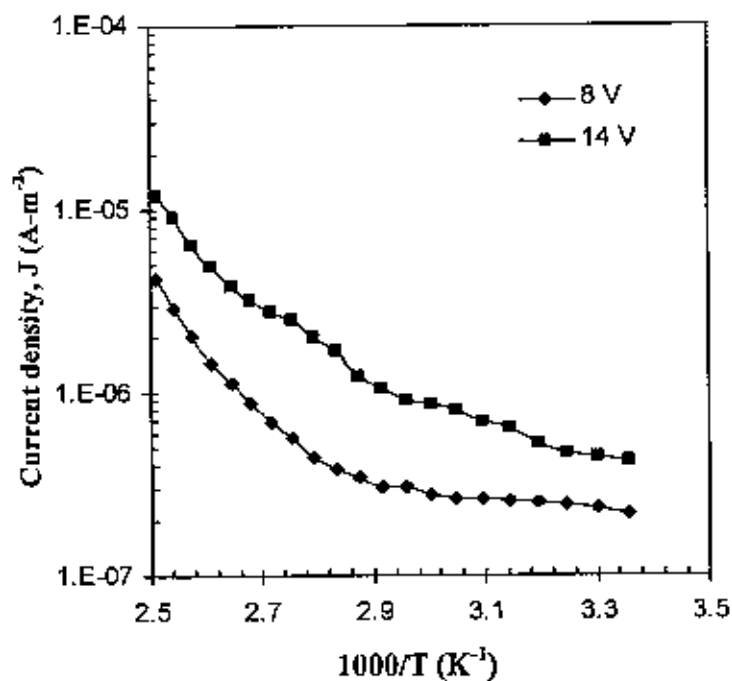


Fig.6.18 Plots of Current density vs. inverse of absolute temperature for PPDEA thin film in Ohmic and non-Ohmic regions ( $d = 250\text{nm}$ ).

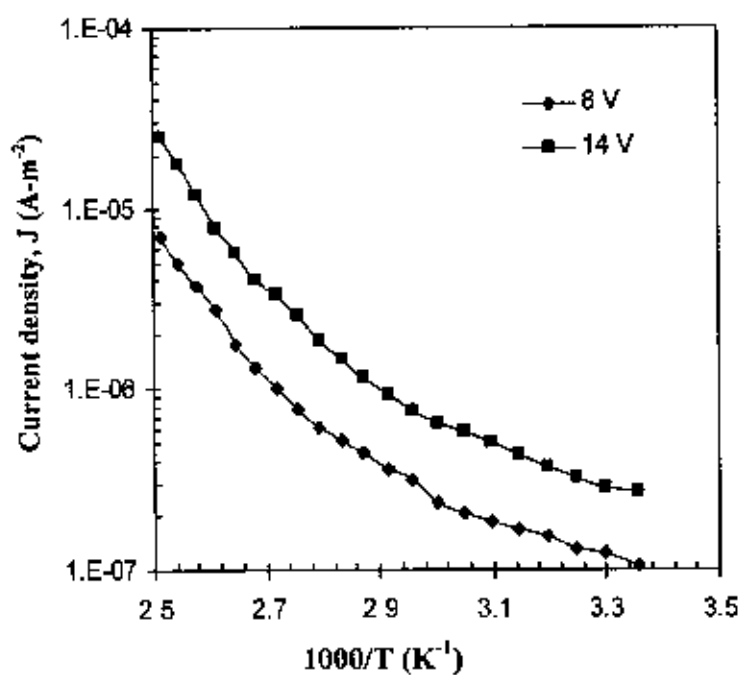


Fig.6.19 Plots of Current density vs. inverse of absolute temperature for PPDEA thin film in Ohmic and non-Ohmic regions ( $d = 150\text{nm}$ ).

**References**

- [1] Chen C. Ku and Raimond Liepins, 'Electrical Properties of Polymers'; Hanser Publishers, Munich - Vienna – New York (1987).
- [2] Yasuda H., 'Plasma Polymerization'; Academic Press, Inc, New York (1985).
- [3] Mathai C. J., Saravanan S., Jayalekshmi S., Venkatachalam S., Anantharaman M. R., 'Conduction mechanism in plasma polymerized aniline thin films' *Mater. Lett.*, **57**, 2253-2257, (2003).
- [4] Nagaraj N., Subba Reddy Ch. V., Sharma A. K., Narasimha Rao V. V. R.. J., 'DC conduction mechanism in polyvinyl alcohol films doped with potassium thiocyanate', *Power Sources*, **112**, 326-330, (2002).
- [5] Sajeev U. S., Mathai, C. J., Saravanan S, Ashokan R, Venkatachalam S., Anantharaman, 'On the optical and electrical properties of rf and a.c. plasma polymerized aniline thin films', *Bull. Mater. Sci.*, **29**, No.2 (2006).
- [6] Sayed W. M. Salem. T. A., 'Preparation of polyaniline and studying its electrical conductivity', *J. Appl. Polym. Sci.*, **77**, 1658-1665,(2000)
- [7] Chowdhury F-U-Z, Bhuiyan A. H., 'The dc electrical conduction mechanism of heat-treated plasma-polymerized diphenyl (PPDP) thin films', *Indi. J. Phys.*, **76**, 239-244,(2002).
- [8] Akther H. and Bhuiyan A. H. 'Space charge limited conduction in plasma polymerized N, N, 3, 5 tetramethylaniline thin films' *New J. Phys.* **7**, 173, (2005).
- [9] Shah Jalal A.B.M., S. Ahmed, A.H. Bhuiyan and M. Ibrahim, 'On the conduction mechanism in plasma-polymerized m-Xylene thin films', *Thin Solid Films*, **288**, 108-111, (1996).
- [10] Kumar. S., Nakamura K., Nishiyama S., Ishii S., Noguchi H., Kashiwagi K., Yoshida Y., 'Optical and electrical characterization of plasma polymerized pyrrole films', *J. Appl. Phys.* **93**, 2705-2711, (2003).
- [11] Silverstein M. S., Visoy-Fisher I., 'Plasma polymerized thiophene: molecular structure and electrical properties', *Polymer*, **43**, 11-20, (2002).
- [12] John R. K., Kumar D. K., 'Structural, Electrical and Optical studies of plasma polymerized and iodine doped polypyrrole', *J. Appl. Polym. Sci.*, **83**, 1856-1859, (2002).

- [13] Valaski R., Ayoub S., Micaroni L., Hummelgen I.A., "Influence of thin thickness on charge transport of electrodeposited polypyrrole thin films", *Thin Solid Films*, **415**, 206-210, (2002).
- [14] El-Nahass M. M., Abd-El-Rahman K. F., Darwish A. A. A., 'Electrical conductivity of 4-tricyanovinyl-N,N-diethylaniline', *Physica B* **403**, 219-223, (2008).
- [15] Bae I.-S., Jung C.-K., Cho S.-J., Song Y.-H., Boo J.-H., "A comprehensive study of plasma polymerized organic thin films on their electrical and optical properties", *J. Alloys and Compounds*, **449**, 393-396, (2008).
- [16] Gould R.D. and Lopez M.G., "Poole-Frenkel conductivity prior to electroforming in evaporated Au-SiO<sub>x</sub>-Au-sandwich structures", *Thin Solid Films* **342-344**, 94-97, (1999).
- [17] Bhattacharyya S., Laha A., and Krupanidhi S. B. 'Analysis of leakage current conduction phenomenon in thin SrBi<sub>2</sub>Ta<sub>2</sub>O<sub>9</sub> films grown by excimer laser ablation.' *J. Appl. Phys.* **91**, 4543-4548, (2002).
- [18] Maisel Leon I, and Glang R., 'Hand Book of Thin Film Technology' McGraw Hill Book Company, NY, (1970).

**CHAPTER 7**  
**CONCLUSIONS**

**7.1 Conclusions**

**7.2 Suggestions for Further Research**



## 7.1 Conclusions

The PPDEA thin films of different thicknesses were prepared from DEA by using a capacitively coupled plasma polymerization technique. The DEA is an aniline derivative with two ethyl group and one aniline group. Although studies on polyaniline have been reported, there are no reports on experimental studies on DEA. So DEA was chosen as a potential organic monomer for thin film preparation and study of its different properties. Conclusions of the results of morphological, structural, optical and dc electrical properties of PPDEA produced from DEA are given below.

The surface morphology and chemical composition of PPDEA are analyzed by SEM and EDX respectively. The SEM micrographs of thin films of PPDEA were taken in various magnifications and various accelerating voltages. Smooth, flawless and pinhole free surface is observed for PPDEA thin films of different thicknesses and no significant difference is observed. EDX analysis indicates the presence of C, N and O in the samples. The main obstacle of EDX is that it cannot detect the presence of H. The presence of O in PPDEA implies incorporation of carbonyl and hydroxyl groups through the reaction of the free radicals. It is also predicted that the PPDEA films are deficient in carbon and nitrogen with respect to the monomer, which may be due to the breakdown of bonds owing to the complex reaction during plasma polymerization.

From the IR spectra it is observed that the absorption peaks in the PPDEA are not sharp when compared with those for DEA and most of the IR absorption features of DEA are noticeable in the spectrum of PPDEA with the shift in wavenumbers i.e. the plasma technique has affected the chemical structure of the deposited films. The presence of C=O indicates that there are trapped free radicals in the PPDEA, which reacts with the atmospheric oxygen.

The values of both allowed direct transition,  $E_{g(d)}$ , and allowed indirect transition,  $E_{g(i)}$  were identified in PPDEA thin films. The values of  $E_{g(d)}$  and  $E_{g(i)}$  increase with increasing thickness. The average values of  $E_{g(d)}$  is, 3.56 eV and that of  $E_{g(i)}$  is 2.40eV.

The J-V characteristics of PPDEA revealed that the dependence of J on V is Ohmic in the lower voltage region and non Ohmic at higher voltage levels. The thickness dependence of current density in the higher voltage region has predicted a contact limited Schottky type conduction mechanism in PPDEA. The experimental  $\beta_{exp}$  value coincided with the theoretical



$\beta_s$  value for the Schottky type mechanism. Thus it is concluded that the conduction mechanism in PPDEA thin films is most probably a Schottky type mechanism.

For applied voltage 8V (Ohmic), the activation energy is observed to be around  $0.10 \pm 0.03$  eV at the low temperature region and that at the higher temperature region is  $0.69 \pm 0.06$  eV. While for applied voltage 14V (Schottky), the activation energies are observed to be around  $0.20 \pm 0.05$  eV at the low temperature region and  $0.63 \pm 0.03$  eV at the higher temperature region. The low temperature activation energy cannot be explained as hopping behavior but the decrease of activation energy with decreasing temperature can be explained as gradual transition to the hopping regime and conduction may be due to movement of carrier between distinct energy level in the high temperature region.

## 7.2 Suggestions for Future work

In this work an attempt was made to investigate the structural, optical and the dc electrical behavior of PPDEA. But, more characteristics of PPDEA thin films can be investigated, which will help finding suitable applications of these materials. The following investigations on PPDEA thin films may be carried out.

The chemical investigation can be done by Elemental analysis. The thermal analysis by DSC, DTA and TGA at different heating rates will be helpful to ascertain the reaction kinetics in the PPDEA films. The XPS investigation should be carried out in order to see the bonding of different functionalities in the PPDEA thin films. It also can provide quantitative information of the element present. The electron spin resonance ( ESR) study may be carried out to see the nature and source of radicals in this material.

The dielectric constant, loss factor and the dielectric strength may be measured to find the dielectric application of the materials. For studying the charge storage and charge relaxation the thermally stimulated depolarization current(TSDC) can be measured.

PPDEA can be modified to change electrical properties by heat treatment and doping. Doping of these films can be carried out while preparing those films in the plasma chamber or by exposing them in dopant gases. It can be also deposited as a coating on other polymers. The PPDEA can be prepared in an asymmetric electrode configuration or inductively coupled, plasma polymerization set-up with rf power and can be characterized by the above mentioned techniques.